Jul 2014

Modelling oxygen dynamics in the Upper Swan estuary and Canning Weir Pool

Final Report

Report prepared for:

Swan River Trust

Government of Western Australia

The University of Western Australia

AED Aquatic Eco Dynamics

Government of Western Australia
Department of Water

Executive Summary

Like many urban waterways around the world, changes in water quality and other pressures are impacting the Swan and Canning river ecosystems with visible signs of stress. The combination of nutrient and organic loading, algal blooms, and low oxygen conditions in the rivers places stress on fish and other aquatic life. Changes in climate, including reduced rainfall and stream flow and increased marine intrusion, adds to the vulnerability. In particular, low oxygen conditions are now a persistent management challenge in the Upper Swan estuary and Canning Weir Pool, with detrimental effects previously reported on estuarine biota and the general amenity and health of the river.

Artificial oxygenation has been a remediation strategy for poor water quality in the upper reaches of the Canning River for more than 16 years, and in the upper Swan River for the past 6 years. There are currently two oxygenation plants on each of the Swan and Canning rivers (and a third plant on the Canning is currently being built). These oxygenation plants pump oxygen-depleted water from near the riverbed, supersaturate it with oxygen, and return the newly oxygenated water to the bottom waters of the estuary. Regular Monitoring of water quality and intensive operational trials around the plants shows obvious improvements in oxygen status due to artificial oxygenation, but a quantitative assessment of the effectiveness of artificial oxygenation in this dynamic estuarine environment had not been previously attempted.

This report summarises a research study started in late 2011 to build coupled hydrodynamic-biogeochemical models for the artificially oxygenated zones in the Swan and Canning Rivers. These models aimed to integrate the substantial data sets that have been collected on water and sediment quality in the rivers since the introduction of the oxygenation plants, and provide a predictive tool for management. It was hoped that, by modelling the dynamic estuarine environments with and without oxygenation intervention, a quantitative measure of the effectiveness of the oxygenation plants could be obtained. Cost-benefit analysis for different operational scenarios would also then be possible.

Following a brief review of a number of model platforms, the model TUFLOW-FV was applied to model at high-resolution the hydrodynamics (water level, velocity, salinity and temperature distribution) coupled with a model for water column biogeochemistry (FABM with AED modules). Two models were developed – one for the Upper Swan that spanned the spatial area from the Narrows Bridge to Great Northern Highway, and one for the Canning Weir Pool upstream of the Kent Street Weir. These models were calibrated against the substantial datasets collected by Department of Water and Swan River Trust for two years: 2008 as a moderately wet flow year, and 2010 as a low flow (dry) year. A one-dimensional (vertical) model for understanding the role of sediment in affecting oxygen status and water quality was developed in parallel and used to define the sediment-water interactions required for the 3D model domains.

The performance of the Swan model was excellent and able to accurately resolve the seasonal and spatial dynamics observed for salinity and temperature (the R^2 values between predicted and observed are 0.85-0.95). Oxygen conditions were generally well captured both spatially and temporally, with an average error of approximately 20%. Model estimates were less accurate for nutrients, although simulation of nutrients was not the focus of the investigation of oxygenation plant performance presented here and is left for subsequent refinement. The sound performance suggests the model is fit-for-purpose in terms of evaluating different operational scenarios under different environmental conditions.

A (passive) oxygen tracer study showed that, when oxygen was not consumed, the area potentially influenced by the addition of oxygen at Guildford and Caversham was up to 30 km, depending on the amount of river flow. However, oxygen is consumed by both biological and chemical processes both within the water column and more significantly by the oxygen demand of the sediment. Therefore a measure was developed to quantify the effectiveness of artificial oxygen by comparing the area of the benthos (riverbed) that was oxygenated when it would have otherwise been experiencing low oxygen (<4 g O_2 m^{-3} or mg L^{-1}) if the oxygen plants were not operating. We refer to this as the "*area of benthos saved*" and can be thought of as a measure of restoration effectiveness.

In 2010, only the Guildford oxygen plant was operating on the Upper Swan as the Caversham plant had not been built yet. Running the Upper Swan model using the actual operation regime of the Guildford plant in 2010 and comparing it to the estuary conditions that would have occurred if it not run at all (the "do nothing" case), allowed us to calculate that the area of benthos saved to be ~0.15 km^2 when the plant was running. This is a significant area compared to the entire riverbed area of 0.38 km^2 between the river reach from King's Meadow Oval to Reg Bond Park – the Swan River Trust

target oxygenation area. With two plants operating the area of benefit could exceed 0.3 km^2, and periodically greater than the target oxygenation zone, and the results therefore confirm the plant significantly improves river benthic habitat.

A number of simplified (hypothetical) operational scenarios were also compared, with an indicative cost of operating these scenarios calculated in order to undertake a cost-benefit analysis. Across the different oxygenation scenarios, with both plants running, the maximum area of benthos saved could extend to as much as 0.6 – 1.0 km^2 depending on the plant operation method and flow conditions, with an estimated operating cost ranging from $200,000-400,000 per annum. The average area restored over the simulation year did increase with increasing inputs of oxygen, however, comparison of different operational regimes highlights how to get the best environmental benefit for the least cost (see below figure).

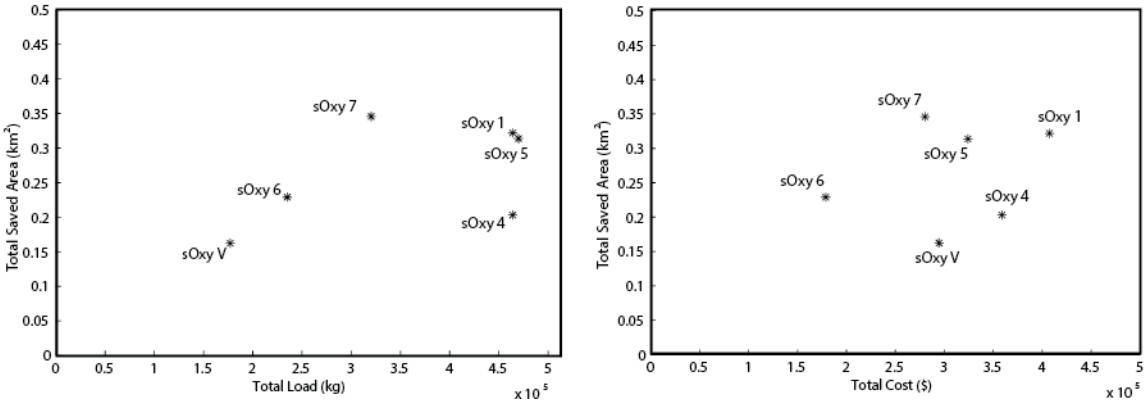

Average area of benthos (river bed) restored in the Upper Swan from critically low oxygen concentrations (<4 g O_2 m^{-3}) relative to total oxygen input (left) and total cost (right). A range of operational scenarios shown highlight the complex relationship between cost and benefit (refer to Table 10 for scenario details).

The Canning model performance was good but had a higher level of error than the Upper Swan model, possibly due to lack of local weather data as inputs to the model. However, the main spatial and temporal features of the water column oxygen status were resolved well and the model was used to explore simplified operational scenarios. The scenarios tested show a clear non-linear relationship to the cost and the environmental benefit (see figure below). In general the plants saved up to 0.05km^2 during the simulation period (of a total area of 1.3km^2 from Kent St weir to Roe Hwy), with average values of ~0.03km^2. The model was used to explore the benefit of the third oxygenation plant on the Canning River, and alternative sparger configurations in order to understand the most effective way to optimise the oxygenation.

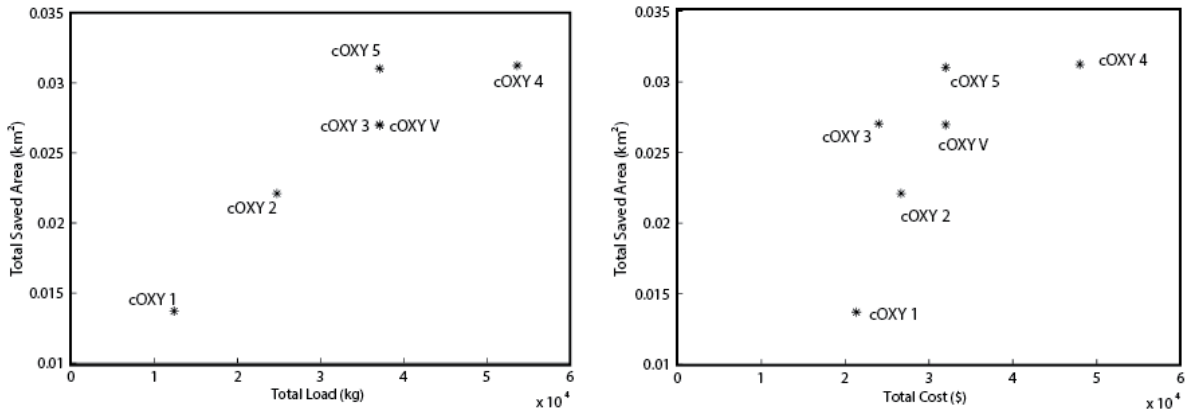

Average area of benthos (river bed) restored in the Canning Weir Pool from critically low oxygen concentrations (<4 g O_2 m^{-3}) relative to total oxygen input (left) and total cost (right). A range of operational scenarios shown highlight the complex relationship between cost and benefit (refer to Table 12 for scenario details).

Overall the modelling of oxygenation zones in the Swan Canning estuary has provided an excellent tool for management. Model comparisons of plant operation versus "do-nothing" show a clear improvement in near-bed water quality and oxygen status. The model simulations therefore confirm the benefits indicated by monitoring data and have further allowed us to more accurately quantify these benefits. Furthermore, the outputs of these models can now be used to develop more cost-effective operational strategies into the future.

General Recommendations and Further Work

Recommendations relating to the operation of the oxygenation plants:

- Implementation of practices to encourage less rapid rising of the oxygenation bubble plume, which may decrease degassing and increase oxygenation plant efficiency.
- Further work to identify how "DO control" (the near real-time operation of oxygenation plants in response to in situ conditions) may perform at the larger system scale, and how this compares with other alternative regimes for plant operation.
- Investment in the collection of local weather station data, including net-radiation. This should be within the upper riverine reaches of the two domains to better capture the local conditions near the oxygenation plants.

Ongoing model development, improvement and further validation will improve the predictive ability of the model for tackling questions relevant to management of the oxygenation plants. Priorities include:

- Sediment flux studies to better describe how nutrient release responds to dynamic benthic oxygen conditions.
- Using the model to run whole operational year scenarios for all years that plants have been in operation to determine 'benthic area saved' versus actual expenditure (ie. to quantify how the management intervention and associated costs have improved the estuarine environment).
- Collection of improved data on organic matter loading in the major and minor tributaries of the Swan.
- Improved spatial mapping of sediment condition to allow specification of localized sediment flux rates within the model.
- Development of a decision-support tool to predict "optimal" operational regime based on forecasts of hydrological, biogeochemical and operational conditions.

For wider use of the model for assessing estuary response, the following further recommendations are made:

- Expansion of model domain to the whole of estuary.
- Improved phytoplankton model setup and validation to better predict surface oxygen conditions.
- Further work on modelling nutrient cycles, which allow the preparation of more detailed nutrient budgets of the estuary to better inform decision making.
- The simulation of benthic oxygen condition and relationships to benthic infauna habitat and community structure.

CONTRIBUTORS

Matthew R. Hipsey [a], *Kieryn Kilminster* [b], *Brendan D. Busch* [a], *Louise C. Bruce* [a], *Sarah Larsen* [b]

[a] Aquatic Ecodynamics, School of Earth and Environment, The University of Western Australia, Crawley WA 6009, Australia.
[b] Water Science Branch, Department of Water, Perth WA 6842, Australia.

ACKNOWLEDGEMENTS

We acknowledge the Swan River Trust for supporting the model development and in particular acknowledge Dr. Kerry Trayler for her leadership and input in development of the model. Detailed review comments on the original draft of this report and advice were also provided by Jim Greenwood, Kerry Trayler, Alex Hams, which together significantly improved the analysis. We also gratefully acknowledge inputs from M. Robb, Z. Goss, and G. Evans from the WA Department of Water for their guidance, operational knowledge about the oxygenation plants and support with data requirements. We also thank I. Teakle from BMTWBM Pty. Ltd. for advice on adjustments and calibration of the TUFLOW-FV model. Sediment biogeochemical model simulations were conducted by Mathias Norlem during his visit to UWA, and Dan Paraska also assisted in compiling sediment nutrient data and setting parameters for the AED model. Samanta Busameyer assisted in the calculation of the error metrics and temperature validation of the model.

REVISION AND DISTRIBUTION HISTORY

Issue	Issued to	Qty	Date	Reviewed	Approved
V1	*DOW / SRT*	*e*	*May 2013*	*K Trayler*	*MH*
V7	*DOW*	*e*	*Aug 2013*	*K Kilminster* *S Evans*	*MH*
V9	*DOW / SRT / CSIRO*	*e*	*Nov 2013*	*K Kilminster* *K Trayler* *A Hams* *J Greenwood*	*LB*
V10	*ALL*	*e*	*1 July 2014*	*K Kilminster* *L Bruce*	*MH*

RELEASE STATUS:

Confidential: No

DOCUMENT DETAILS

Citing this report:
Hipsey, M.R., Busch, B.D., Bruce, L.C., Kilminster, K., 2014. Modelling oxygen dynamics in the Upper Swan estuary and Canning Weir Pool. AED Report #R25, The University of Western Australia, Perth, Australia. 91pp.

ISBN: 978-1-74052-304-2

Contents

1. Introduction & Objectives

Background

Poorly oxygenated water is often observed in the bottom waters of many salt-wedge riverine estuaries (e.g., Paerl *et al.*, 1998; Roberts *et al.*, 2013). This is defined as water that is significantly below saturation level, and can be classified as experiencing *low oxygen* (<4 mg L^{-1}), *hypoxia* (<2 mg L^{-1}) or *anoxia* (0 mg L^{-1}). The balance of tidally driven pulsing of oceanic water into the estuary with river inflows discharging to the coastal margin, typically sets up a salt-wedge stratification pattern that restricts vertical mixing between oxygen deplete bottom waters and the atmosphere. The extent and severity of oxygen depletion is highly variable across the length of an estuary and throughout the year since it depends both on physical circulation patterns and biogeochemical processes such as organic matter mineralization, photosynthesis and the sediment oxygen demand (Bruce *et al.*, 2014).

Low oxygen conditions, including periods of both hypoxia and anoxia in the upper reaches of the Swan Canning estuary (WA) is a now a persistent management challenge, with detrimental effects on estuarine biodiversity and the overall amenity and health of the river (Kurup and Hamilton, 2002; Tweedley *et al.*, 2011; Wildsmith *et al.*, 2011; Storer *et al.*, 2013; Cottingham *et al.*, 2014). This is largely a result of reduced flows in the surrounding Swan-Avon River catchments (Petrone *et al.*, 2010; Silberstein *et al.*, 2012), that have led to reduced flushing of nutrients and organic matter from the upper estuary reaches, and penetration and persistence of the salt-wedge further upstream (Cottingham et al., 2014). In parallel to the changing hydrology, land-use development within the Swan Coastal Plain has further increased the loading of labile organic material to the estuary (Petrone *et al.*, 2009), much of which accumulates in the poorly flushed upper reaches of the estuary and leads to very high sediment oxygen demand rates (Smith *et al.*, 2010). In order to tackle the problem of oxygen depletion, the Western Australian State Government has conducted artificial oxygenation of the stratified upper river reaches as a remediation strategy for poor water quality within the Canning River for more than 16 years, and in the upper reaches of the Swan River for the past 6 years. There are currently two oxygenation plants on each of the Swan and Canning Rivers. These oxygenation plants pump oxygen-depleted water from near the riverbed, supersaturate it with oxygen, and return the newly oxygenated water to the bottom waters of the estuary through a local array of diffusers.

Data from weekly monitoring of water quality (e.g., http://www.swanrivertrust.wa.gov.au/swan-river-trust/publications/monitoring-and-evaluation), and assessments of intensive operational trials around the plants (Department of Water, 2010 and 2011; Kilminster *et al.*, 2011; Storer *et al.*, 2013) has indicated a reduction in the extent of low oxygen concentrations due to artificial oxygenation. However, the horizontal dispersion and overall persistence of the oxygenated water plume can vary significantly depending on environmental conditions such as the wind, tide and riverine inflows. Projections of a drying climate for south-west Western Australia and increases in temperature are likely to further exacerbate the problem of hypoxia into the future (Vaquer-Sunyer and Duarte, 2011; Bruce *et al.*, 2014). It is therefore essential to better understand how oxygenation plant efficiency varies under a range of environmental conditions, the extent to which it can improve water quality, and how this would differ under a range of operational strategies. For this purpose, predictive modelling is able to complement on-the-ground data collection activities and support scenario predictions. Given the oxygenation plants are energy and resource intensive to operate, a simulation model able to quantify conditions where oxygenation is either more or less effective also opens up the opportunity to conduct a cost-benefit analysis.

Further, the impact of oxygenation on nutrient cycling and overall nutrient budgets is unclear. For example, the negative impacts of low oxygen on higher organisms is well documented (Vaquer-Sunyer and Duarte, 2008), but the impacts on the nitrogen (N) and phosphorus (P) cycles are less well understood due to complex redox-sensitive biogeochemical processes that occur (Middleburg and Levin, 2009; Pena *et al.*, 2010; Zhang *et al.*, 2012). An advanced mechanistic understanding of the effects of variability and manipulation of oxygen concentrations on N and P cycling is critical because it has been found that persistent hypoxia is likely to enhance internal nutrient loading, and this can potentially further fuel algal growth compounding the problems of eutrophication (Kemp *et al.*, 2009; Howarth *et al.*, 2011). In particular, denitrification is as an important loss of N in estuarine environments (e.g., Crowe *et al.*, 2012) that occurs under anaerobic conditions, however, its success in removing N is generally linked to a supply of nitrate from an oxygenated water column. Somewhat counter-intuitively, persistent hypoxia in the water column is therefore associated with less efficient N loss via denitrification and replacement with alternative nitrogen metabolism pathways such as dis-assimilatory nitrate reduction to ammonia (DNRA) (Roberts *et al.*, 2013). Given the highly variable conditions that occur

in the estuary across a range of spatial and temporal scales, it is not straightforward to unravel the interactions between observed physico-chemical properties, the rates of nutrient processing, and the overall nutrient budgets, and predictive models can therefore be used to unravel these pathways. From an environmental management point of view, a well-validated model can serve to help us better understand and quantify the effects artificial oxygenation on promoting denitrification, and enhancing P sorption and sedimentation in addition to general habitat benefits.

Following this rationale, a project was undertaken from 2012-2013 by the University of Western Australia and Department of Water that aimed to gain further insights into these questions through development of a spatially-resolved coupled hydrodynamic-biogeochemical model of the Upper Swan estuary and the Canning Weir Pool. This report summarises the development and validation of the model with a focus on the oxygen dynamics. The model simulates the interactions between physical and biogeochemical processes that govern estuarine response to oxygenation, and in particular provides the ability to quantify the pathways of oxygen, nutrients and organic matter. The model is used to conduct a cost-benefit analysis of hypothetical oxygenation plant operational regimes, by introducing a method for assessing how estuarine habitat is improved by oxygenation at the estuary system-scale.

Scope of work

Specifically the scope of the project was to:

1. Briefly **review the range of models** that have previously been applied to the Swan estuary or are relevant to the current application.

2. Define **requirements of the estuary model** for the purposes of studying the oxygenation dynamics.

3. **Implement the most suitable model** for the study regions, including the Upper Swan River and Canning Weir Pool. The challenge for this study region is that it is highly curved and experiences strong vertical stratification, which together make accurate simulation difficult. Sensitivity to resolution of the computational domain should therefore be considered.

4. **Configure a biogeochemical model** that resolves the interactions between oxygen, carbon, nutrients, and phytoplankton, with a focus on simulation of oxygen dynamics. The coupled model must simulate the transport and kinetics of temperature, salinity, carbon and nutrients (including organic and inorganic components), phytoplankton and sediment fluxes.

5. **Validate the model** against measured physical (salinity, temperature), and biogeochemical variables using profile data from intensive monitoring by the State Government agencies and also other monitoring data that is available.

6. **Run a selection of operational scenarios** under different conditions to be defined in consultation with the estuary management team, and assess the relative effectiveness in combating hypoxia and anoxia.

This report is structured by first presenting a review of the available data and historical research (Section 2), followed by a description of the model approach and rationale for model parameterisation (Section 3). Objectives 3 - 6, are then addressed independently for the Swan in Section 4 and for the Canning in Section 5. A summary and recommendations are presented in Section 6.

2. Previous research & available data

A substantial amount of prior research and data collection has been conducted on the Swan Canning river system relevant to the current model development. Since the model heavily relies on this data for setup, parameterisation and validation an overview of data that was reviewed as part of the analysis is summarised in Table 1.

Table 1: Summary table of available data and previous research on the Swan Canning catchment relevant to the present model development.

Data	Station Names	Variables	Time period	Reference
Routine water quality sampling (surface, bottom water)	**Lower Swan Estuary**: BLA and ARM **Narrows Bridge**: NAR **Middle Swan Estuary**: NIL, STJ and MAY **Upper Swan Estuary**: RON, KIN and SUC **Swan River**: WMP and MSB **Canning Estuary**: SCB, SAL, RIV and CASMID **Lower Canning River**: KEN, BAC, NIC and ELL	Total N Ammonium N Total Oxidised N Dissolved Organic N Total P Soluble Reactive P Silica Dissolved Organic C Total Suspended Solids Alkalinity Chlorophyll-a Secchi Depth Phytoplankton	Ongoing, weekly/fortnightly Main sites available from 1995	Published in quarterly reports by the Department of Water
		Dissolved O_2 Temperature Salinity	Ongoing, weekly	Published weekly
O_2 plant studies	Guildford region	DO, T, salinity	February – June 2009	Operational report for the oxygenation trial of Turbolox technology in the upper Swan River estuary 2009
	Numerous (see Figure 25)	DO, T, salinity, WQ	Jan 2010; April 2010; June 2010	DoW intensive sampling data
Microbial population surveys	BLA, ARM, NAR, STJ, RON, SUC	Bacteria, virus, picoplankton	Jan – Dec 2010 fortnightly	Gedaria and Hipsey (2013)
Dissolved organic matter studies	Upper estuary and catchment	DOC/DON Hydrophobic/philic fraction	January 2007	Petrone *et al.*, (2009)
		POC/PON DOC/DON	2007 Weekly	Petrone (2010)
	Lower estuary	Organic matter fluorescence against water quality	April August November 2009	Fellman *et al.*, (2011)
Light data	Upper estuary	PAR profiles	2012	Department of Water (unpublished data)
Simulated flows and water quality	Many catchment sites	Flow, TN, TP	2001 – 2006	SQUARE model
	Ron Courtney Island	Flow, salt wedge location DO	1973, 74 1993, 94 Monthly	Kurup *et al.*, (1998)
			June – August 1994 Weekly	Kurup and Hamilton (2002)
	Ron Courtney Island Tonkin Hwy Overpass	Flow NH_4 PO_4 Na K Ca Mg HCO_3 Cl SO_4 EC S	1993 – 1994 Weekly – monthly	Hamilton *et al.*, (2006)

Determining benthic fluxes is a key component of this work since oxygen depletion is a direct consequence of organic matter breakdown in the sediment. From various technical documents available, and a search of the academic literature, an overview of sediment data taken from numerous sites over different time periods was compiled (Table 2).

This highlights the spatial variability in the nutrient fluxes, and also the relatively high sediment oxygen demand (SOD) values reported consistently via different investigators and from different methods. As outlined in more detail in the next section, the sediment data is used to validate a detailed sediment biogeochemistry model that is used to inform the main model investigation.

Table 2: Summary table of available sediment data and previous research on the Swan Canning estuary relevant to the present model development.

Data	Station Names	Variables	Time period	Reference
Sediment surface grab samples	KMO WMP VIT RPB	NH_4^+ NO_X N_2 PO_4^{3-} SiO_4^{4-} DIC	May 2008	Smith *et al.*, (2010) Geoscience Australia Report
		DIC TOC – gives R_{OM}	12 – 24 h incubation	
	RON RCE BRW10 KIN KMO VIT SUC BBO MEA MUL WMP-RB SCS01 CAV REG MBS MSB JBC POL	NH_4^+ NO_X N_2 PO_4^{3-} SiO_4^{4-} DIC	September 2007	
		DIC TOC – gives R_{OM}	12 – 24 h incubation	
Cores	KMO WMP VIT RPB	NH_4^+ NO_X N_2 PO_4^{3-} SiO_4^{4-}	May 2008	Smith *et al.*, (2010) Geoscience Australia Report
	KMO WMP	NH_4^+ NO_X N_2 PO_4^{3-} SiO_4^{4-} DIC O_2TN TP		
	SR32 SR33 SR34	NH_4^+ NO_x PO_4^{3-} SiO_4^{4-} TCO_2 DON	October 2006	Smith *et al.*, (2006) Geoscience Australia Report
	SR33	Al As Cd Cu Fe Mn Ni V Zn		
Benthic fluxes	SR32 SR1 KMO WMP	NH_4^+ NO_X N_2 PO_4^{3-} SiO_4^{4-} DIC O_2	October 2006 May 2008	Smith *et al.*, (2010) Geoscience Australia Report
	SR33	Al As Cd Cu Fe Mn Ni V Zn	October 2006	Smith *et al.*, (2006) Geoscience Australia Report
	Pelican Pt Melville Water Lucky Bay Perth Water Garrat Rd Br Ron Courtney Island Guildford	SOD NH_4^+ NO_3^- DIN FRP	February 1997	Lavery *et al.*, (2001)
	Kent St Weir	SRP before and after application of Phoslock	February 2010	Application of Phoslock™ to the Canning River 2010 – DoW Report on methods and results.
	Guildford	O_2	April – May 2010	Department of Water, unpublished data

3. Model Approach

In general terms the requirements for an estuarine model able to simulate oxygenation dynamics include:

- potential for curvilinear (boundary following) structured grid, or flexible mesh to capture complex bathymetry with reasonable run-times;
- ability to resolve tight vertical stratification associated with the salt-wedge;
- biogeochemical model to consider sources, sinks of oxygen, organic matter and nutrients;
- transformation kinetics of oxygen, carbon and nutrients (particulate & dissolved);
- sediment-water interaction and atmosphere-water interaction;
- the ability to allow for the source term of oxygen from the oxygenation plant at the appropriate locations.
- Ability to run the model for long time periods (multiple years) without excessive simulation times.

A range of various models that either have been or have potential to be applied to the Swan Canning river system are summarised in Table 3. The project team had experience with several of these platforms and initially the Upper Swan estuary domain was setup using GETM. However, initial runs indicated relatively long run-times to capture this domain and periodic instabilities in the model outputs. After considering this initial experience with running GETM, favourable initial runs with TUFLOW-FV, and also general experience with other model platforms, the combination of hydrodynamic model TUFLOW-FV coupled with the AED water quality modules within FABM (described below) was chosen for the study and is reported here. This combination was chosen due to the high level of flexibility in grid generation, wide range of contemporary turbulent closure models and flexible and customisable open-source water quality modules. These elements are summarised below. The model is also currently also applied in a similar capacity to simulate biogeochemistry within the Yarra River Estuary (Bruce *et al.*, 2014), Hawkesbury-Nepean River (BMTWBM, 2014) and Caboolture Estuary (Adiyanti *et al.*, 2014).

The project simulates two independent domains: one for the Upper Swan estuary from the Narrows Bridge to Great Northern Hwy, and one from downstream of Kent St Weir to the Canning and Southern River gauging stations; the extent of domains used for the simulations are shown in detail in subsequent sections. Both the Swan and Canning domains were optimised to have relatively coarse resolution away from the focus areas and finer detail in the focus regions (i.e., areas of low oxygen and areas influenced by the oxygenation plants). Both model domains are driven by available data for inflows, meteorology and tides.

Hydrodynamics

The TUFLOW-FV (http://tuflow.com, BMTWBM, 2013a) package is applied for this investigation as a 3D flexible-mesh (finite volume) hydrodynamic model to simulate the water level, velocity, salinity and temperature distribution in the both the Swan and the Canning domain areas. The model accounts for variations in water level, the horizontal salinity distribution and vertical density stratification in response to inflows, salt-wedge dynamics and surface thermodynamics.

The mesh (in plan view), consists of triangular and quadrilateral elements of different size that are suited to simulating areas of complex estuarine morphometries. The vertical mesh discretization has options for sigma-coordinates, or z-coordinates, with the latter also allowing multiple surface Lagrangian layers, as adopted in this study. The finite volume numerical scheme solves the conservative integral form of the non linear shallow water equations in addition to the advection and transport of scalar constituents such as salinity and temperature as well as the state variables from the coupled biogeochemical model. The equations are solved in 3D with baroclinic coupling from both salinity and temperature using the UNESCO equation of state (Fofonoff and Millard, 1983). Both 1st and 2nd order spatial integration schemes are available within TUFLOW-FV. The temporal integration scheme is explicit and uses both mode splitting and dynamically varying time-steps to maximize computational efficiency subject to Courant and Peclet stability constraints.

Surface momentum exchange and heat dynamics are solved internally within TUFLOW-FV, where appropriate meteorological boundary conditions are supplied. In the current application, turbulent mixing of momentum and scalars has been calculated using the Smagorinsky scheme in a horizontal plane and through coupling with the General Ocean Turbulence Model (GOTM, (Umlauf and Burchard, 2003) for vertical mixing.

Table 3: Summary of available model platforms for estuary hydrodynamic-biogeochemistry modelling (Note: H = horizontal; V = vertical).

	GETM-FABM	TUFLOWFV-FABM	ELCOM-CAEDYM	CE-QUAL-W2	MIKE3	EFDC	CSIRO-EMS
Grid approach	Structured H: Curvilinear V: Sigma	Unstructured H: Finite volume V: Z-coordinate & Sigma	Structured H: Orthogonal V: Z-coordinate	Structured H: Laterally averaged sections V: Z-coordinate	Unstructured H: Mesh V: Z-coordinate	Structured H: Curvilinear	Structured H: Curvilinear V: Z-coordinate & Sigma
Vertical stratification approach	Extensive options via GOTM library (www.gotm.net)	Extensive options via GOTM library (www.gotm.net)	Mixing energy model	Various empirical options available	Various options available	Various options available	Various options available
Availability	Free	Commercial (hydrodynamics) Free (biogeochemistry)	Commercial	Free	Commercial	Free	Free
Source code	Open Source (GPL)	TFV: No FABM: Open Source (GPL)	License agreement & CWR membership	Open Source	No	Open Source	License agreement
Example applications in similar Australian systems	Shark Bay (Kangas *et al.*, 2012) Yarra River Estuary (Bruce *et al.*, 2011)	Hawkesbury-Nepean (BMTWBM, 2014) Yarra River Estuary (Bruce *et al.* 2014) Caboolture River Estuary (Adiyanti *et al.*, 2014) Maroochy Estuary (BMTWBM, 2013b)	Lower Lakes and Coorong (Hipsey & Busch, 2012) Cockburn Sound (Yeates *et al.*, 2008) Swan River Estuary (Chan *et al.*, 2002; Robson & Hamilton, 2004; Vilhena, 2013)	Swan River Estuary (Kurup *et al.*, 1998)	Gippsland Lakes (Zhu *et al.*, 2013)	E. Tanner (pers comm.)	Derwent Estuary (Wild-Allen *et al.*, 2013) Moreton Bay (Herzfeld *et al.*, 2014) Leschenault (Gillibrand *et al.*, 2012) Fitzroy River (Robson *et al.*, 2006; Robson *et al.*, 2008)
Suitability to Swan Canning and oxygenation scenarios	Suitable but requires high level of technical proficiency; engineering structures not implemented. Optimised for parallel computation on supercomputers (MPI)	Suitable, modern code with good range of hydraulic structures (e.g. weir) and boundary options; Optimised for parallel computation on multi-core machines (OpenMP)	Suitable for lower and mid estuary, but structured grid is less suited for riverine reaches. At the time the project was undertaken, the code was not optimized for parallel computing	Not suited since laterally averaged	Potentially suitable but limited reports in high curvature rivers.	Potentially suitable but limited reports in high curvature rivers.	Potentially suitable; Optimised for parallel computation on multi-core machines (OpenMP)

Water column biogeochemistry

The *Framework for Aquatic Biogeochemical Models* (FABM) is a relatively new state-of-the-art code-base to support the simulation of aquatic biogeochemical and ecological dynamics. It has been developed in response to the need to develop improved standards and flexibility in model integration in as part of an active development community (Trolle *et al.*, 2012; Bruggeman & Bolding, 2014). FABM itself is not a water quality model, but rather it is an object-oriented code framework that supports a common library of biogeochemical and ecological models and model 'components'. It has been designed to facilitate integration of different biogeochemical/ecological model approaches (both process-based and empirical), model currencies and to enable coupling with a diverse array of physical (hydrodynamic) driver models. In this study, we adopted the Aquatic Ecodynamic (AED) modules developed at UWA. The mathematical approach implemented in the AED modules is similar to the aquatic ecological models of the other platforms, and specific details of the approach can be read in Hipsey *et al.*, (2014) and a similar application in the Yarra estuary by Bruce *et al.*, (2014).

The AED modules are highly flexible and support simulation of various water quality aspects, but in this study the modules are configured to simulate the C, N, P and DO, including the inorganic nutrients, organic matter, and phytoplankton. Since the focus of this study was not on simulating algal dynamics in detail, the configuration was limited to nutrients with no Chl-a or no zooplankton. Therefore, for this configuration, four dissolved inorganic nutrients (FRP, NO_3, NH_4, PIP), three dissolved (DOC, DON, DOP) and three particulate (POC, PON, POP) detrital organic matter groups, and dissolved oxygen (DO) were modelled. The simulated state variables, which are mixed, transported and subject to boundary forcing by the hydrodynamic driver, are listed in Table 4, along with other derived properties for comparison with field data (e.g., TN, TP). Biogeochemistry parameters adopted are in Table 5.

Table 4: Simulated variables as part of TUFLOW-FV–FABM–AED oxygenation simulations.

Variable	Units *	Common Name	Process Description
T	°C	Temperature	Temperature modelled by TUFLOW-FV, subject to surface heating and cooling processes
S	psu	Salinity	Salinity simulated by TUFLOW-FV, impacting density. Subject to inputs and evapo-concentration
EC	uS cm^{-1}	Electrical conductivity	Derived from salinity variable
I	mE m^{-2} s^{-1}	Shortwave light intensity	Incident light, I_0, is attenuated as a function of depth
η_{PAR}	m^{-1}	PAR extinction coefficient	Extinction coefficient is computed based on organic matter and suspended solids
DO	mmol O_2 m^{-3}	Dissolved oxygen	Impacted by photosynthesis, organic decomposition, nitrification, surface exchange, and sediment oxygen demand
DOC	mmol C m^{-3}	Dissolved organic carbon	Mineralization, algal mortality/excretion
POC	mmol C m^{-3}	Particulate organic carbon	Breakdown, settling, algal mortality/excretion
FRP	mmol P m^{-3}	Filterable reactive phosphorus	Algal uptake, organic mineralization, sediment flux
DOP	mmol P m^{-3}	Dissolved organic phosphorus	Mineralization, algal mortality/excretion
POP	mmol P m^{-3}	Particulate organic phosphorus	Breakdown, settling, algal mortality/excretion
PIP	mmol P m^{-3}	Particulate inorganic phosphorus	Adsoprtion/desorption of/to free FRP
TP	mmol P m^{-3}	Total Phosphorus	Sum of all P state variables
NH_4^+	mmol N m^{-3}	Ammonium	Algal uptake, nitrification, organic mineralization, sediment flux
NO_3^-	mmol N m^{-3}	Nitrate	Algal uptake, nitrification, denitrification, sediment flux
DON	mmol N m^{-3}	Dissolved organic nitrogen	Mineralization , algal mortality/excretion
PON	mmol N m^{-3}	Particulate organic nitrogen	Breakdown, settling, algal mortality/excretion
TN	mmol N m^{-3}	Total Nitrogen	Sum of all N state variables

* Note that core units in FABM-AED are mmol m^{-3}, however, for the remainder of the report results of DO are converted to g m^{-3} (equivalent to mg L^{-1})

Sediment oxygen and nutrient fluxes

One of the key drivers for estuarine deoxygenation is the sediment oxygen demand (SOD). Several reported attempts have been made to measure SOD (See Table 2), however these are not easily transferable to the main 3D model described in this report due to highly variable conditions under which they were measured. A parallel study to develop a sediment biogeochemical model was therefore undertaken (Norlem *et al.*, 2013), where the high-resolution dynamics of surficial sediment was simulated under various conditions, including the highly dynamic conditions as created by the diel changes in redox conditions created by periodic oxygenation.

Table 5: Summary of water column biogeochemical parameter descriptions, units and typical values.

Symbol	Description	Units	Assigned value	*Comment*
$k_{atm}^{O_2}$	oxygen transfer coefficient	m/s	calculated	*Wanninkhof (1992)*
$[O_2]_{atm}$	atmospheric oxygen concentration	mmol O_2/m^3	calculated	*Riley and Skirrow (1975)*
$\chi_{C:O_2}^{miner}$, $\chi_{C:O_2}^{PHY}$	Stoichiometric conversion of C to O2	g C/ g O_2		*12/32*
$\chi_{N:O_2}^{nitrif}$	Stoichiometric conversion of N to O2	g N/ g O_2		*14/32*
R_{nitrif}	maximum rate of nitrification	/d	0.5	*Lake*: 0.03 – 0.05 [A]; 0.037 [C] *Estuary*: 0.5 [B]
K_{nitrif}	half saturation constant for oxygen dependence of nitrification rate	mmol O_2/m^3	78.1	*Lake*: 62.5 – 93.7 [A] *Estuary*: 78.1 [B]
θ_{nitrif}	temperature multiplier for temperature dependence of nitrification rate	-	1.08	*Lake*: 1.08 [A]; 1.03 [C] *Estuary*: 1.08 [B]
R_{denit}	maximum rate of denitrification	/d	0.5	*Lake*: 0.01 – 0.04 [A] *Estuary*: 0.5 [B]
K_{denit}	half saturation constant for oxygen dependence of denitrification	mmol O_2/m^3	21.8	*Lake*: 12.5 – 15.6 [A] *Estuary*: 21.8 [B]
θ_{denit}	temperature multiplier for temperature dependence of denitrification	-	1.08	*Lake*: 1.05 [A] *Estuary*: 1.08 [B]
R_{decom}^{PON}	maximum rate of decomposition of particulate organic nitrogen	/d	0.5	*Lake*: 0.005 – 0.01 [A]; 0.03 [C] *Estuary*: 0.5 [B]
K_{decom}^{PON}	half saturation constant for oxygen dependence of mineralisation rate	mmol O_2/m^3	31.25	*Lake*: 47 – 78 [A] *Estuary*: 31.25 [B]
θ_{decom}^{PON}	temperature multiplier for temperature dependence of mineralisation rate	-	$= \theta_{OM}$ =1.08	*Lake*: 1.08 [A] *Estuary*: 1.08 [B]
R_{miner}^{DON}	maximum rate of mineralisation of dissolved organic nitrogen	/d	0.5	*Lake*: 0.003 – 0.05 [A] *Estuary*: 0.001 – 0.028 [D]
K_{decom}^{DON}	half saturation constant for oxygen dependence of mineralisation rate	mmol O_2/m^3	31.25	47 – 78 [A]
θ_{miner}^{DON}	temperature multiplier for temperature dependence of mineralisation rate	-	$= \theta_{OM}$ =1.08	1.04 – 1.10 [A]
ω_{PON}	settling rate of particulate organic matter	m/d	$= \omega_{OM}$ =-1.0	-1.0 [B]
R_{decom}^{POC}	maximum rate of decomposition of particulate organic carbon	/d	0.5	0.01 – 0.07 [A]; 0.008 [C]
K_{decom}^{POC}	half saturation constant for oxygen dependence of mineralisation rate	mmol O_2/m^3	31.25	47 – 78 [A]
θ_{decom}^{POC}	temperature multiplier for temperature dependence of mineralisation rate	-	$= \theta_{OM}$ =1.08	1.04 – 1.10 [A]
R_{miner}^{DOC}	maximum rate of mineralisation of dissolved organic carbon	/d	0.5	*Lake*: 0.003 – 0.05 [A] *Estuary*: 0.001 – 0.006 [D]
K_{decom}^{DOC}	half saturation constant for oxygen dependence of mineralisation rate	mmol O_2/m^3	31.25	47 – 78 [A]
θ_{miner}^{DOC}	temperature multiplier for temperature dependence of mineralisation rate	-	$= \theta_{OM}$ =1.08	1.04 – 1.10 [A]
ω_{POC}	settling rate of particulate organic matter	m/day	$= \omega_{OM}$ =-1.0	
R_{decom}^{POP}	maximum rate of decomposition of particulate organic phosphorus	/d	0.5	0.01 – 0.03 [A]; 0.099 [C]
K_{decom}^{POP}	half saturation constant for oxygen dependence of mineralisation rate	mmol O_2/m^3	31.25	47 – 78 [A]
θ_{decom}^{POP}	temperature multiplier for temperature dependence of mineralisation rate	-	$= \theta_{OM}$ =1.08	1.04 – 1.10 [A]
R_{miner}^{DOP}	maximum rate of mineralisation of dissolved organic phosphorus	/d	0.5	0.01 – 0.05 [A]
K_{decom}^{DOP}	half saturation constant for oxygen dependence of mineralisation rate	mmol O_2/m^3	31.25	47 – 78 [A]
θ_{miner}^{DOP}	temperature multiplier for temperature dependence of mineralisation rate	-	$= \theta_{OM}$ =1.08	1.04 – 1.10 [A]
ω_{POP}	settling rate of particulate organic matter	m/d	$= \omega_{OM}$ =-1.0	

$\Phi_{ads}^{pH}(pH)$	Function characterizing pH effect on	-	calculated	-0.0088(pH)^2 + 0.0347(pH) + 0.9768 [E]
c_{ads}^{r}	ratio of adsorption and desorption rate coefficients	l/mg		0.7 [F]
c_{ads}^{max}	maximum adsorption capacity of SS	mmol P/mg SS		0.00016 [F]

[A] Converted from data on oligotrophic lakes (Romero *et al.*, 2004) to eutrophic lakes (Gal *et al.*, 2009), and justifications therein .
[B] Based on Bruce et al. (*2011*) FABM-AED application on the Yarra Estuary (Victoria); estimated from data from Roberts *et al.* (2013).
[C] Based on Hamilton and Schladow (1997) for Prospect Reservoir
[D] Based on incubations by Petrone *et al.* (2009) for Swan Estuary (Western Australia)
[E] Based on regression of data from Salmon *et al.* (2014) based on data review from 6 papers therein
[F] Based on model of Chao *et al.* (2010).

The high-resolution results from the sediment biogeochemical model were then used to guide estimates of nutrient and oxygen fluxes from the sediment and how they are impacted by oxygenation. They were subsequently used to define the model parameters used in the estuary models.

The results from this high-resolution model were used to develop a simpler sediment oxygen demand, F_{SOD}, equation:

$$F_{SOD}^{O_2} = F_{max}^{O_2}\left[\frac{DO_e}{DO_e+K_{sed}^{O_2}}\right]\left(\theta_{sed}^{O_2}\right)^{T_e-20} \quad (1)$$

where *e* refers to specific conditions in each model element in which the flux is being computed, DO is the dissolved oxygen concentration in the element, and $\theta_{sed}^{O_2}$ is an Arrhenius temperature scaling factor. This was used within the 3D model domain allowing us to capture the essential dynamics relevant to the environmental conditions experienced here without the overhead of the detailed sediment diagenesis model. Based on the diagenesis model outputs and relevant field estimates of SOD (Figure 1), we then estimated an indicative maximum flux rate ($F_{max}^{O_2}$) of 2.5 g O_2 m^{-2} day^{-1} (80 mmol O_2 m^{-2} day^{-1} input to FABM) when used with an oxygen half saturation constant ($K_{sed}^{O_2}$) of 4 g O_2 m^{-3} (130 mmol m^{-3} input to FABM). Herzfeld *et al.* (2001) also reported similar flux rates as those described here. Sediment nutrient flux parameter values are summarised in Table 6.

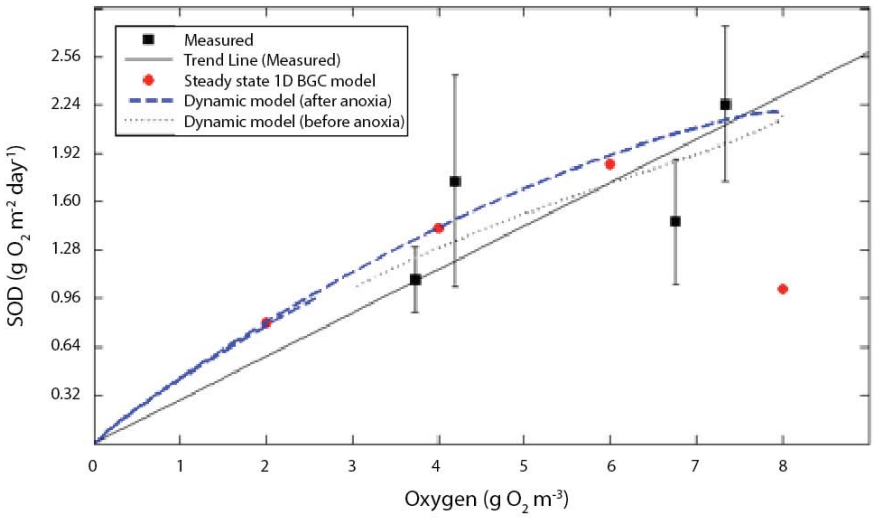

Figure 1: Sediment oxygen demand predictions from the 1D sediment diagenesis model of Norlem *et al.* (2013) under different bottom water oxygen conditions. Measured values are given as average +/- one standard deviation and based on data presented in Smith *et al.* (2010). Model simulations were run in steady state for a given bottom water condition, and also under dynamic oxygenation scenarios with variable bottom water concentrations. The latter accounts for hysteresis and delayed effects due to oxygen penetration and reaction rates.

Table 6: Summary of sediment parameter descriptions, units and typical values.

Symbol	Description	Units	Assigned value	Comment
$F_{max}^{O_2}$	maximum flux of oxygen across the sediment water interface into the sediment	mmol $O_2/m^2/d$	80.0	*Lake*: 6 – 38 [A] *River*: 9.4 – 20.3 [B] *Estuary*: 48 [C]; 79 [D]; ~50 [E]
$K_{sed}^{O_2}$	half saturation constant for oxygen dependence of sediment oxygen flux	mmol O_2/m^3	130	*Lake*: 15.6 [A] *Estuary*: 150 [C]; ~50 [F]
$\theta_{sed}^{O_2}$	temperature multiplier for temperature dependence of sediment oxygen flux	-	$= \theta_{sed}$ =1.08	1.04 – 1.10 [A]
F_{max}^{RSi}	maximum flux of silica across the sediment water interface	mmol $Si/m^2/d$	4	*Lake*: 0.6 [A] *Estuary*: 4 – 40 [E]
K_{sed}^{RSi}	half saturation constant for oxygen dependence of sediment silica flux	mmol Si/m^3	150	estimated
θ_{sed}^{RSi}	temperature multiplier for temperature dependence of sediment silica flux	-	$= \theta_{sed}$ =1.08	1.04 – 1.10 [A]
$F_{max}^{PO_4}$	maximum flux of phosphate across the sediment water interface	mmol $P/m^2/d$	0.2	*Lake*: 0.080 – 0.125 [A] *River*: 0.0 – 0.10 [B] *Estuary*: 0.3 – 4 [E]
$K_{sed}^{PO_4}$	half saturation constant for oxygen dependence of sediment phosphate flux	mmol O_2/m^3	20	*Lake*: 15.6 [A, J] *Estuary*: >200 [F]
$\theta_{sed}^{PO_4}$	temperature multiplier for temperature dependence of sediment phosphate flux	-	$= \theta_{sed}$ =1.08	1.04 – 1.10 [A]
F_{max}^{DOP}	maximum flux of dissolved organic phosphorus across the sediment water interface	mmol $P/m^2/d$	0.05	*Lake*: 0.03 [A] *River*: 0.05 – 0.10 [B]
K_{sed}^{DOP}	half saturation constant for oxygen dependence of sediment dissolved organic phosphorus flux	mmol O_2/m^3	150	estimated
θ_{sed}^{DOP}	temperature multiplier for temperature dependence of sediment dissolved organic phosphorus flux	-	$= \theta_{sed}$ =1.08	1.04 – 1.10 [A]
$F_{max}^{NH_4}$	maximum flux of ammonium across the sediment water interface	mmol $N/m^2/d$	30.0	*Lake*: 1.35 – 6.42 [A] *River*: 4.3 – 12.8 [B] *Estuary*: 30 [C]; 5 – 25 [E]
$K_{sed}^{NH_4}$	half saturation constant for oxygen dependence of sediment ammonium flux	mmol N/m^3	31.25	*Lake*: 1.56 – 15.6 [A] *Estuary*: 31.25 [C]
$\theta_{sed}^{NH_4}$	temperature multiplier for temperature dependence of sediment ammonium flux	-	1.08	1.04 – 1.10 [A]
$F_{max}^{NO_3}$	maximum flux of nitrate across the sediment water interface	mmol $N/m^2/d$	5.2	*Lake*: -21.4 – -7.14 [A] *River*: 4.3 – 12.8 [B] *Estuary*: 5.2 [C]; -7.2 – 7.1 [E]
$K_{sed}^{NO_3}$	half saturation constant for oxygen dependence of sediment nitrate flux	mmol O_2/m^3	100.0	*Lake*: 2.14 – 15.6 [A] *Estuary*: 100 [C]
$\theta_{sed}^{NO_3}$	temperature multiplier for temperature dependence of sediment nitrate flux	-	$= \theta_{sed}$ =1.08	1.04 – 1.10 [A]
F_{max}^{DON}	maximum flux of dissolved organic nitrogen across the sediment water interface	mmol $N/m^2/d$	5.2	*Lake*: 0.07 – 0.57 [A] *River*: 1.28 – 2.20 [B]
K_{sed}^{DON}	half saturation constant for oxygen dependence of sediment dissolved organic nitrogen flux	mmol N/m^3	100.0	estimated
θ_{sed}^{DON}	temperature multiplier for temperature dependence of sediment dissolved organic nitrogen flux	-	$= \theta_{sed}$ =1.08	1.04 – 1.10 [A]

[A] Converted from data on oligotrophic lakes (Romero *et al.*, 2004) to eutrophic lakes (Gal *et al.*, 2009), and justifications therein.

[B] Based on Hipsey *et al.* (2010) ELCOM-CAEDYM model of the lower Murray River); estimated from data from Prof. Justin Brookes.

[C] Based on Bruce *et al.* (2011) GETM-FABM-AED application on the Yarra Estuary (Victoria); estimated from data from Roberts *et al.* (2013).

[D] Net flux measured during eddy correlation experiment in the Upper Swan Estuary (Department of Water, unpublished data); varied in the range 20 – 150 mmol $O_2/m^2/d$ with a background concentration of 260 mmol O_2/m^3, therefore $F_{max}^{O_2}$ ~ 50/(260/(260+150)) = 79 mmol $O_2/m^2/d$.

[E] Based on benthic chamber studies showing an average net flux of 50 mmol $O_2/m^2/d$ the Upper Swan estuary (Smith *et al.*, 2007).

[F] Based on Smith *et al.*, (2007) assessment of data from the Upper Swan estuary, limitation at low oxygen concentrations is not observed

Economic assessment of oxygenation

In order to undertake a cost-benefit analysis of oxygenation plant performance an indicative operational cost was defined. The cost is calculated for each oxygenation plant based on i) the electricity cost, Θ_{power}, and ii) the oxygen input cost, Θ_{oxygen}. Note that these are the primary costs accounted for and we do not consider the capital cost of plant construction, or the indirect costs associated with running such as maintenance and repair. The total cost is therefore:

$$\Theta_{plant} = \Theta_{power} + \Theta_{oxygen} \quad (2)$$

and

$$\Theta_{power} = \sum_t E_j \ \kappa_t \ p_{j,t} \quad (3)$$

where E is the energy units consumed (kWh) for the j^{th} plant, κ_t is a binary flag (0,1) indicating if the plant is operational or not at any time t, and p_j is the price of energy (\$ kWh^{-1}). The price is set to vary between peak and off-peak times, and hence is defined for each plant, and each time-step (2 hourly). The price of oxygen is computed based on the flow rate of oxygen consumed:

$$\Theta_{oxygen} = \sum_t Q_{oxy}(t) \ p_o \quad (4)$$

where $Q_{oxy}(t)$ is the flow rate of oxygen as a function of time, and p_o is the price of oxygen (\$ kg^{-1}). For the analysis p_o was constant at 0.62, and off peak was from 10pm to 8am.

4. Upper Swan Estuary Model

Model application

The Upper Swan estuary domain spans from the Narrows Bridge to the Great Northern Hwy bridge. The mesh is loosely based on a curvilinear designed grid, but with custom elements around complex areas (Figure 2). The channel has approximately 4-8 elements across the river below Caversham, with 1 cell across from the region upstream of Caversham to the Avon River boundary point (the Department of Water S616076 flow gauging station). The depths on the grid were interpolated from recently collected bathymetric data available from the Department of Transport from the Narrows to Caversham, and upstream of this point raw depth sounder data collected from the centre of the channel was interpolated and joined to the high-resolution data set (Figure 3). Bathymetric smoothing of the centre of the channel was also performed (Figure 4). The vertical resolution consisted of 0.25 m thick vertical layers from 0.0 mAHD to 2.0 mAHD, and then 0.5 m thick vertical layers from 2.0 m to the bottom of the domain. Above 0.0 mAHD, 3 sigma layers of variable thickness were used to capture vertical differences between the tidal minimum and maximum.

The domain is forced by inflows, meteorological and tidal information from various locations (Figure 5):

- *Tidal data* – 15 minute water level data from was input directly to the model, and weekly water quality data interpolated to daily resolution;
    - Barrack St Jetty (Department of Transport water level gauge) & Narrows Bridge (Department of Water profile data for temperature, salinity and oxygen, and grab data for nutrients)
- *Meteorological data* – Hourly South Perth data from the Department of Agriculture was used uniformly across the domain:
    - Solar radiation, wind, air temperature, humidity, rain & cloud cover
- *Inflow data* – daily gauging station flow data from the Department of Water was input and available water quality data was interpolated to daily resolution for:
    - Swan River, Ellen Brook, Jane Brook, Susannah Brook, Helena River, Bennett Brook, Bayswater Drain (Table 7; Figure 6).

Table 7: Details of inflow stations input to the model domain showing the UTM input location and associated Department of Water station ID (refer also to Figures 5 and 6)

Inflow	X	Y	BC ID	Name
0	407488	6483347	S616076	Upper Swan River @ Great Northern Highway
1	398521.1768	6466744.225	S616082	Bayswater Drain
2	401873.5369	6470737.257	S616084	Bennet Brook
3	402026.775	6469681.576	S616086	Helena River
4	406477.8351	6478763.48	S616178	Jane Brook
5	405648.6555	6474549.506	S616099	Susannah Brook
6	405790.5906	6481841.906	S616189	Ellen Brook

Numerous processing scripts were used to create model input files from the Department of Water raw data files including:

a) interpolation to relevant input data frequency (usually daily, as summarised above)

b) derivation of non-measured but simulated variables (e.g. POM, DOM attributes)

Two time periods were simulated to assess the model under different flow regimes.

- 2008 – moderately "wet" year (~182 GL)
- 2010 – a low flow "dry" year (~24 GL)

The model was run from January 1st – December 31st for each of these two years. For the 2010 simulation the Guildford oxygenation plant was periodically operational and this was also included as a boundary condition (the lower station as indicated in Figure 2). Data for oxygenation plant input was based on oxygenation consumption data logs and specifications of plant flow rate, and it was configured to come in over the bottom 1 m of the centre cell across the river.

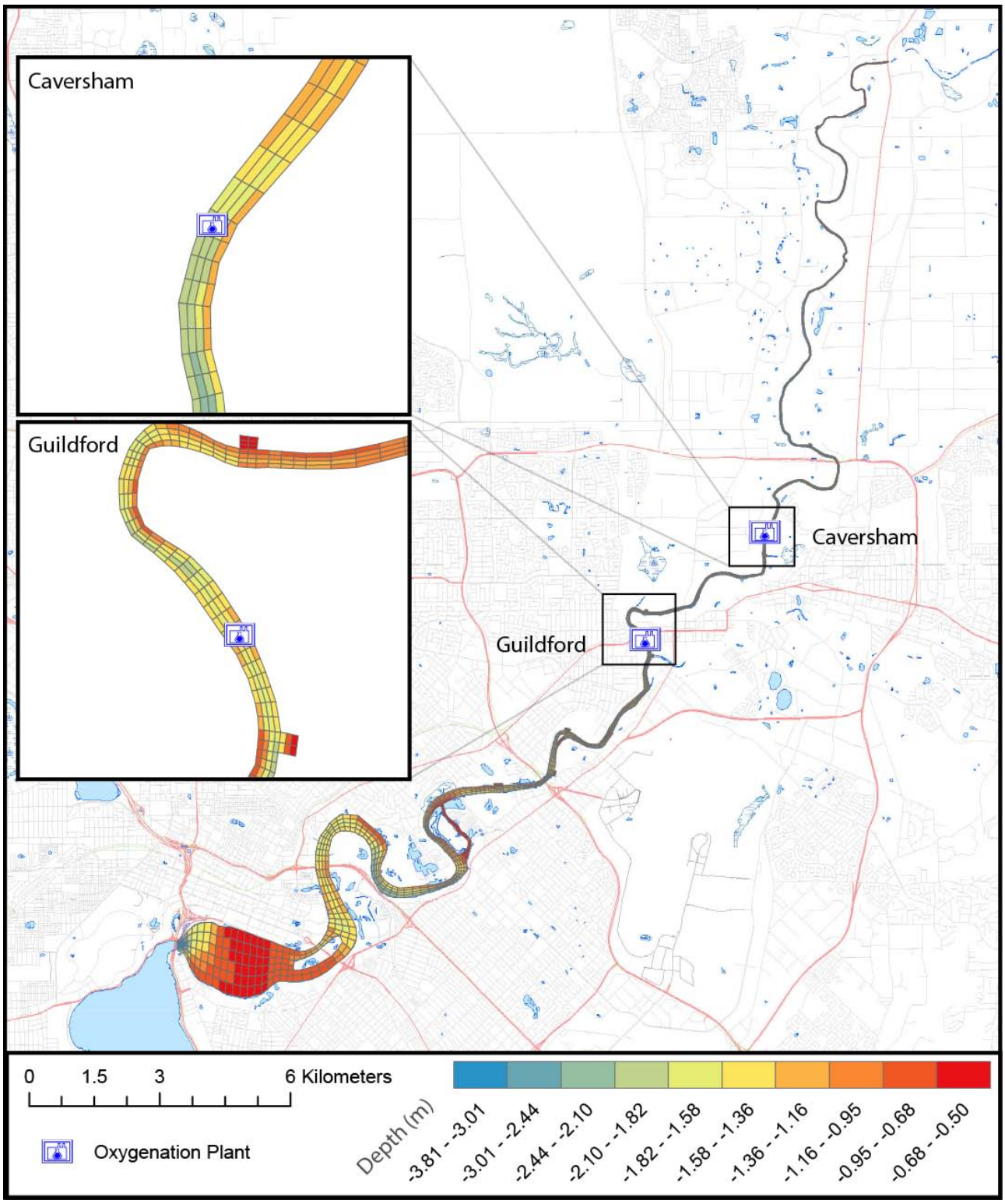

Figure 2: Upper Swan estuary computational mesh from the Narrows Bridge to Great Northern Hwy, with two zoom regions shown near the Guildford and Caversham oxygenation plants.

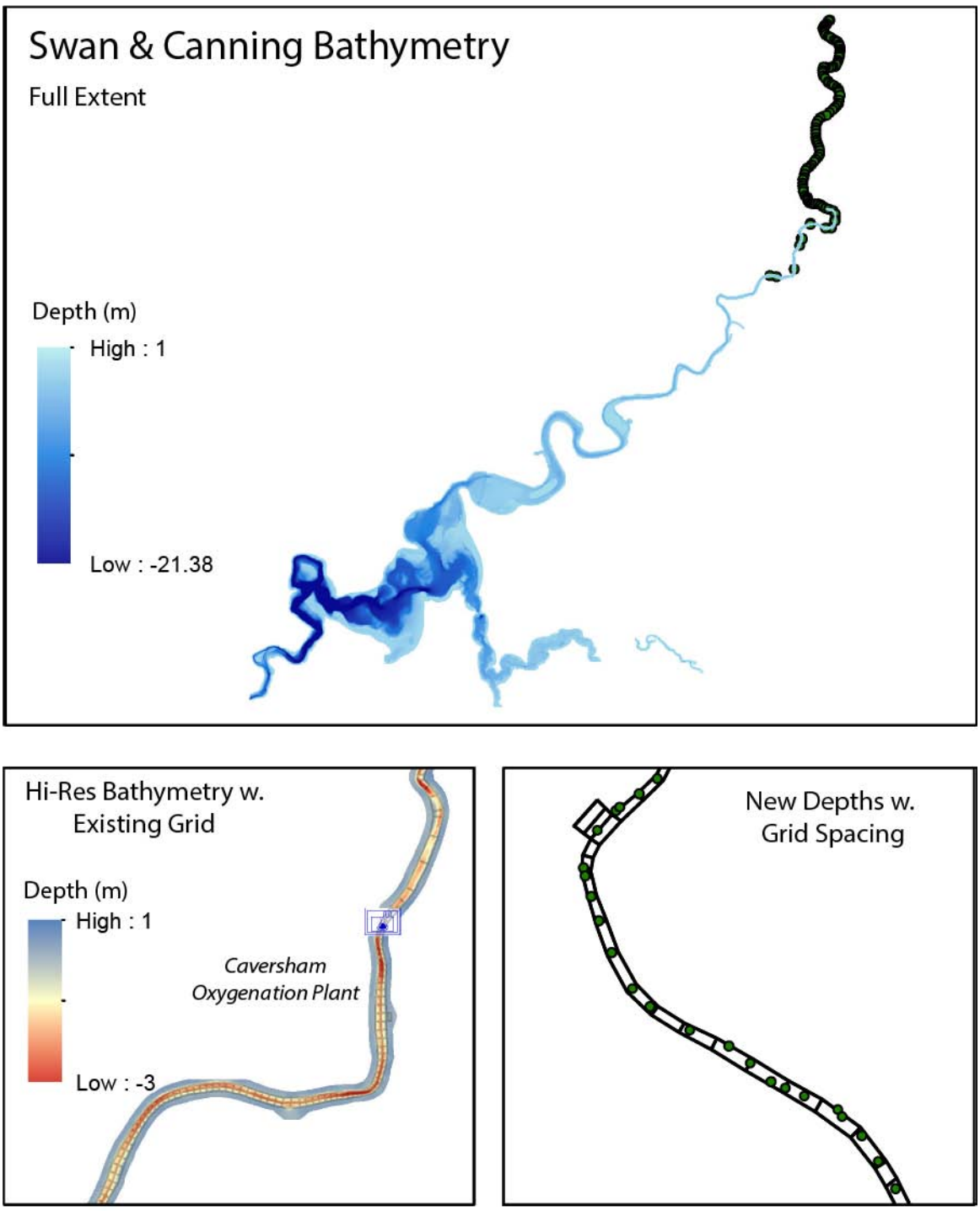

Figure 3: Image of the available bathymetric data supplied by the Department of Transport (top), and supplemented with point survey data from the region from Caversham to Great Northern Hwy.

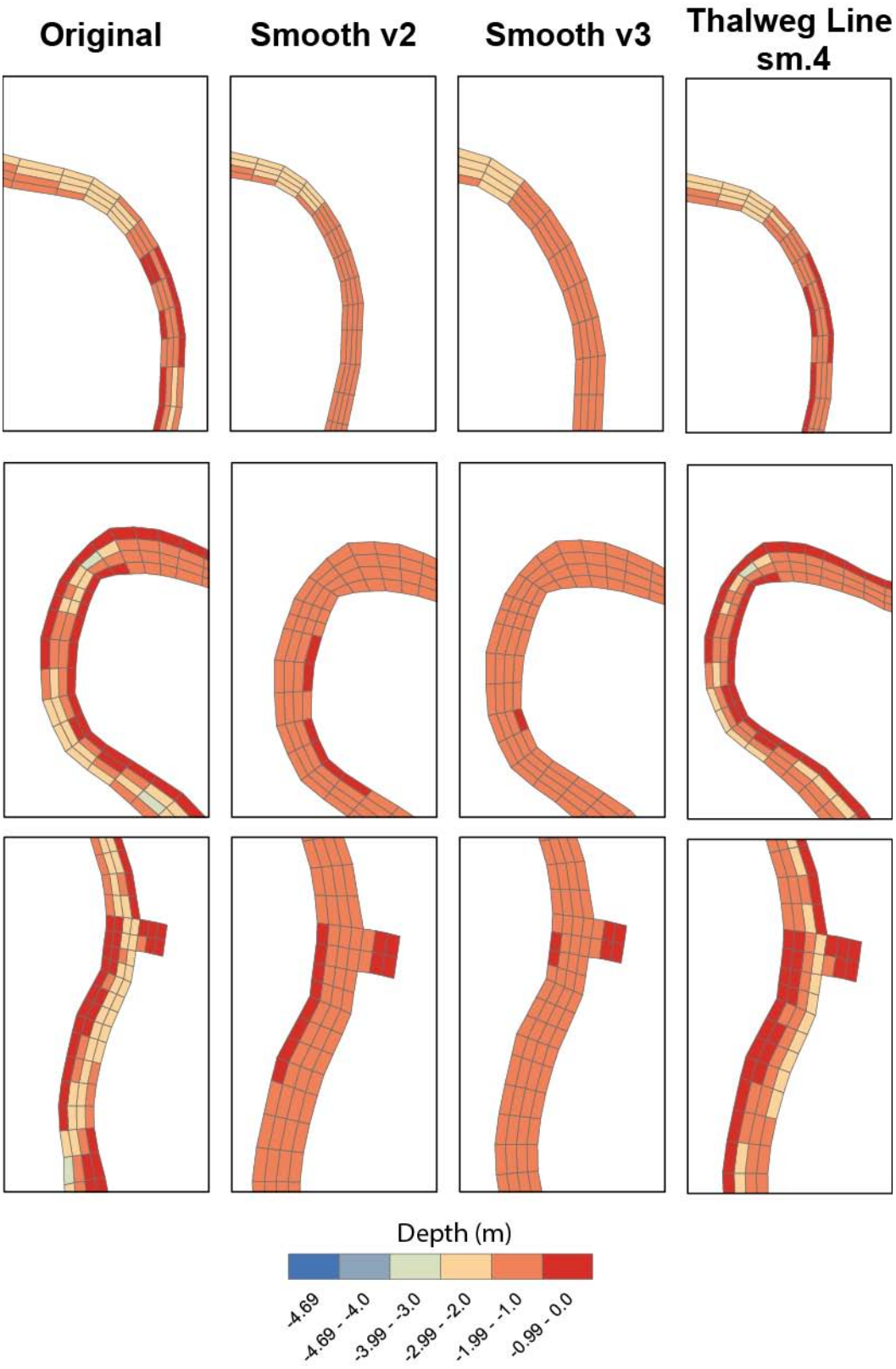

Figure 4: Example of the approach to testing the modelled salt-wedge sensitivity to the degree of bathymetric smoothing. The raw (left) grid did not propagate the salt-wedge fast enough due to rough element on the river edge, where as over-smoothing was the opposite. The best results were achieved by leaving undulations in the bottom, but passing a modest smoothing filter over the centre (thalweg) line of cells.

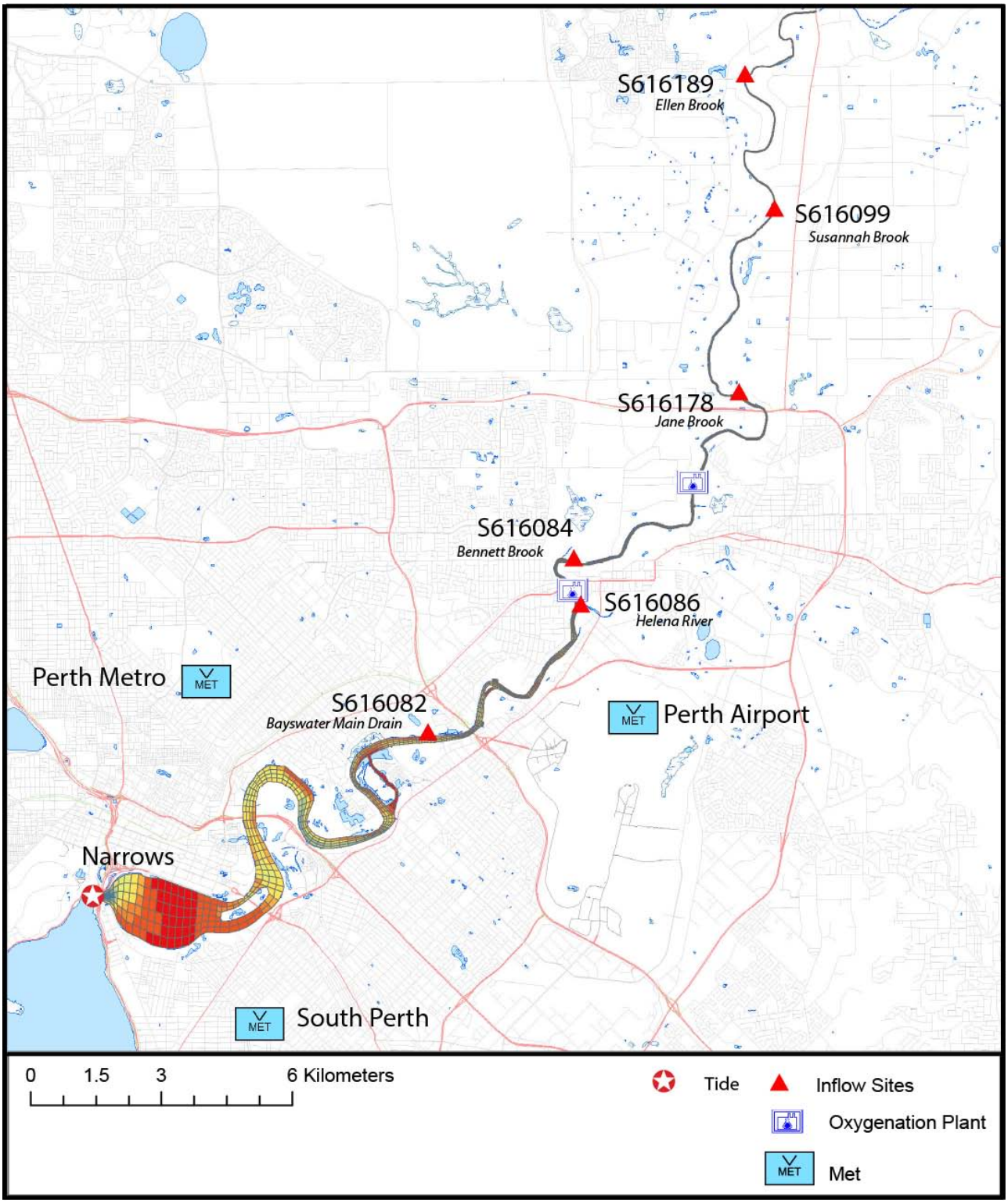

Figure 5: Location of boundary condition data points for the Upper Swan estuary model showing the six main tributary inflows and Department of Water gauge identifier, the two oxygenation plant diffuser input points, and the ocean-side open boundary tidal forcing location. Note the main inflow to the domain (S616076) is input at the top limit of the domain. Meteorological data that was considered is form the three stations shown, however, South Perth data was applied uniformly over the domain in the final simulations.

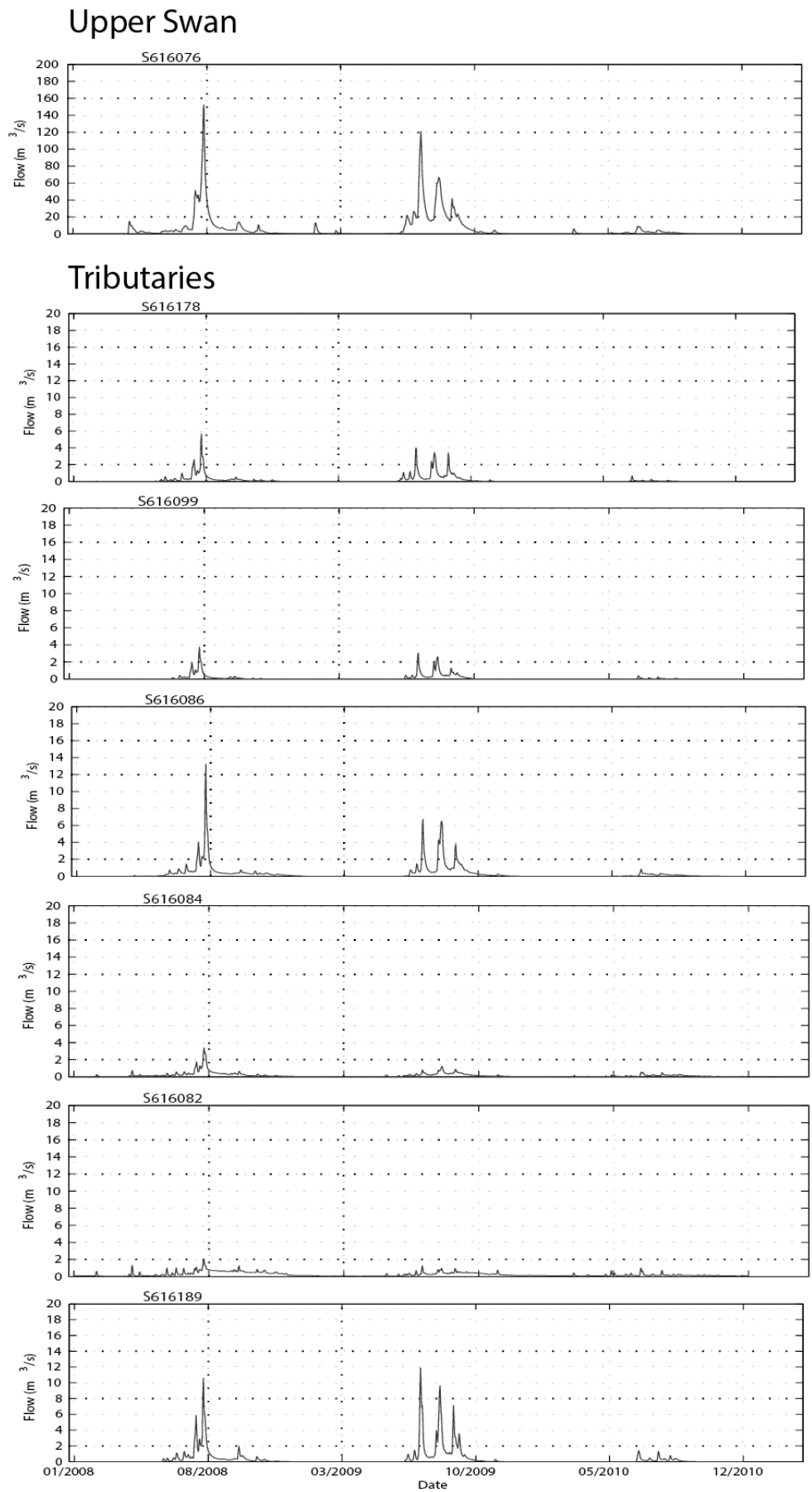

Figure 6: Inflows entering the Upper Swan estuary domain from 2008-2010 (refer to Table 10). Note the very low 2010 flows.

Model validation and assessment

Available validation data & validation approach

An extensive set of data has been collected for the Upper Swan estuary over the simulation periods as part of the weekly Swan River Trust / Department of Water monitoring program. This is conducted at 20 main regular monitoring sites (Figure 7; Table 8) at which physical and biogeochemical parameters, including both profile data and grab samples for laboratory analyses are taken. This data has been used to validate the model across the annual time-scale, both for 2008 and 2010.

Assessment of water quality models is often challenging given normal indicators like R^2 are not always a good indicator of model performance (e.g., Ahronditsis *et al.*, 2006). Here a multi-pronged validation approach was used to test the performance of the model including:

- Time series comparison at the 20 sites listed in Table 8, for both 2008 and 2010. This was conducted for:
    - Salinity
    - Temperature
    - Oxygen
    - Ammonium *(note this is presented in Appendix A)*
    - Nitrate *(note this is presented in Appendix A)*
    - Phosphate *(note this is presented in Appendix A)*
- Individual depth-profile comparison plot comparison, available for Salinity and Oxygen
- Full domain "curtain" longitudinal comparison, based on comparison of the contoured model output and contoured plots of the weekly profile data, available for Salinity and Oxygen
- Cumulative frequency distribution comparison of Oxygen in the surface and bottom waters of each site
- Seasonal transect comparisons of bottom water Oxygen
- Estuary wide total anoxic area and hypoxic area comparisons.

In addition to these regularly sampled sites, extensive profiling and other water quality data was collected at high resolution around the Guildford Oxygenation Plant in 2010 (e.g., see Figure 25). This covered several periods with snapshots around the Guildford plant in January, April and June. The model is therefore also tested against the:

- "Oxy domain" high resolution "curtain" comparison – contoured comparisons of the intensive experimental data collected periodically within 2010, available for Salinity and Oxygen.

For the time series comparisons, several error statistics were calculated. These included: NMAE, RMSE and the Nash-Sutcliffe Efficiency (NSE), and a correlation coefficient:

1) Normalised mean absolute error (NMAE):

$$NMAE = \frac{\sum_{i=1}^{N}(|P_i - O_i|)}{N\bar{O}} \quad (5)$$

2) Root mean square error (RMSE):

$$RMSE = \sqrt{\frac{\sum_{i=1}^{N}(P_i - O_i)^2}{N}} \quad (6)$$

3) Model efficiency (NSE):

$$NSE = 1 - \frac{\sum_{i=1}^{N}(P_i - O_i)^2}{\sum_{i=1}^{N}(O_i - \bar{O})^2} \quad (7)$$

4) Correlation coefficient (R)

$$R = \frac{\sum_{i=1}^{N}(P_i - \bar{P})(O_i - \bar{O})}{\left[\sum_{i=1}^{N}(P_i - \bar{P})^2 \sum_{i=1}^{N}(O_i - \bar{O})^2\right]^{1/2}} \quad (8)$$

where N is the number of observations, O_i and P_i, the "i^{th}" observed and model predicted data and $\bar{O}$ and $\bar{P}$ the mean observed and model predicted data respectively. Ahronditsis and Brett (2004) highlight that different metrics are appropriate for assessing different aspects of model behaviour and give typical values reported in aquatic system modelling publications. For example, a model can have a poor R^2 but also a very low MAE or RMSE. Efficiency metrics like NSE are useful to explain whether the model is able to capture the variance in the data more than simply assuming the average of the data. During our calibration of the model we considered all four metrics, reporting the R^2 and MAE below.

Table 8: Validation sites adopted in the Upper Swan estuary domain, indicating their UTM location, and the focus sites presented in the below validation time-series plots (denoted A-J).
Note data from all 20 sites were used in curtain comparisons.

Station number	SiteID	Name	X	Y	Time series panel ID
1	NAR	Narrows Bridge	391215	6463014	
2	NIL	Nile Street	394660	6464027	A
3	STJ	St John's Hospital	397308	6464439	B
4	MAY	Maylands Pool	396801	6465716	C
5	RON	Ron Courtney Island	399802	6467786	D
6	BWR10	Sandy Beach	400826	6467654	
7	KIN	Kingsley	401768	6468783	E
8	KMO	Kings Meadow Oval	401966	6469695	F
9	VIT	Vitox Plant	401818	6470125	
10	SUC	Success Hill	401585	6470349	G
11	MEA	Meadow Street Bridge	402739	6470849	
12	LLH	Lilac Hill	403082	6471153	
13	WMP	West Midland Pool	404439	6471549	H
14	SCS01	Black Adder Creek	404596	6471992	
15	WBRP	Woodbridge Riverside Park	404598	6472300	
16	CAV	Caversham	404634	6472665	I
17	REG	Reg Bond Park	404894	6473496	
18	MSB	Middle Swan Bridge	406263	6474166	J
19	JBC	Jane Brook confluence	405656	6474493	
20	POL	Power line crossing	404979	6475053	

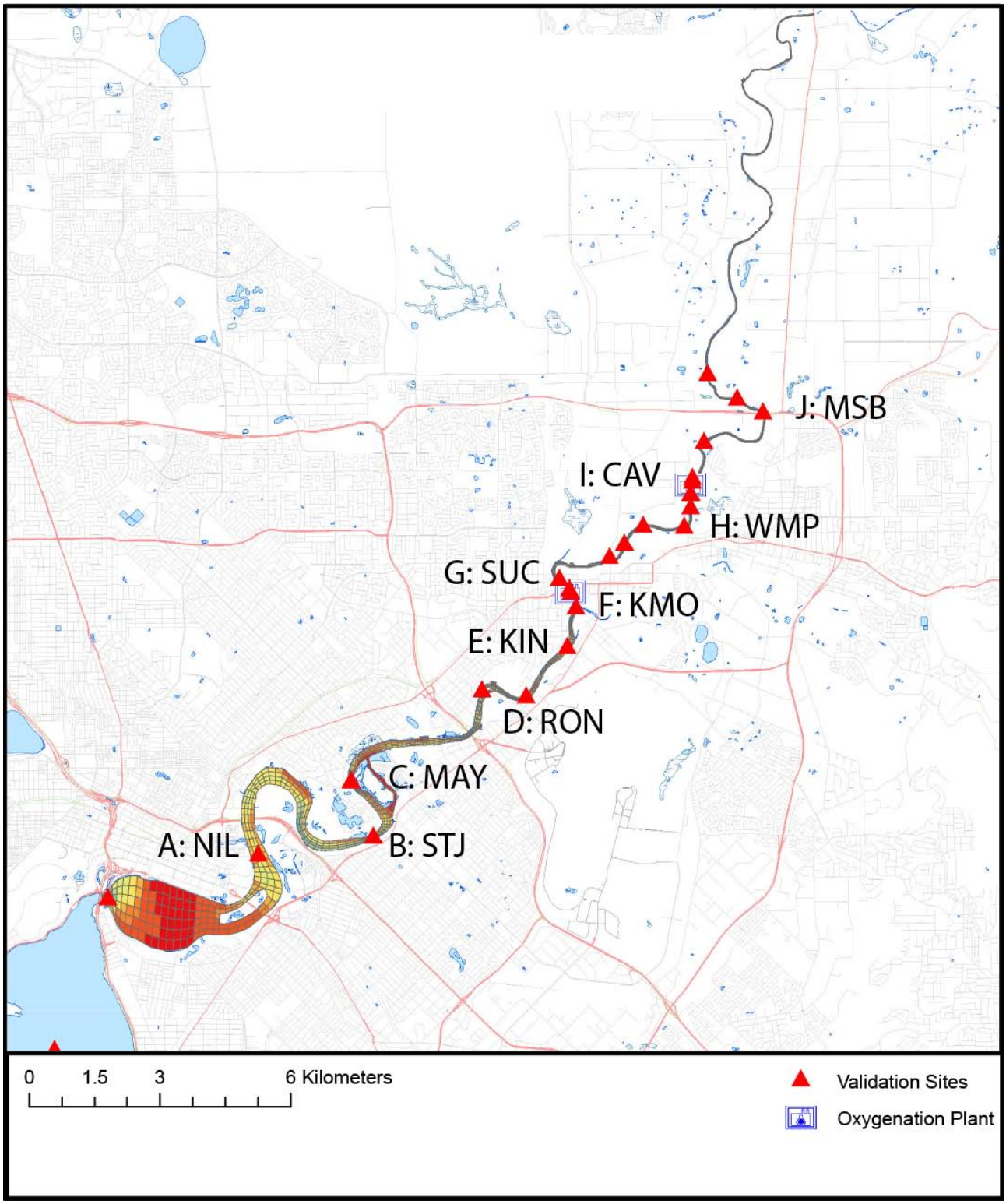

Figure 7: Upper Swan estuary domain showing the 20 validation sites used, with labels for the 10 reported on in the below validation plots (A-J).

Large-scale estuary validation

Salinity:

Comparison of the modelled and observed surface and bottom salinity is shown in Figure 8 for 2008 and Figure 9 for 2010. In general terms the salt-wedge is very well predicted up to CAV, with the model accurately capturing the horizontal variation in salinity in addition to the differences between the surface and bottom waters during small and large flow events.

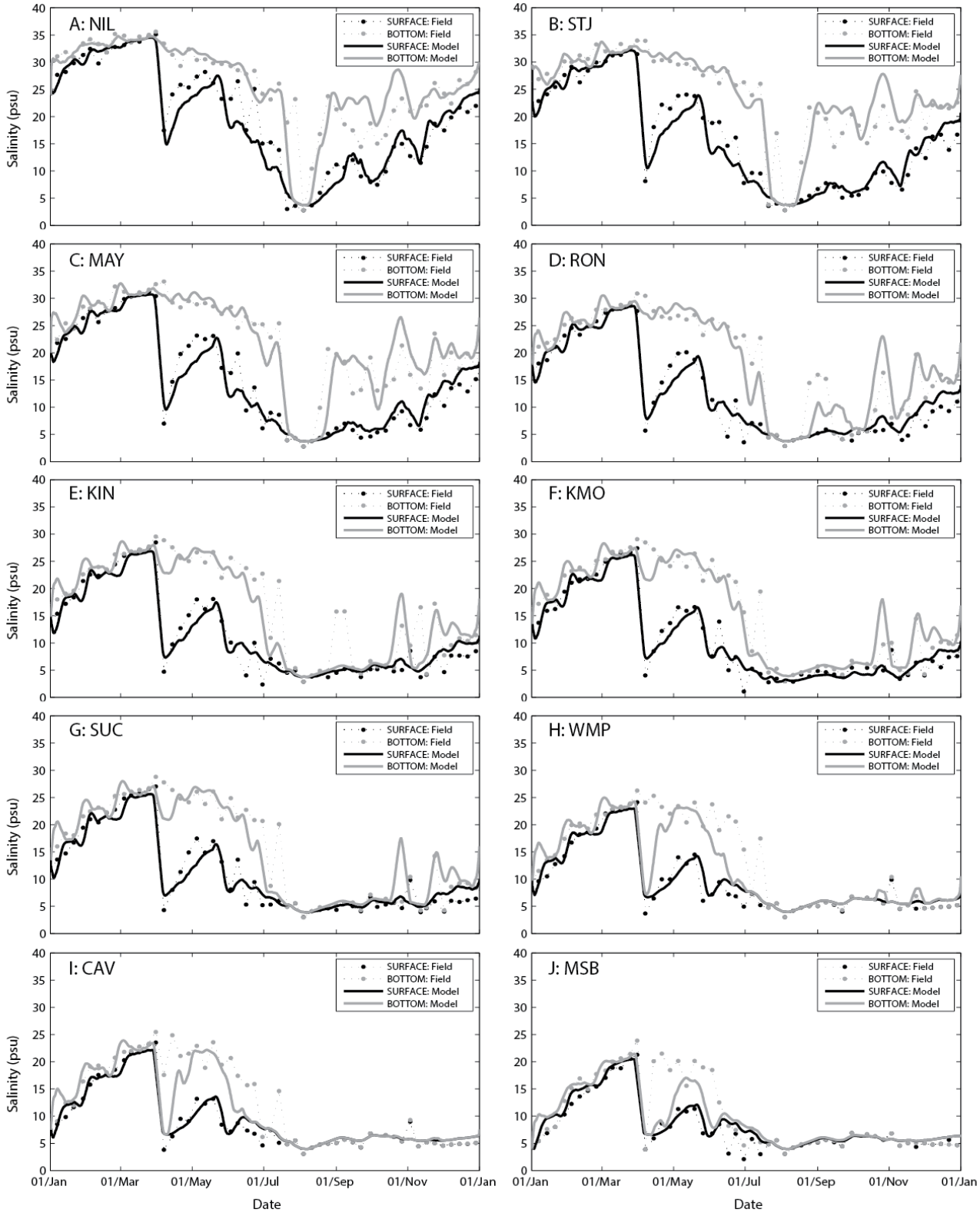

Figure 8: Upper Swan estuary salinity (psu) for the year 2008 comparing simulated and observed values at 10 sites, labelled A-J.

The model uses the same parameters and grid for both the 2008 (wet) and 2010 (dry) simulations, and confidently predicts the dynamics in both these years. The R^2 values for salinity (Figures 10-11, Table 9) vary between 0.85-0.95, with Nash-Sutcliffe efficiency (NSE) parameters of ~0.95 indicating a very high level of agreement.

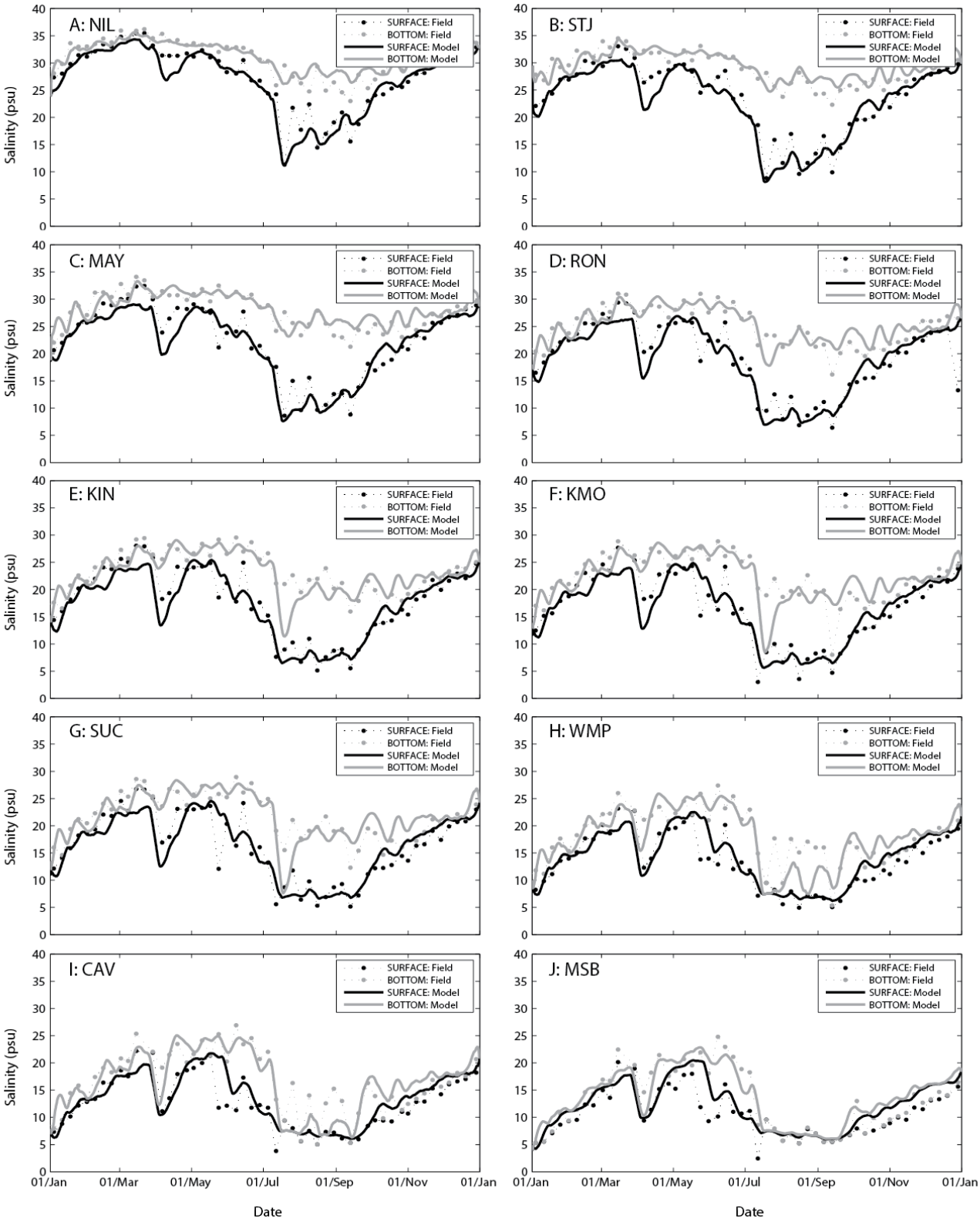

Figure 9: Upper Swan estuary salinity (psu) for the year 2010 comparing simulated and observed values at 10 sites, labelled A-J.

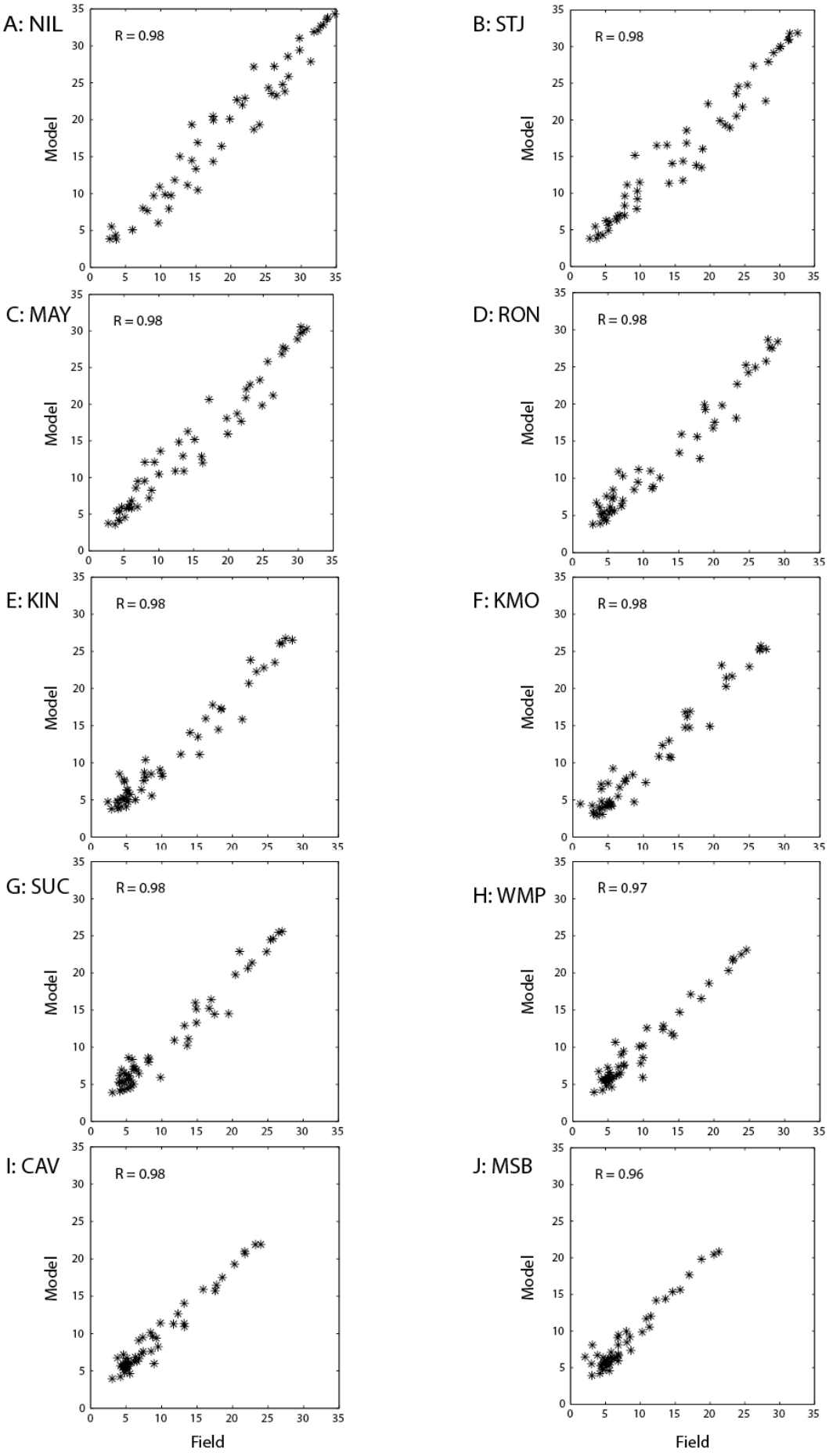

Figure 10: Scatter plot comparison of simulated versus observed salinity for several stations for 2008.

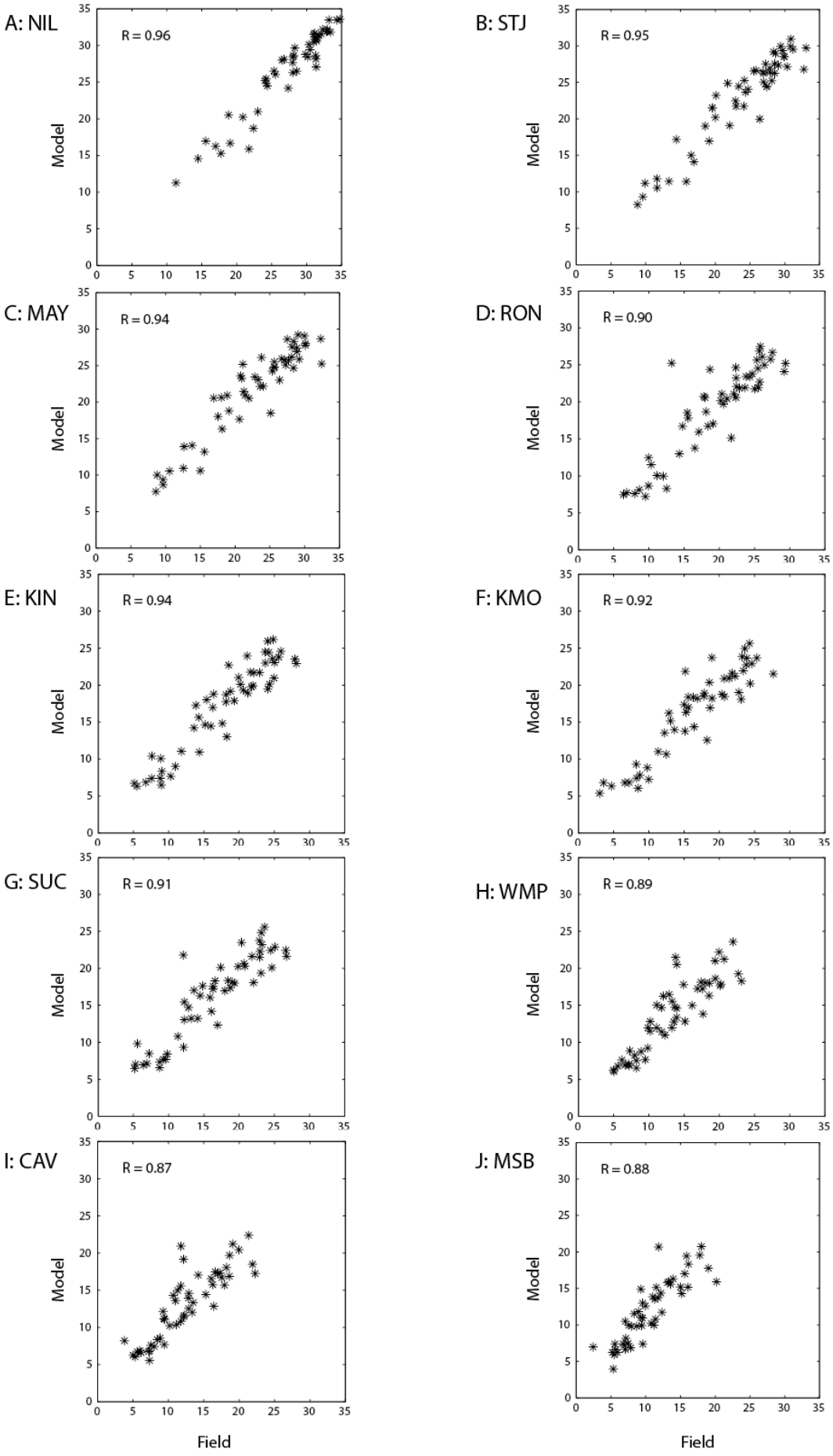

Figure 11: Scatter plot comparison of simulated versus observed salinity for several stations for 2010.

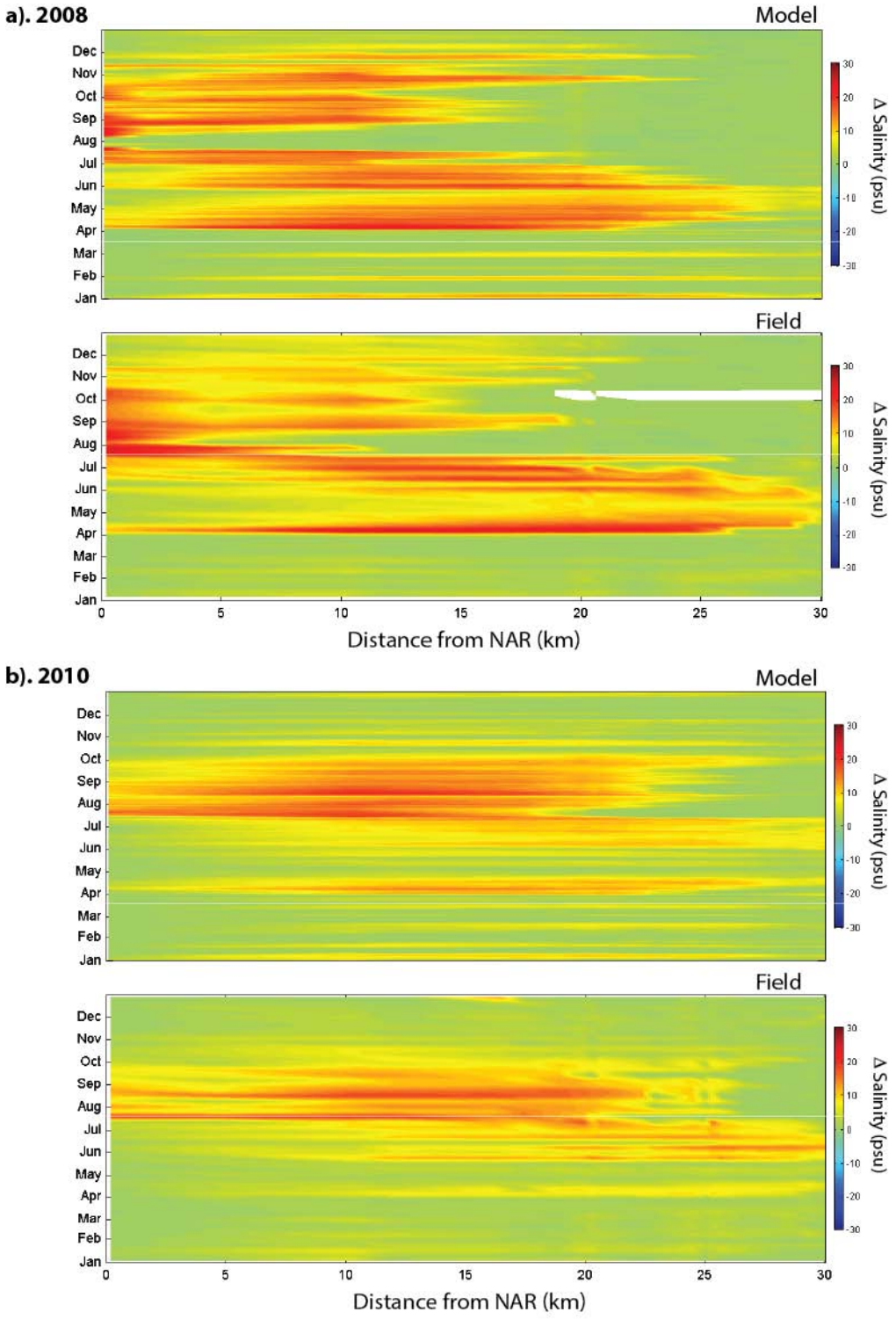

Figure 12: Degree of salinity stratification (ΔSalinity = bottom – surface; psu) compared along the estuary (x-axis) versus time (y-axis) for: a) 2008 and b) 2010 model output (top panel) and observed data (bottom panel). The field data is interpolated between the 20 profiling locations in Table 8 prior to enable plotting.

A time-distance plot of modelled and observed stratification strength and extent (Figure 12) gives a good visual guide of model performance at capturing the salt-wedge, and how the different patterns seen in the estuary in the two years.

The longitudinal sections of salinity from interpolated field data and equivalent model output for 2008 show monthly changes in the state of the estuary and nature of the salt-wedge (Figure 13). The model performance here is further demonstrated since not only is the horizontal pattern well reproduced, but also the shape of the salt-wedge and shape

of the vertical variation is accurately captured, with limited to no evidence of problems with vertical numerical diffusion of the bottom salinity into the surface layer. Despite the overall good performance of the model in reproducing the salinity structure, the model appears to misplace the upstream position of the main salinity front during April and May (seen also in the time-series plot (Figure 8). The mismatch is not accompanied by evidence of excessive diffusion of the front, and it is likely the result of inaccuracies in the tributary water inputs and/or tidal propagation.

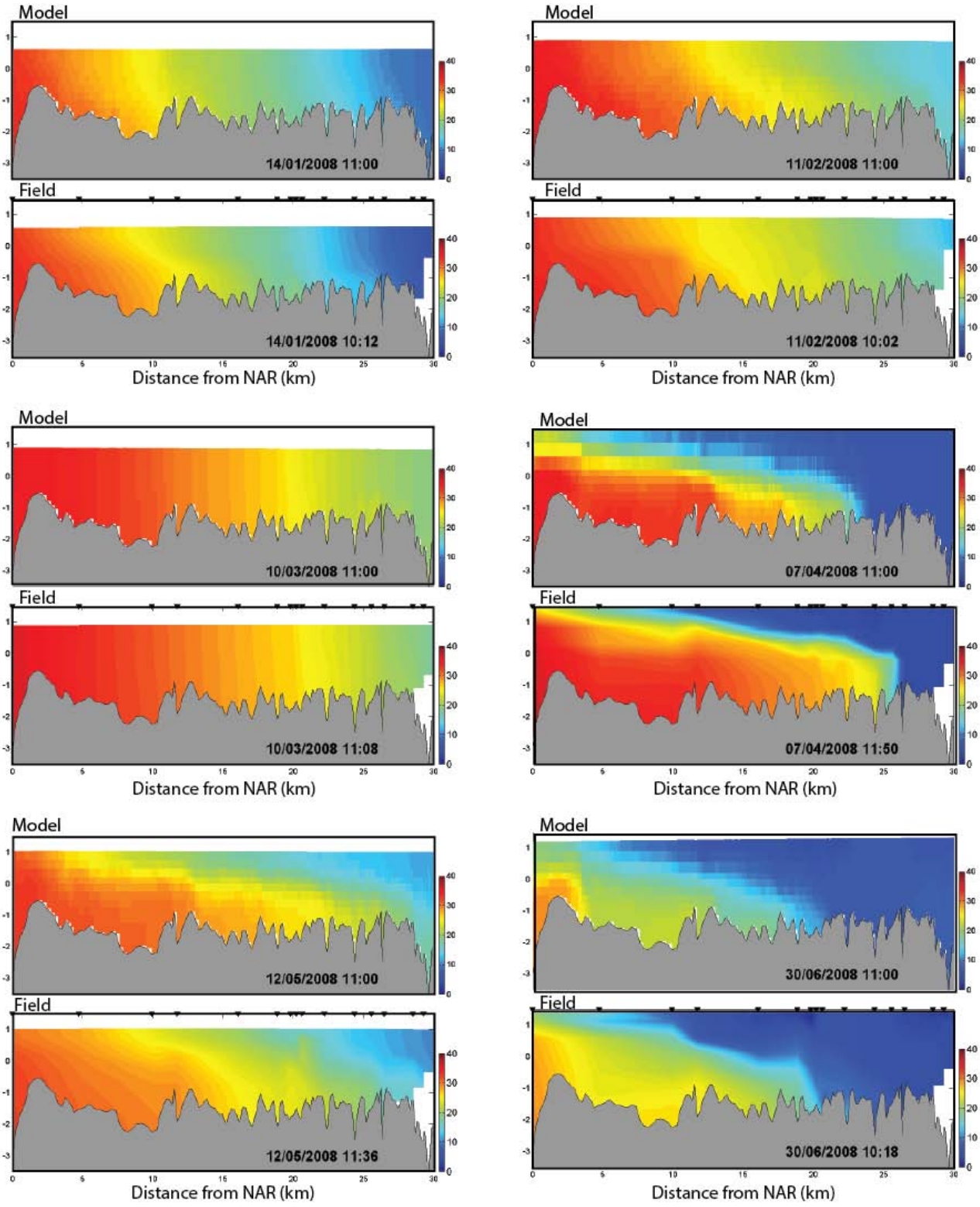

Figure 13a: Cross-section ('curtain') plots showing depth variation (y-axis, m AHD) of salinity (psu) along the centre of the estuary (x-axis, distance upstream from NAR in km). Plots are comparing modelled and observed salinity for several monthly snapshots (January-June 2008). The field plots are based on a linear contouring around the 20 profile data points (Table 8), identified as triangles on the water surface.

Given capturing the spatial and temporal evolution of the salinity structure of the estuary is essential for accurate simulation of oxygen and nutrients, the results presented demonstrate the model is fit-for-purpose for the investigation from a hydrodynamic point of view.

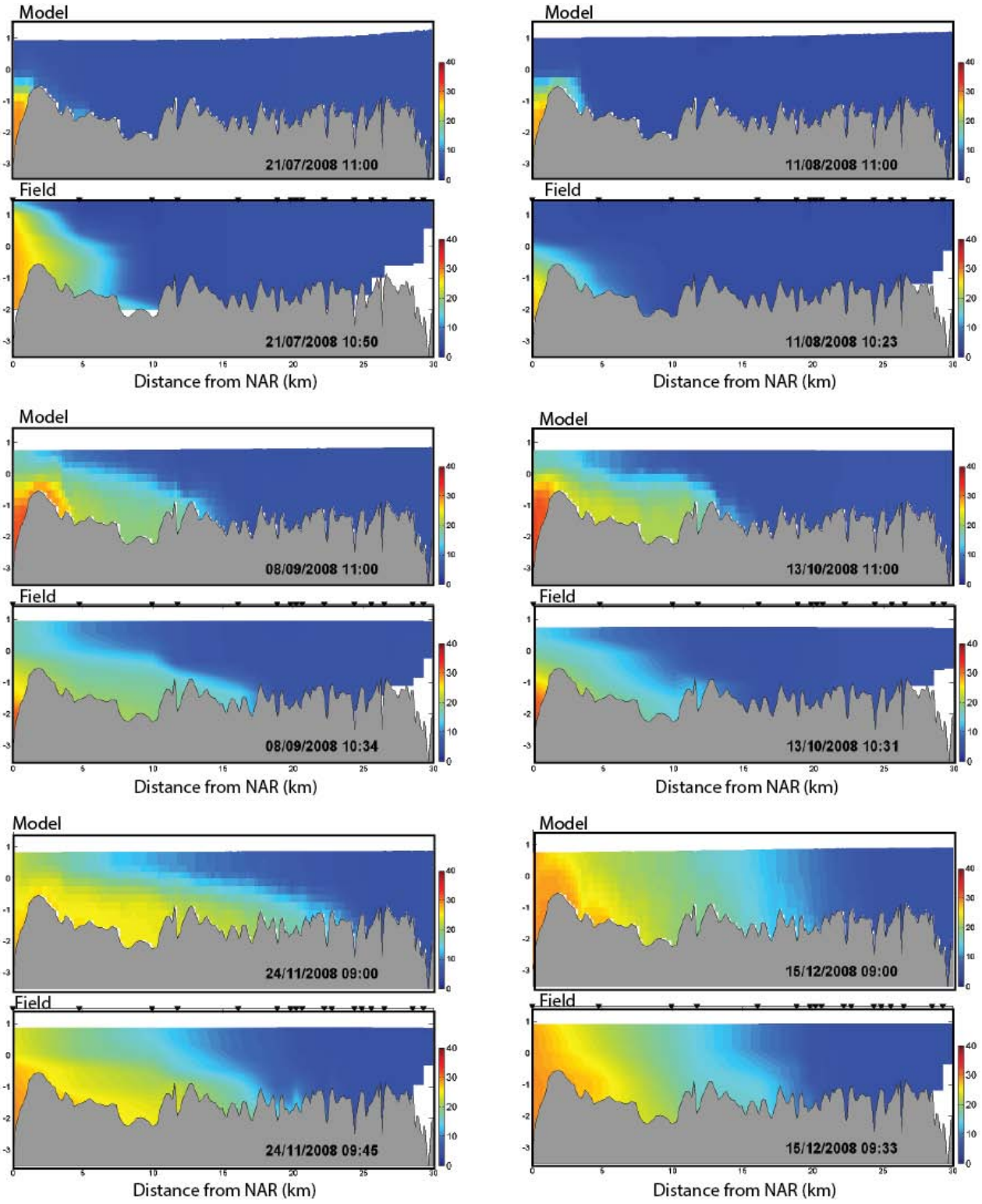

Figure 13b: Cross-section ('curtain') plots showing depth variation (y-axis, m AHD) of salinity (psu) along the centre of the estuary (x-axis, distance upstream from NAR in km). Plots are comparing modelled and observed salinity for several monthly snapshots (July-December 2008). The field plots are based on a linear contouring around the 20 profile data points (Table 8), identified as triangles on the water surface.

Temperature:

The comparison of surface and bottom temperature for 2008 (Figure 14) and 2010 (Figure 15) demonstrate the seasonal variation and the relatively minor differences between the surface and bottom waters. On average the R^2 for temperature is ~0.9 with a mean error of ~1.1°C (Table 9), with a general tendency for overheating of the bottom waters during the periods of lower flows.

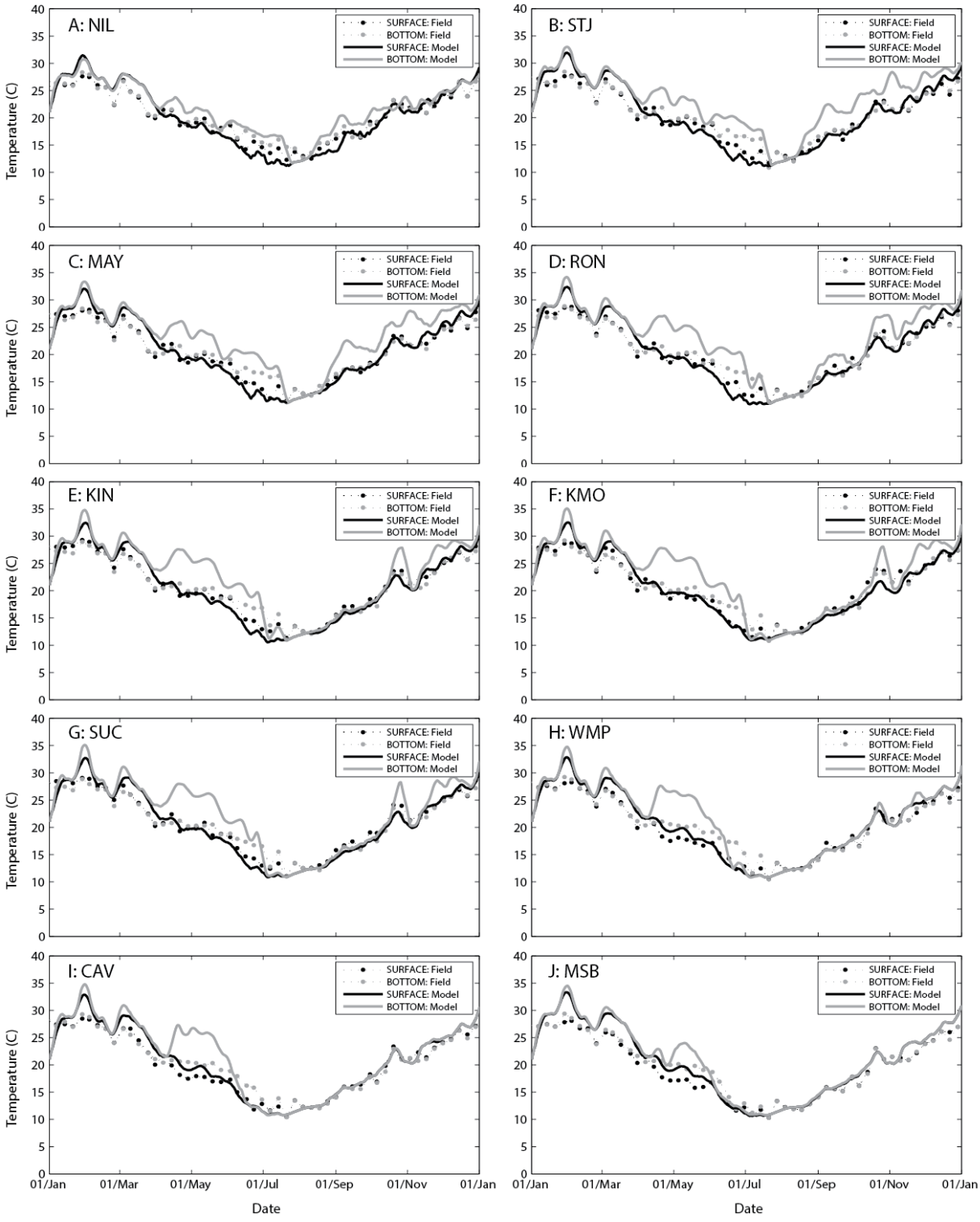

Figure 14: Upper Swan estuary temperature (°C) for the year 2008 comparing simulated and observed values at 10 sites, labelled A-J.

The errors in the temperature simulation are likely due to simplifications made in specification of surface meteorological forcing, including lack of long-wave radiation data, and inflow temperature estimates. Minor adjustments (scaling factors) were made to the available wind speed data and solar radiation data to give the best possible temperature, since oxygen solubility is tightly linked to water column temperature and salinity.

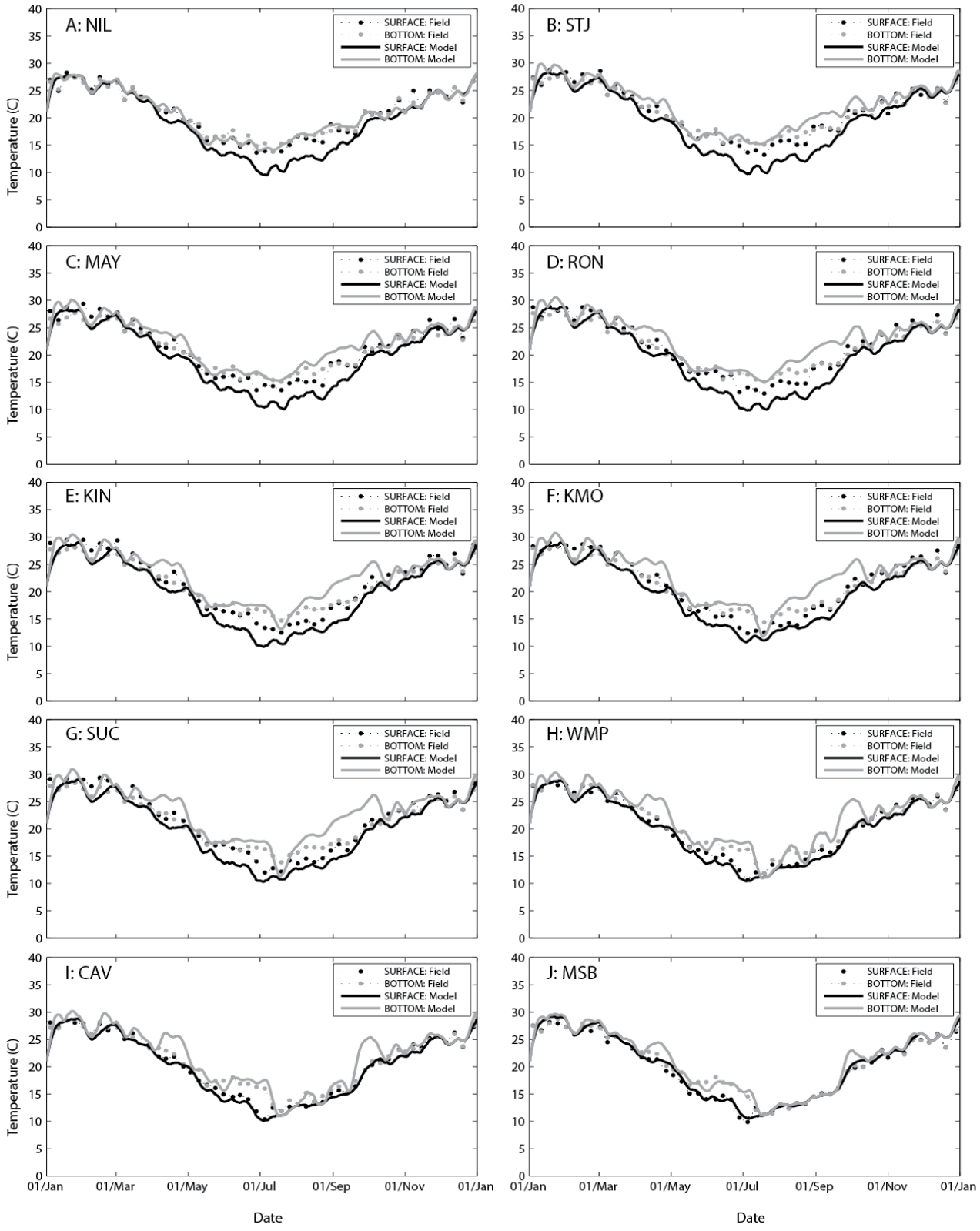

Figure 15: Upper Swan Estuary temperature (°C) for the year 2010 comparing simulated and observed values at 10 sites, labelled A-J.

Oxygen:

Time-series comparisons of oxygen concentrations for 2008 (Figure 16) and 2010 (Figure 17) demonstrate that the model captures the significant spatial and seasonal variability and differences between the two years. In 2008 the moderate autumn flows led to long periods of hypoxia, which were then replaced by well-mixed conditions in winter and the recovery of the low bottom-water oxygen in the upper river during the autumn coincides with a break-down in the salinity stratification.

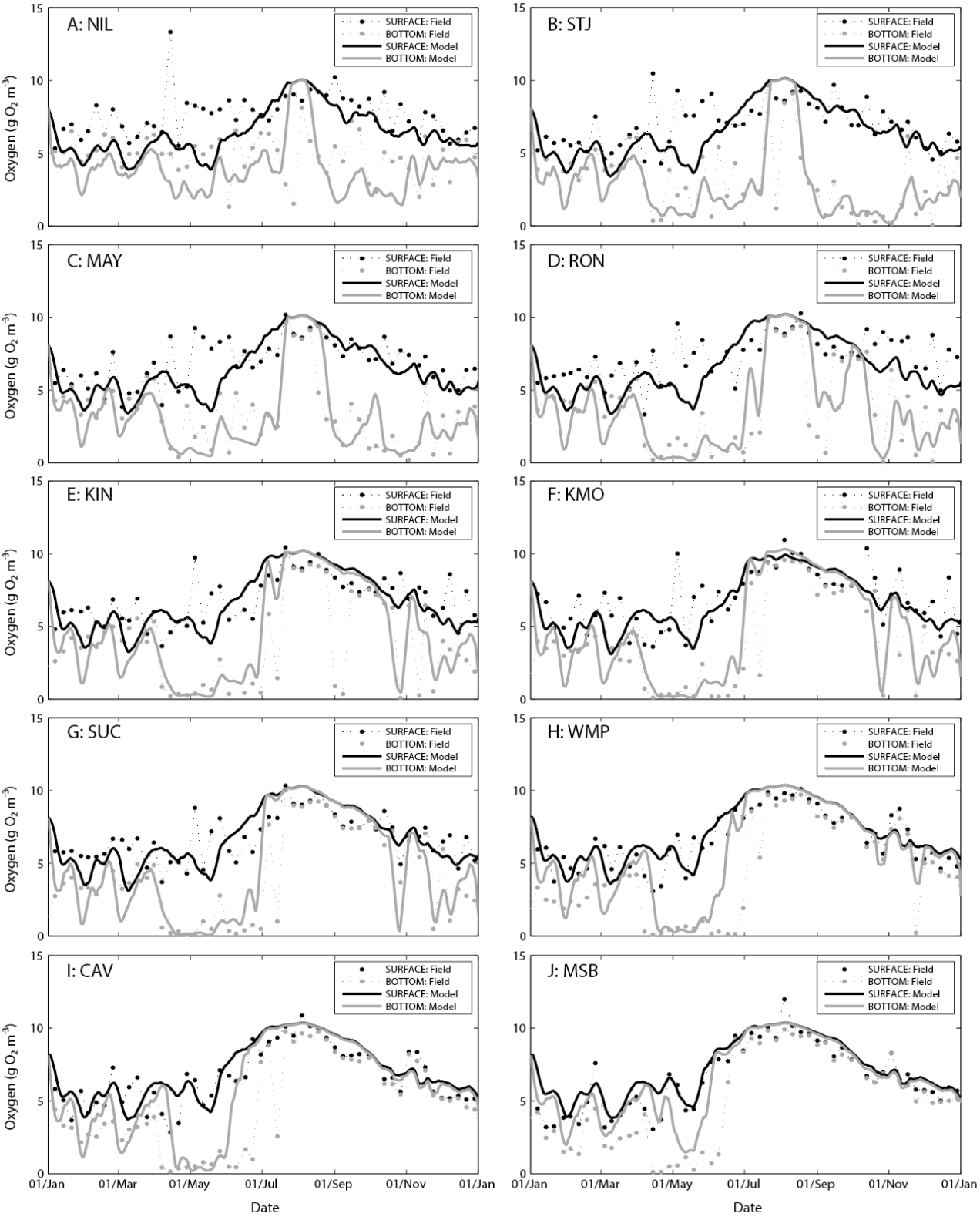

Figure 16: Upper Swan Estuary dissolved oxygen concentration (g O_2 m^{-3}) for the year 2008 comparing simulated and observed values at 10 sites, labelled A-J.

In 2010 the lower flows persisted all year and created a different pattern; the signal is also complicated by occasional operation of the Guildford oxygenation plant during the months Jan to July. Overall the model predictions capture the seasonal changes well and the changes in both the surface and bottom waters. Higher R^2 values were recorded in 2008 (Figure 18) due to the much larger month-to-month variability in 2010 (Figure 19) making the point comparisons less effective. The data suggest the phytoplankton in 2010 (not shown) played a more influential role in surface O_2 than in 2008, with very high values in the warm months. Nonetheless, the essential features in both years are captured and the model has a MAE of 20-25%, which is considered to be very high level of model performance for biogeochemical variables in estuarine systems (e.g., Ahronditsis and Brett, 2004).

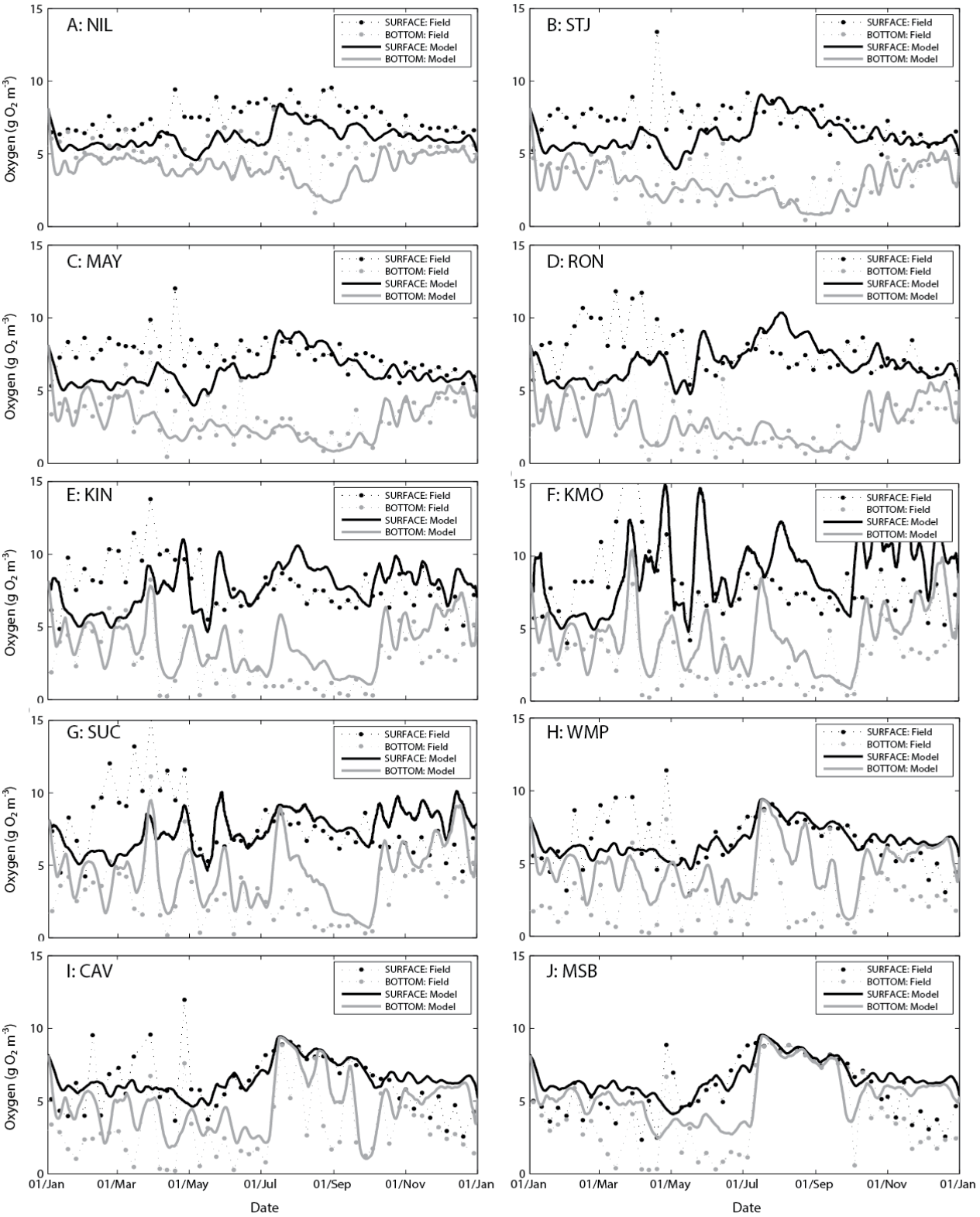

Figure 17: Upper Swan Estuary dissolved oxygen concentration (g O_2 m^{-3}) for the year 2010 comparing simulated and observed values at 10 sites, labelled A-J.

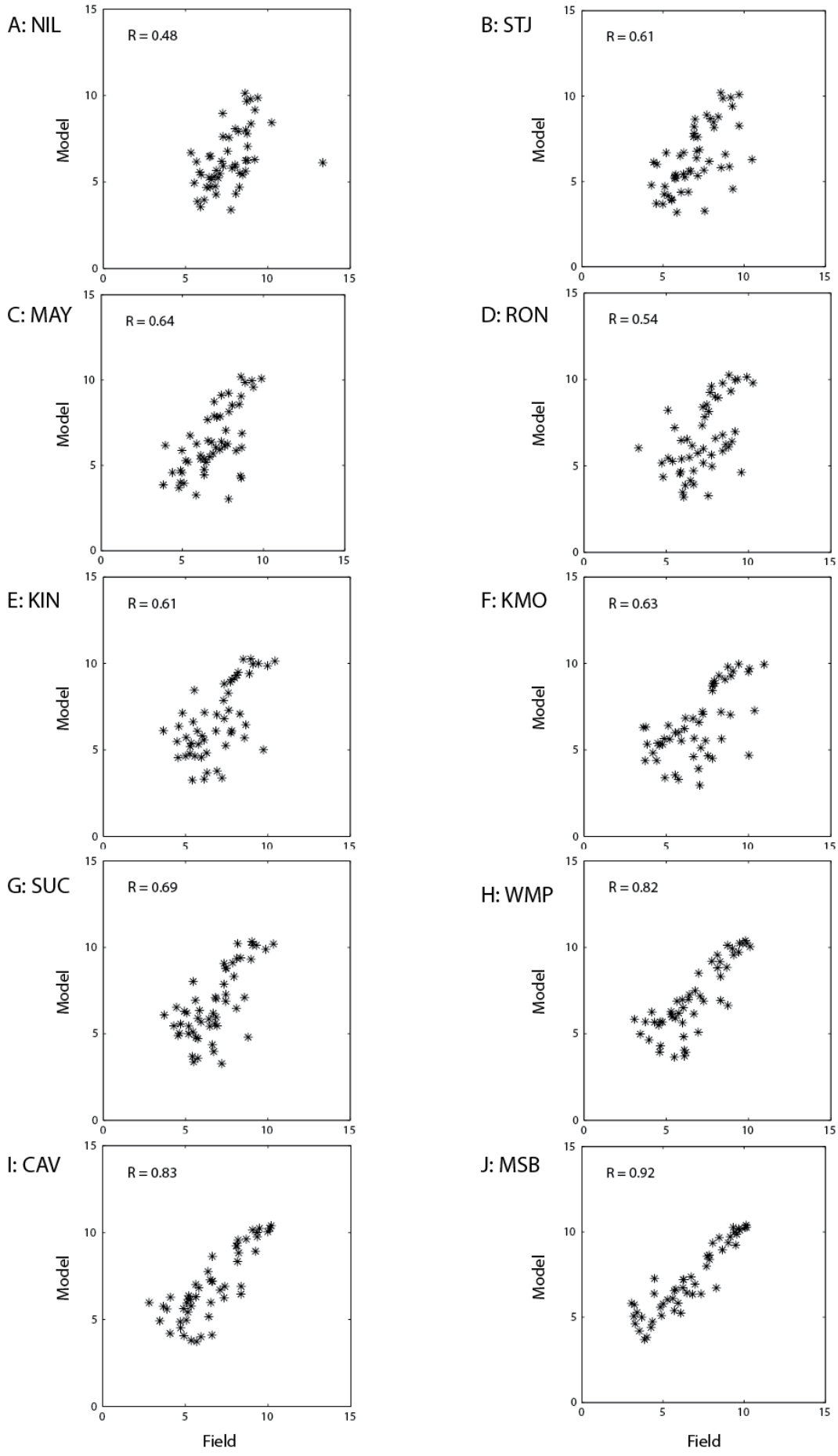

Figure 18: Scatter plot comparison of simulated versus observed dissolved oxygen in 2008 at 10 sites, labelled A-J.

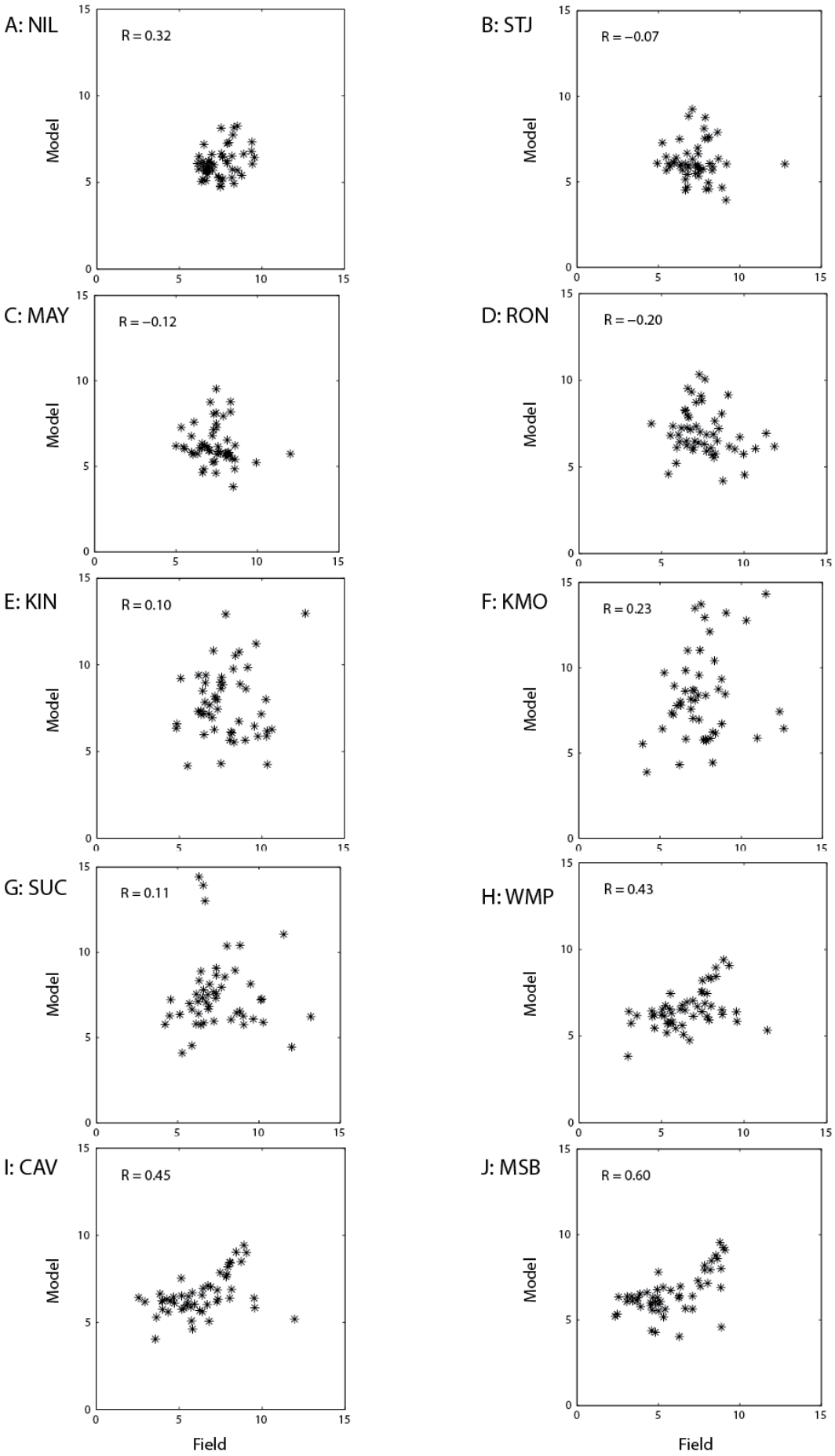

Figure 19: Scatter plot comparison of simulated versus observed dissolved oxygen in 2010 at 10 sites, labelled A-J.

For the oxygen comparison, the assessment of time-series and correlation coefficient is not always the best indicator of model performance and so to further assess if the model is fit for purpose several support analyses are also developed. First, cumulative frequency distribution plots highlight the range and likelihood of certain conditions being experienced; this is shown for the 10 stations for 2008 (Figure 20) and 2010 (Figure 21).

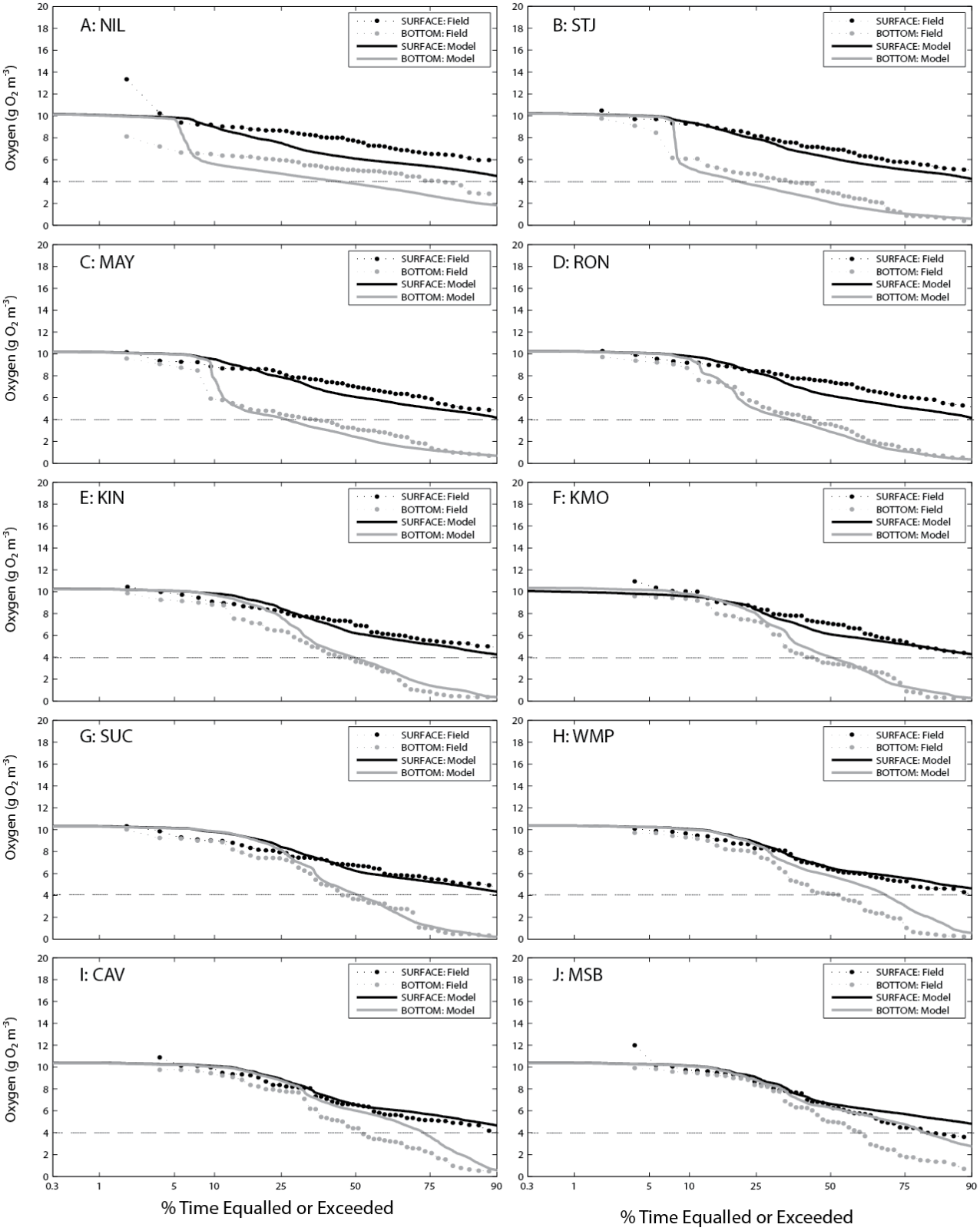

Figure 20: Cumulative frequency distribution (%) of simulated and observed dissolved oxygen (g O_2 m^{-3}) for several stations (A-J) in 2008.

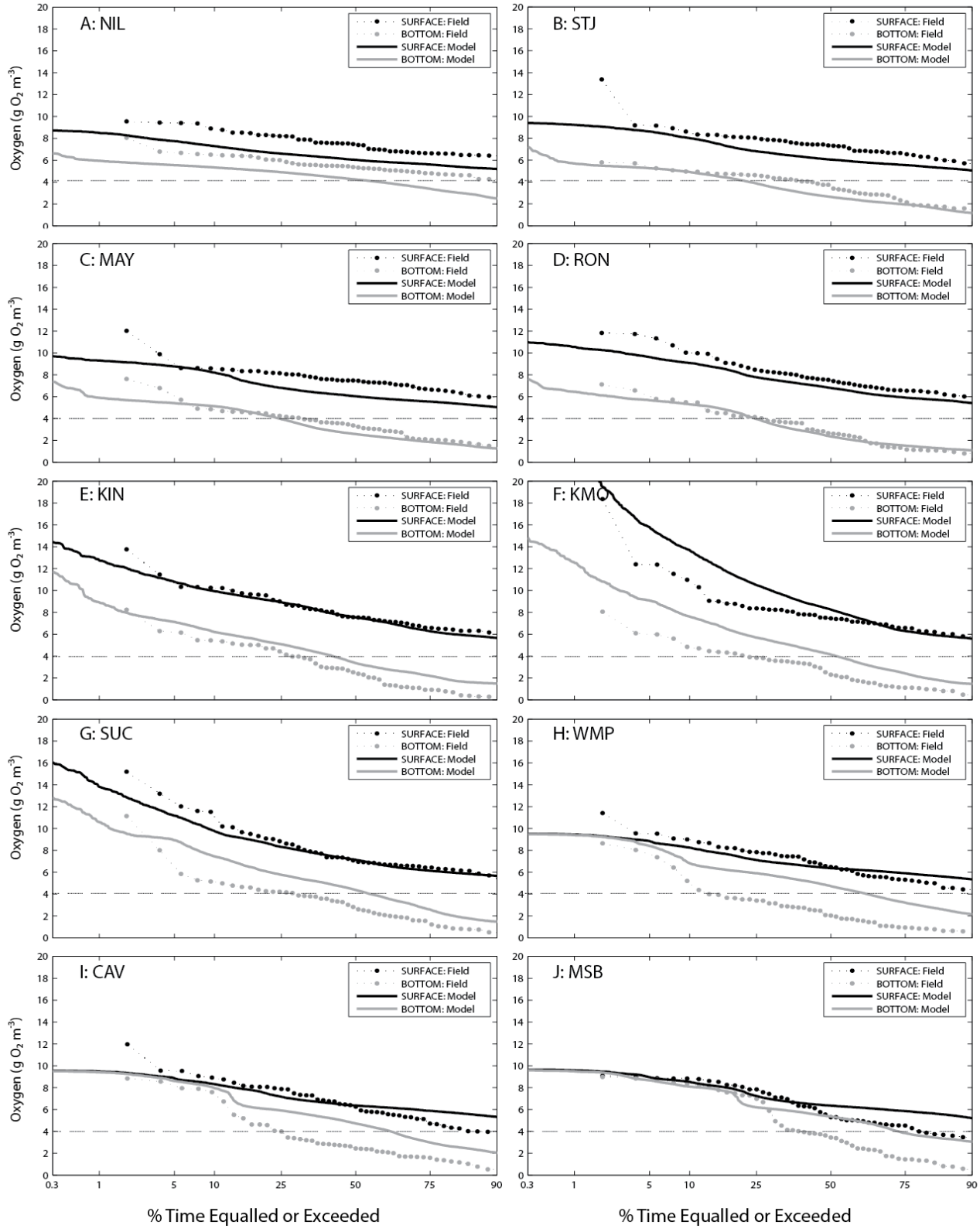

Figure 21: Cumulative frequency distribution (%) of simulated and observed dissolved oxygen (mg O_2 L^{-1}) for several stations (A-J) in 2010.

Bearing in mind the non-uniform exceedance scale on these plots (which amplifies the relatively infrequent portion of the distribution), the model demonstrates a high level of similarity at most sites, highlighting the model accurately captures the range of spatio-temporal variability in the data. This analysis makes clear a notable over-prediction of the bottom water in the most upstream stations (WMP, CAV and MSB) by 1 – 2 g O_2 m^{-3}. Nonetheless, the spatio-temporal

extent of the periods of oxygen stratification were well predicted, with a slight under-prediction noted in 2010 (Figure 22).

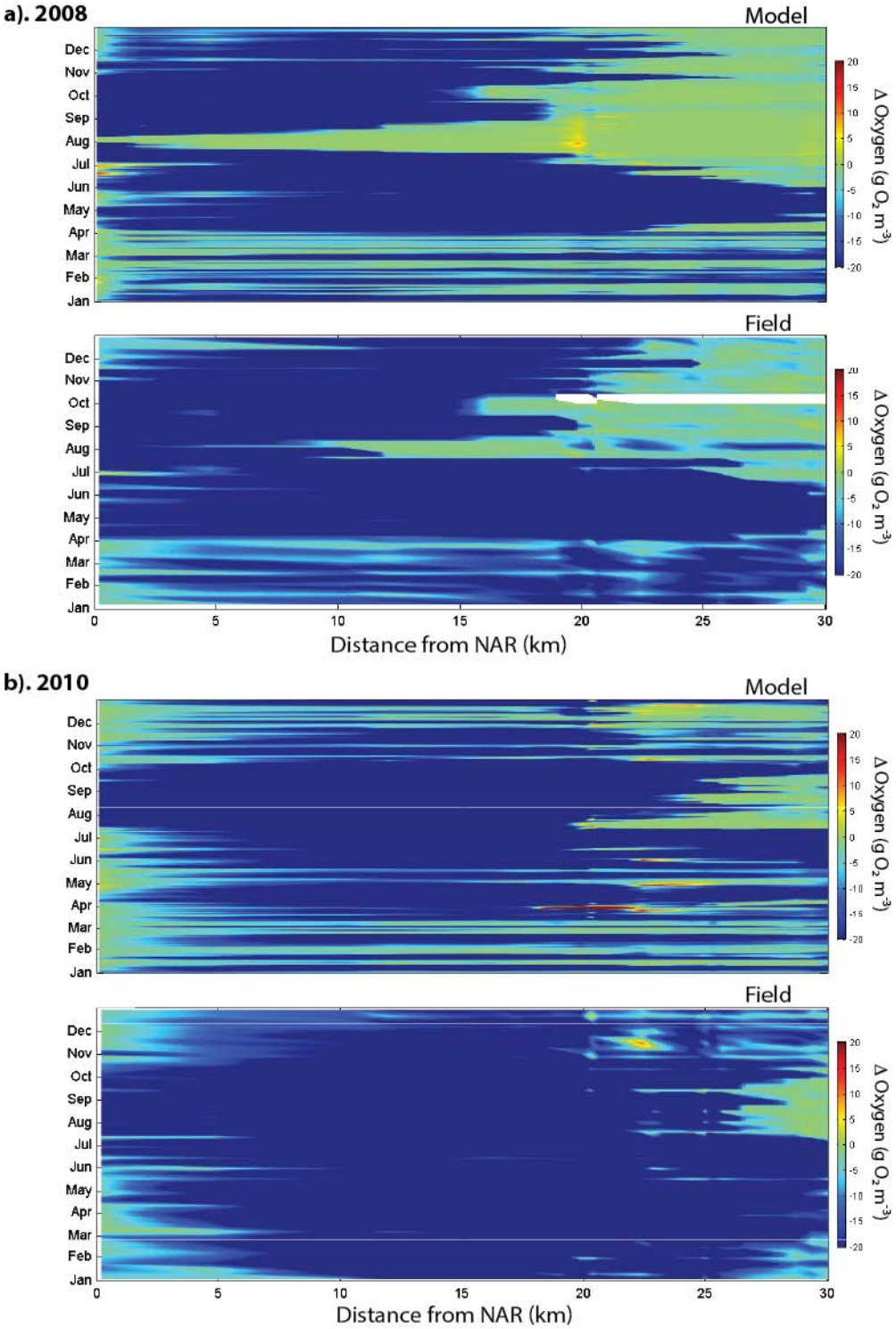

Figure 22: Degree of oxygen stratification (ΔOxygen = bottom – surface; mg O_2 L^{-1}) compared along the estuary (x-axis) versus time (y-axis) for: a) 2008 and b) 2010 model output (top panel) and observed data (bottom panel). The field data is interpolated between the 20 profiling locations in Table 8 prior to enable plotting.

The nature of the oxygen stratification is tightly linked to the salt-wedge and flow characteristics, with the longitudinal transect comparisons demonstrating fairly accurate reproduction of the vertical profiles of oxygen along the length of the estuary (Figure 23a & b).

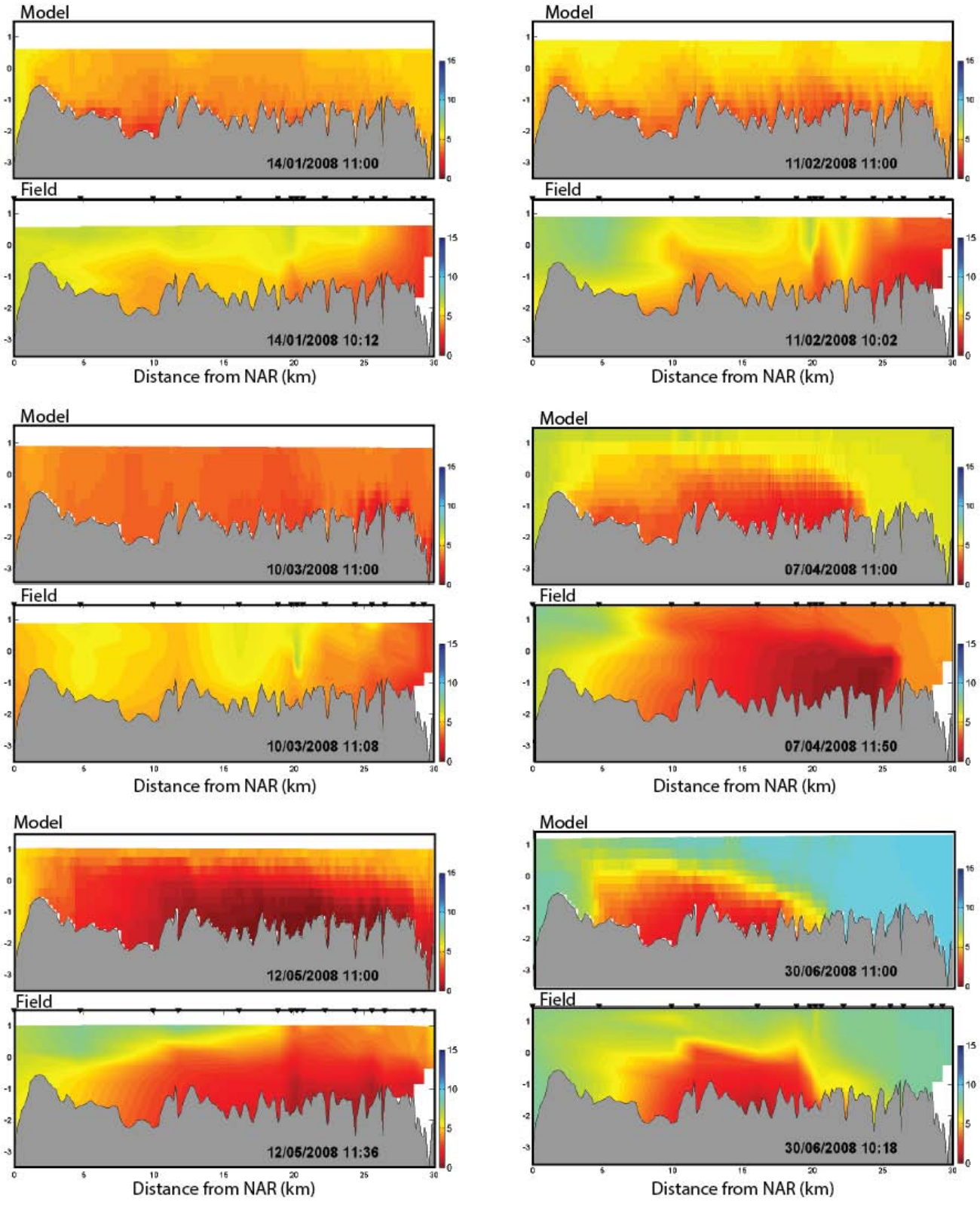

Figure 23a: Cross-section ('curtain') plots showing depth variation (y-axis, m AHD) of dissolved oxygen (g O_2 m^{-3}) along the centre of the estuary (x-axis, distance upstream from NAR in km). Plots are comparing modelled and observed oxygen for several monthly snapshots (January-June 2008). The field plots are based on a linear contouring around the 20 profile data points (Table 8), identified as triangles on the water surface.

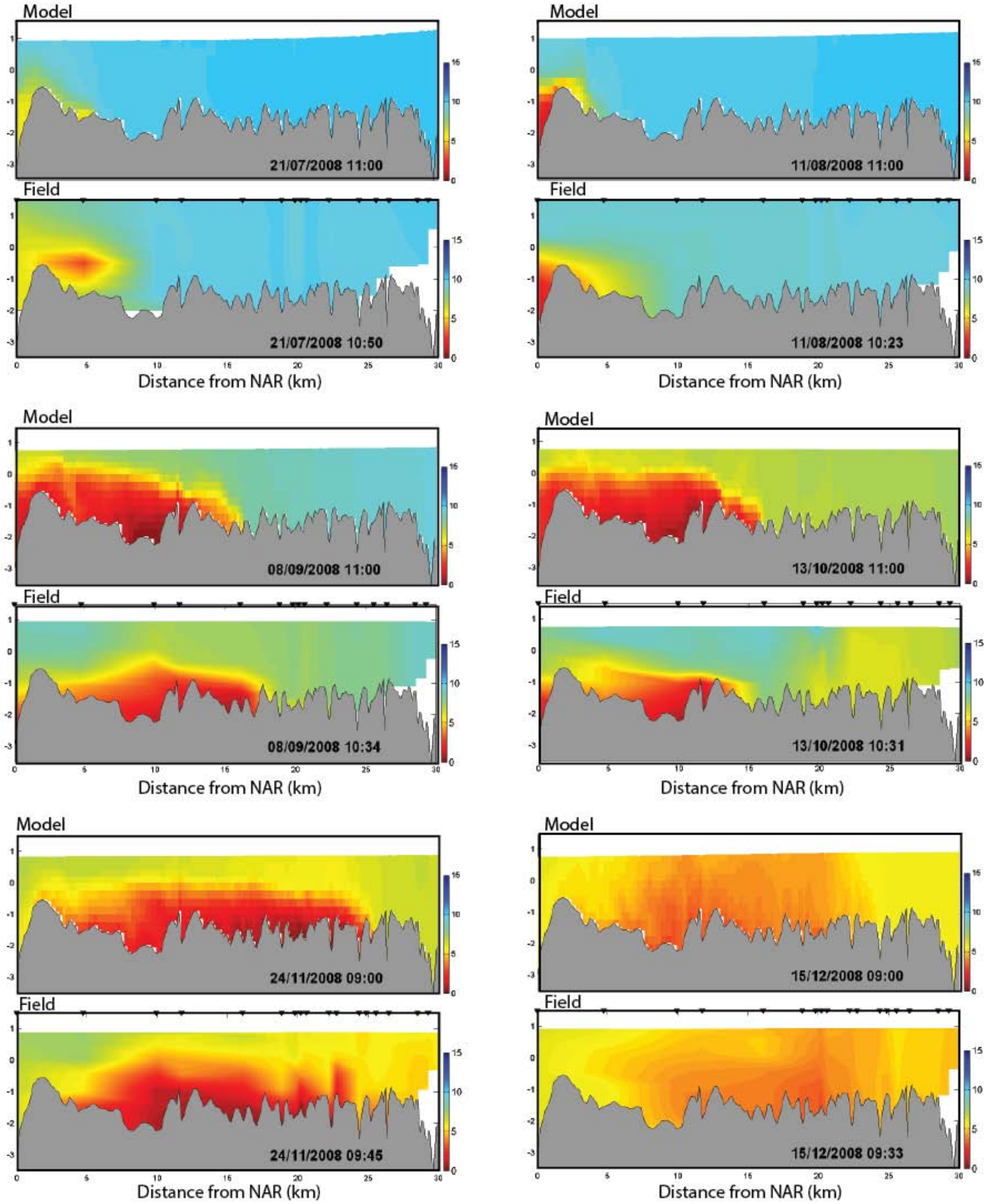

Figure 23b: Cross-section ('curtain') plots showing depth variation (y-axis, m AHD) of dissolved oxygen (g O_2 m^{-3}) along the centre of the estuary (x-axis, distance upstream from NAR in km). Plots are comparing modelled and observed oxygen for several monthly snapshots (January-June 2008). The field plots are based on a linear contouring around the 20 profile data points (Table 8), identified as triangles on the water surface.

There is under-prediction of oxygen peaks in the surface layer of the lower reaches of the domain during January-May, which is thought to be due to high levels of algal production not captured in the model at these locations. However, given the focus of this study was on oxygen dynamics in the upper reaches we did not pursue improvements in these regions and further improvements to the model in this area are left to a further study.

The spatial extent and degree of the low bottom-water oxygen region is generally well predicted however, particularly the low oxygen period from September-November. The overall extent of low oxygen (<4) and hypoxia (<2), at the estuary scale, is further analysed in Figure 24. At this scale the model captures the benthic area under low oxygen / hypoxia very well, and how these areas change from week to week.

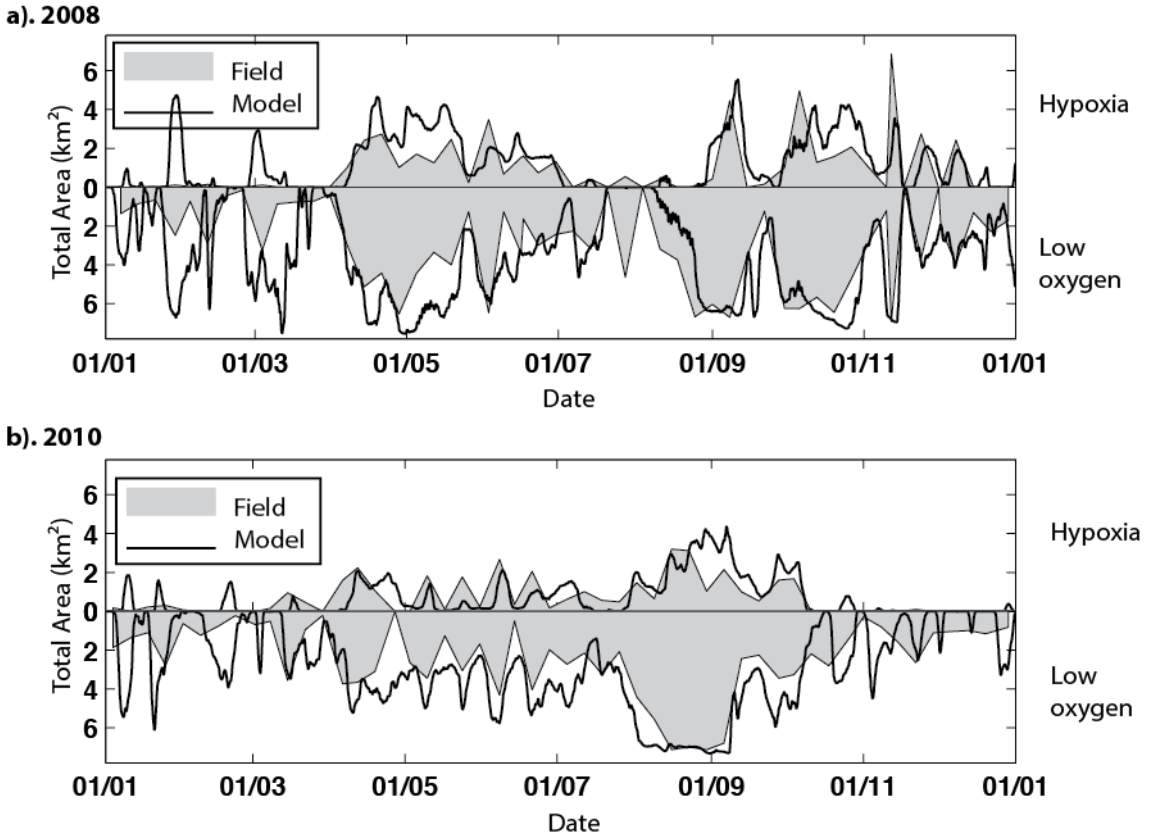

Figure 24: The total area of hypoxia (above) and low oxygen (below) for a) 2008 and b) 2010, comparing the model (black line) and interpolated data (shaded region). This is for the entire simulation domain, with hypoxia defined as <2 g O_2 m^{-3} and low oxygen as <4 g O_2 m^{-3}.

Table 9: Summary of error statistics for several key stations along the domain for salinity, oxygen and temperature

	NashSutcliffe			MAE			NMAE			RMS			NRMS		
Site	SAL	TEMP	OXY	SAL	TEMP	OXY	SAL	TEMP	OXY	SAL	TEMP	OXY	SAL	TEMP	OXY
KIN	0.952	0.934	-0.064	1.317	1.086	40.611	0.115	0.053	0.187	12.56	9.585	368.47	0.022	0.009	0.034
MAY	0.954	0.914	-0.188	1.468	1.163	38.614	0.099	0.057	0.177	14.089	10.409	373.83	0.018	0.01	0.033
NAR	0.964	0.902	-0.044	1.4	1.033	29.955	0.057	0.053	0.13	12.919	9.583	289.29	0.01	0.009	0.024
NIL	0.945	0.852	-1.125	1.716	1.446	50.619	0.087	0.071	0.212	16.051	12.284	462.8	0.016	0.012	0.038
RON	0.946	0.903	-0.671	1.395	1.288	48.94	0.113	0.063	0.214	14.021	11.338	420.83	0.023	0.011	0.037
STJ	0.945	0.876	-0.25	1.538	1.368	41.756	0.097	0.068	0.19	15.75	11.88	382.83	0.019	0.012	0.034
SUC	0.951	0.945	0.138	1.268	0.939	35.645	0.117	0.046	0.167	11.752	9.178	326.59	0.021	0.009	0.03

Validation against 2010 high-resolution Guildford profiling data

An intensive profiling exercise was undertaken at several times during 2010 at locations shown in Figure 25. To determine the performance of the model at this scale we have plotted the model predictions against the contoured field profile data for salinity and oxygen. Note that we have plotted 45 individual contour comparisons throughout this period, with 6 key snapshots presented here to demonstrate the range of modelled conditions.

Over the 10 km region, the model comparisons generally capture the trends seen in the profile data (Figure 26). In particular the position of the pycnocline and degree of salinity stratification is well represented. The oxygen plume (blue) and hypoxic regions (red) are generally well captured in terms of the position in the water column and lateral extent, though the magnitude or exact position is sometimes out.

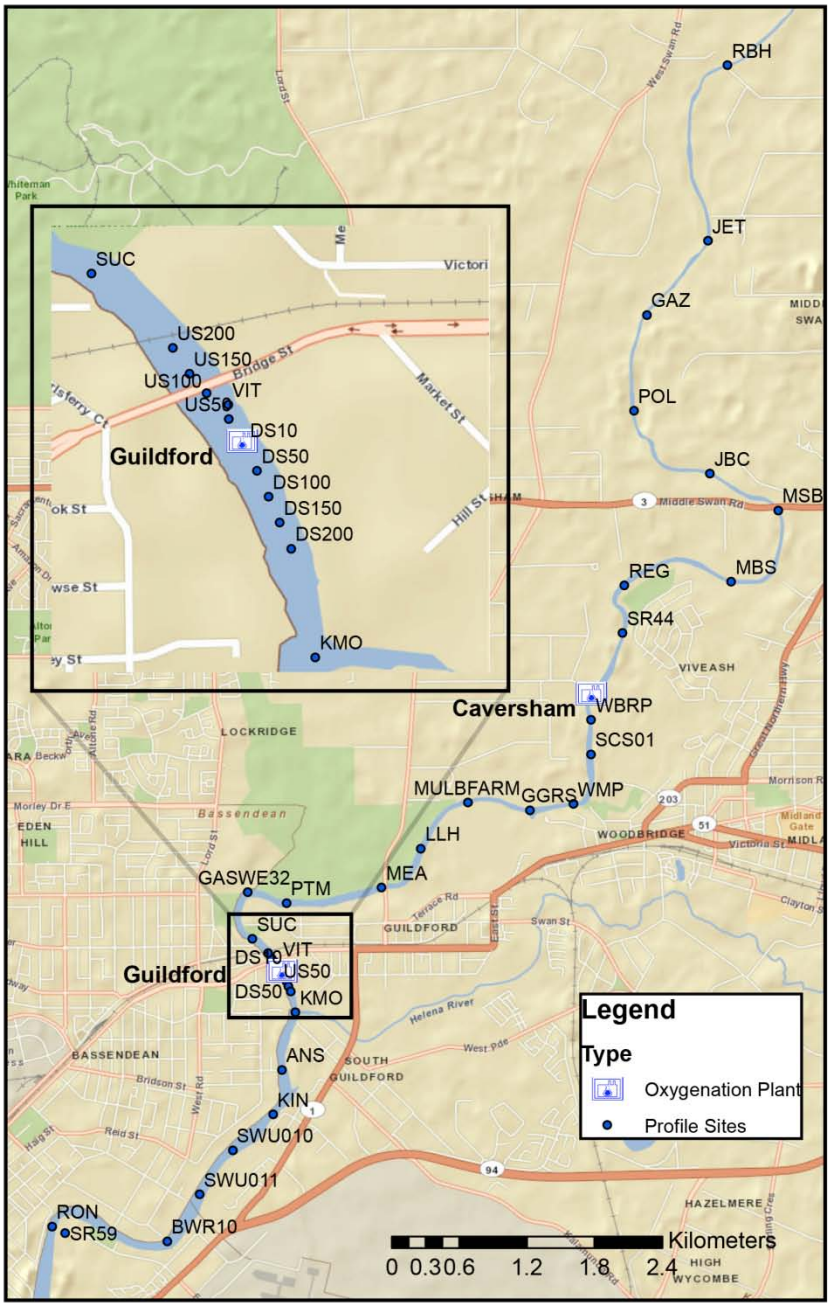

Figure 25: Strategic data collection points around the Guildford and Caversham oxygenation plants, for detailed sampling conducted in January, April and June 2010.

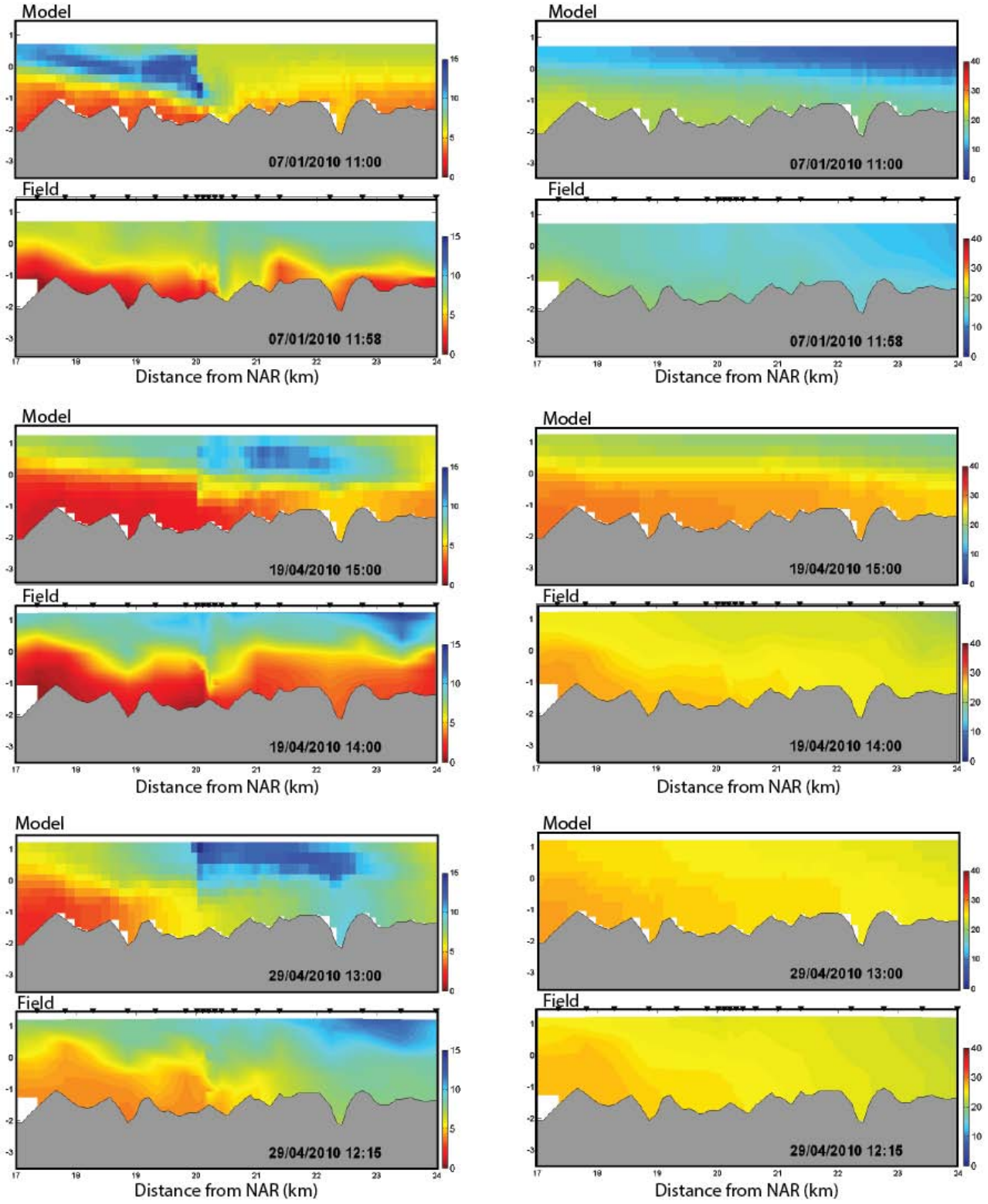

Figure 26a: Cross-section ('curtain') plots showing depth variation (y-axis, m AHD) of dissolved oxygen (left; g O_2 m^{-3}) and salinity (right; psu) along the centre of the estuary near Guildford (x-axis, distance upstream from NAR in km). Plots are comparing modelled and observed oxygen for several snapshots (January-April 2010) where profile data was available, identified as triangles on the water surface.

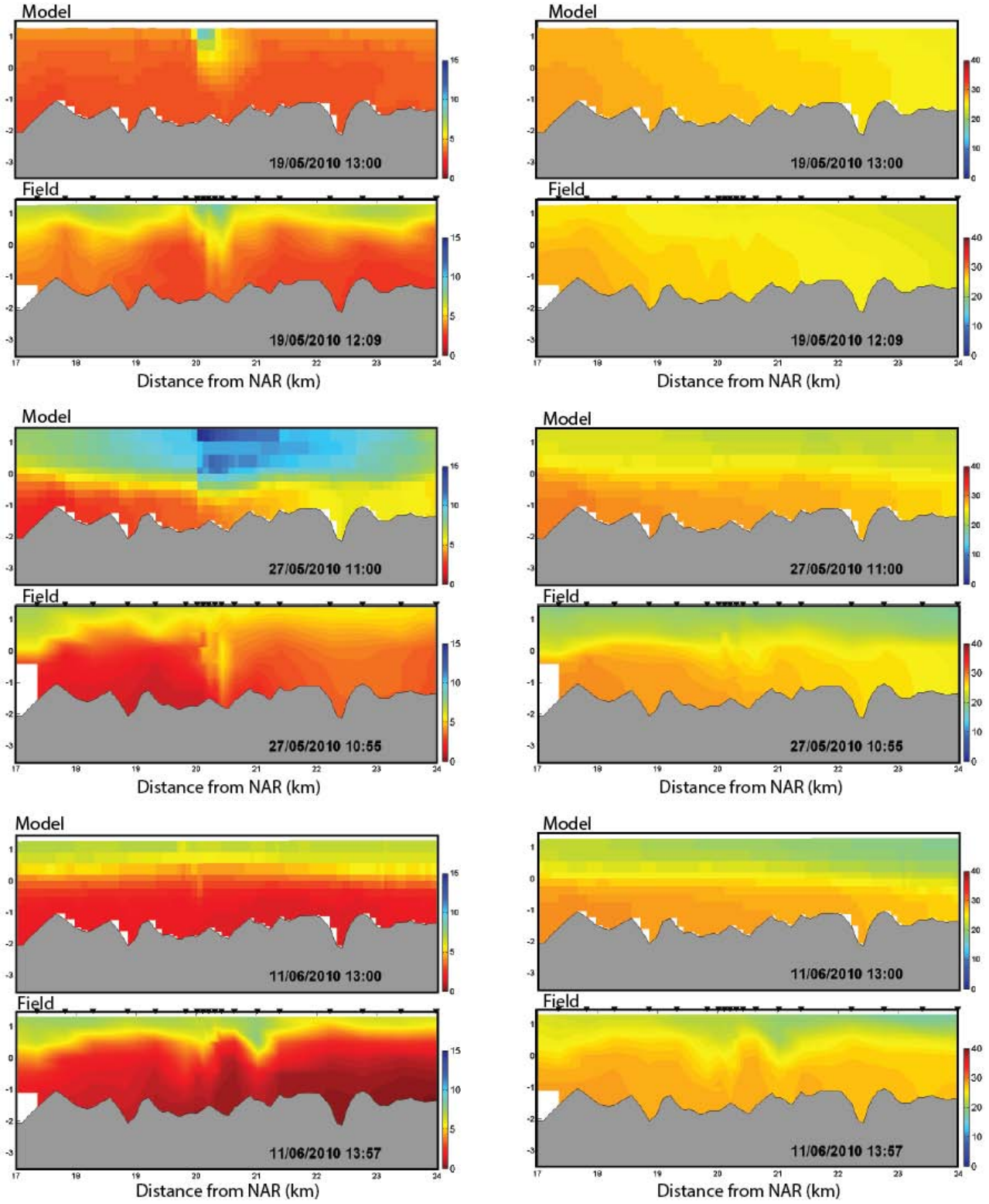

Figure 26b: Cross-section ('curtain') plots showing depth variation (y-axis, m AHD) of dissolved oxygen (left; g O_2 m^{-3}) and salinity (right; psu) along the centre of the estuary near Guildford (x-axis, distance upstream from NAR in km). Plots are comparing modelled and observed oxygen for several snapshots (May-June 2010) where profile data was available, identified as triangles on the water surface.

Oxygenation plant scenario assessment

A range of scenarios were explored to assess how sensitive the river oxygen would be to hypothetical oxygenation plant operational scenarios. These were chosen in consultation with relevant stakeholders and are presented as an initial set of "what-if" scenarios to provide a broad indication of how the river responds to oxygenation under different flow regimes. These scenarios were simplified from current operational practices that were being implemented at the time of model development. It is important to note that the simplification of these scenarios sometimes resulted in non-realistic oxygen concentrations (i.e., super-saturation) that would not be supported operationally if they were to occur. The overarching rationale was to evaluate plant efficiency under different operational regimes. Additionally a smaller subset of scenarios looked to explore the effect of changing hydrologic conditions (i.e., wet year versus dry year). All scenarios had a relevant 'control scenario', where no artificial oxygenation took place, by which they could be compared.

Scenarios tested

The scenarios tested are listed in Table 10 and range from **sOxy0** – **sOxy9**, with the main validation 2010 simulation denoted as **sOxyV**. They each run for 12 months and are designed to explore sensitivity to:

- Amount of oxygen input: ***BASE*** = 30 kg hr^{-1}; ***HIGH*** = 60 kg hr^{-1}
- The timing of oxygenation input, in particular, whether it is input at night time (during hours of cheaper electricity prices), or whether it is input on certain phases of the tidal cycle:
  Constant = 24hr/day constant input from the oxygenation plant;
  Economic = Night-time input only, with zero during the day;
  Flood/Ebb tide = Analysis of tidal level at Narrows Bridge to only put in oxygenated water when on a flood/ebb portion of tidal cycle.
- The location of input, for example whether it is input at Guildford, Caversham, or both.

Table 10: Summary of scenarios run to assess effectiveness of the oxygenation plants

Scenario Name	Flow condition	Guildford plant operational regime	Caversham plant operational regime
sOxy0 [A]	2010 – low flow year	No oxygenation	No oxygenation
sOxyV	2010 – low flow year	Actual 2010 input rates	No oxygenation
sOxy1	2010 – low flow year	Constant at the "BASE" input rate	Constant at the "BASE" input rate
sOxy4	2010 – low flow year	No oxygenation	Constant at the "HIGH" input rate
sOxy5	2010 – low flow year	Economic timing of inputs at the "HIGH" input rate	Economic timing of inputs at the "HIGH" input rate
sOxy6	2010 – low flow year	Economic timing of inputs at the "BASE" input rate	Economic timing of inputs at the "BASE" input rate
sOxy7	2010 – low flow year	Flood-tide timing of inputs at the "BASE" input rate	Ebb-tide timing of inputs at the "BASE" input rate
sOxy8 [B]	2010 modified to have 2011 scale post-winter flow Avon	No oxygenation	No oxygenation
sOxy9	2010 modified to have 2011 scale post-winter flow in Avon	Constant at the "BASE" input rate	Constant at the "BASE" input rate

[A] Control scenario which sOxyV – sOxy7 are compared to.

[B] Control scenario for high winter flow conditions which sOxy 9 is compared to.

Bottom water oxygen comparison

The scenario results indicate the different bottom water oxygen predictions (Figure 27) for the 10 sites across the river. These highlight the extent of the improvement the plants have both downstream to KIN and upstream past MSB.

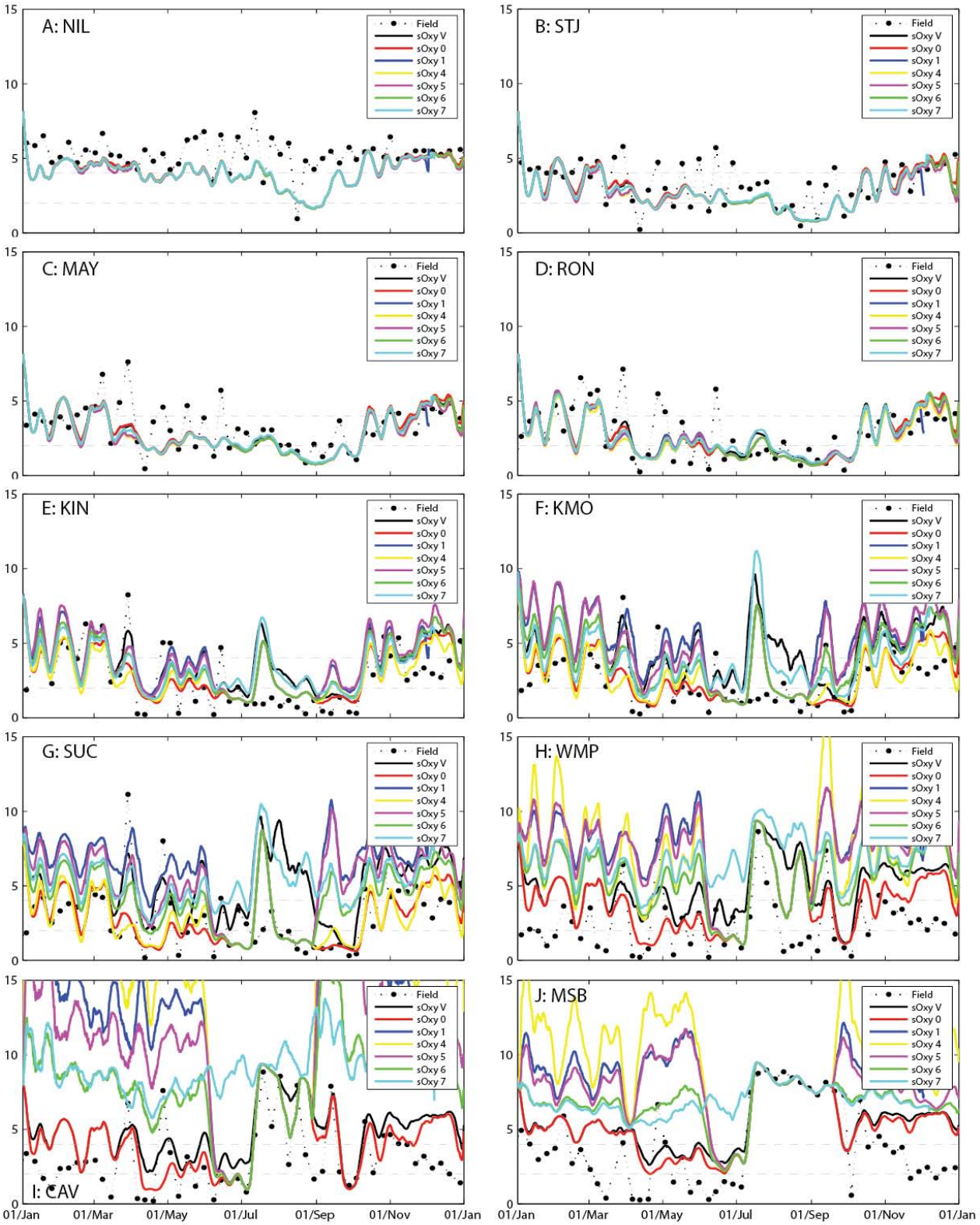

Figure 27: Bottom water oxygen concentrations (g O_2 m^{-3}) at the 10 sites previously reported on for 7 simulations, including the sOxy0 (no oxygenation, red) and sOxyV (actual 2010 oxygenation, black) reference results (refer to Table 10).

Substantial increases of the order of 100-200% greater than the no oxygenation reference simulation are seen in the region from KMO – MSB, demonstrating the simulations with the high flow rates of oxygen showed very large increases to the concentrations. Note that the upstream sites (WMP and beyond) have supersaturated oxygen concentrations that are reached; in reality that would mean that the plants would be turned off. Downstream of KIN all scenarios overlap since, highlighting this as the limit of the zone of influence.

Potential extent of the oxygenation influence

Figure 28 extends the above observation and illustrates the maximum range that the oxygenation plant flows can influence, measured as total range (includes the km downstream + km upstream) where the tracer concentration is >5% of the oxygenation plant inflow water concentration for each of the scenarios where the plant is running. As the economic and tidal optimum scenarios (sOxy6 & sOxy7) operate for 12 hours/day compared to the base case (sOxy1) that runs for 24 hours it would be expected that the maximum range of influence would be considerably lower. However, the predicted range for these was ~70-80% of sOxy1, which peaked at a range of 35km, highlighting that the reduction of range is not linearly proportional to the reduction in oxygen plant flow rates. The high river flow scenario (sOxy9) predicted a reduced level of influence when compared to the base case (sOxy1) in the months of September and October where the upper Swan River flow rates were increased. These predictions are expected as increased riverine flow rates lead to increased rates of dilution and thus reduced efficiency for the oxygenation plants.

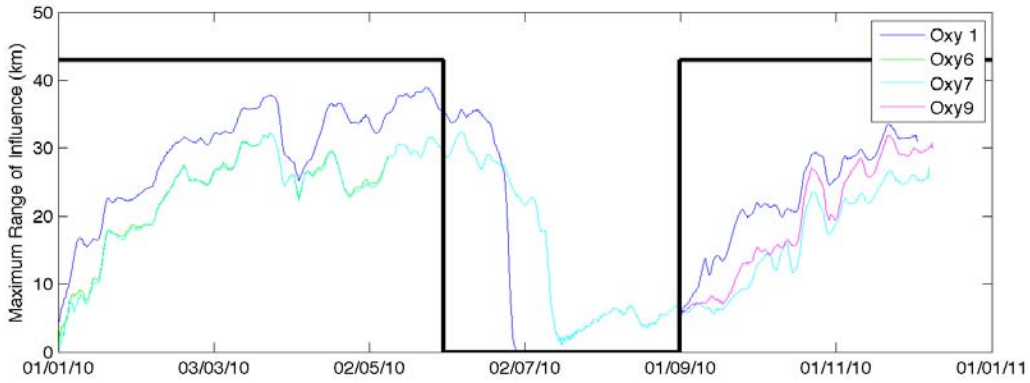

Figure 28: Extent of oxygen plant influence (tracer concentration > 5%) and black line represents oxygenation period (indicating on/off).

Effect on net % area of benthos experiencing low oxygen and hypoxia

Whilst the overall extent of influence is interesting to know, the ultimate benefit of the oxygenation plant on the health of the estuary is through restoration of oxygenated conditions to benthic habitat that would have otherwise been anoxic or hypoxic. For the scenarios where the oxygenation plants were running (sOxy1,6,7,9) the per cent of bottom water area experiencing low oxygen and hypoxia (integrated over the full model domain, Narrows Bridge to Great Northern Highway), are slightly reduced when compared to the scenarios when the oxygenation plants are switched off (Figure 29). However, the differences across this whole domain are slight, which is not surprising since the oxygenated zone is only a small proportion of the whole domain. For the high flow scenarios (sOxy8&9) the percentage of the domain experiencing hypoxia or general low oxygen conditions is greater than when compared to the low flow scenarios (sOxy0,1,6&7).

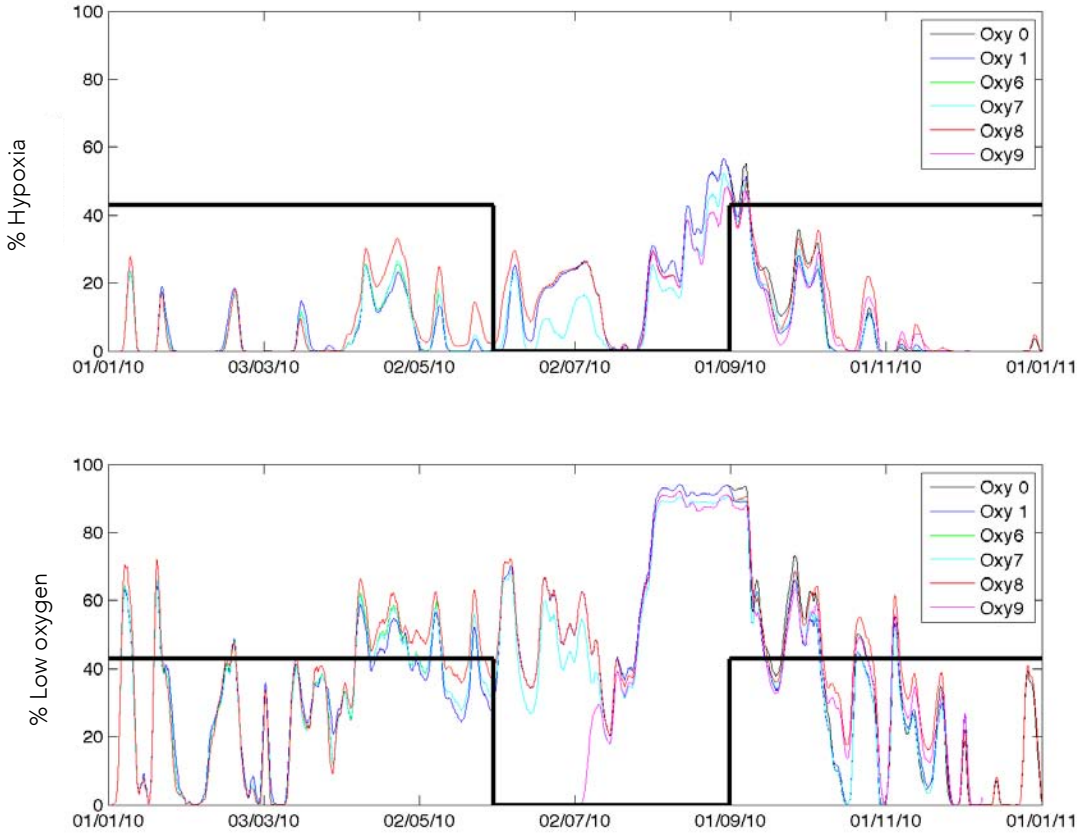

Figure 29: Percent (%) of bottom waters under hypoxia (< 2 g O_2 m^{-3}) and low oxygen (< 4 g O_2 $m3^{-1}$) for the full model domain. Thick black line represents operation period of oxygenation plants.

The extent of anoxia and hypoxia in the bottom waters of the upper Swan region is clearly heavily influenced by riverine flow events. High flows replenish bottom water oxygen concentrations effectively removing anoxia and hypoxia. When these flow events are followed by periods of low flow, salinity stratification sets up and anoxia and hypoxia return. These patterns can be observed in the model-simulated results for each of the oxygenation plant scenarios.

The rate of return to anoxic and hypoxic conditions is greatest when the oxygen plants are switched off (sOxy0) and slowest when both plants are operating at moderate capacity (sOxy1). For both the economic scenario (sOxy6) and the tidal optimum (sOxy7) both plants are operating for 12 hours per day and the model predicts reduced conditions of anoxia and hypoxia when operation occurs on the ebb tide for Caversham and the flood tide for Guildford. These results suggest that timing the injection of oxygenated water with the tide is a more efficient operational practice although operating at off-peak times would be more economic.

While differences between the scenarios are relatively small across the whole domain, considering the area that could be affected by the oxygenation plants, the effect of the different scenarios is much larger (Figures 30 and 31). The extent of bottom water anoxia and hypoxia is greater for the 2010 dry flow regime (sOxy0) compared to the hypothetical 2011 wet flow regime scenario (sOxy8) during the months July to mid October. The flow regime then switches in November and December with the 2011 flow being less than the 2010 flow (refer to Figure 31). For the scenarios where both plants are operating under maximum capacity (sOxy1&9) a similar pattern of switching is observed.

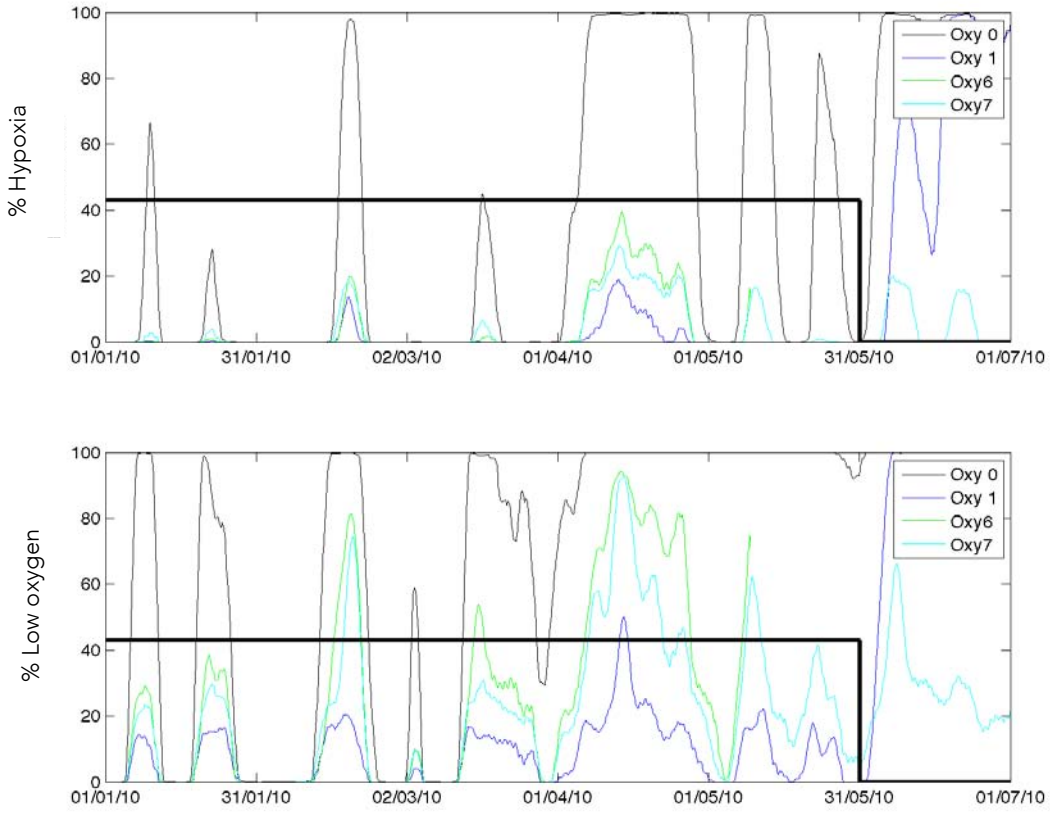

Figure 30: Percent (%) of bottom waters under hypoxia (< 2 g O_2 m^{-3}) and low oxygen (< 4 g O_2 m^{-3}) for the smaller oxygenation plant domain. Thick black line represents operation period of oxygenation plants. Note date range.

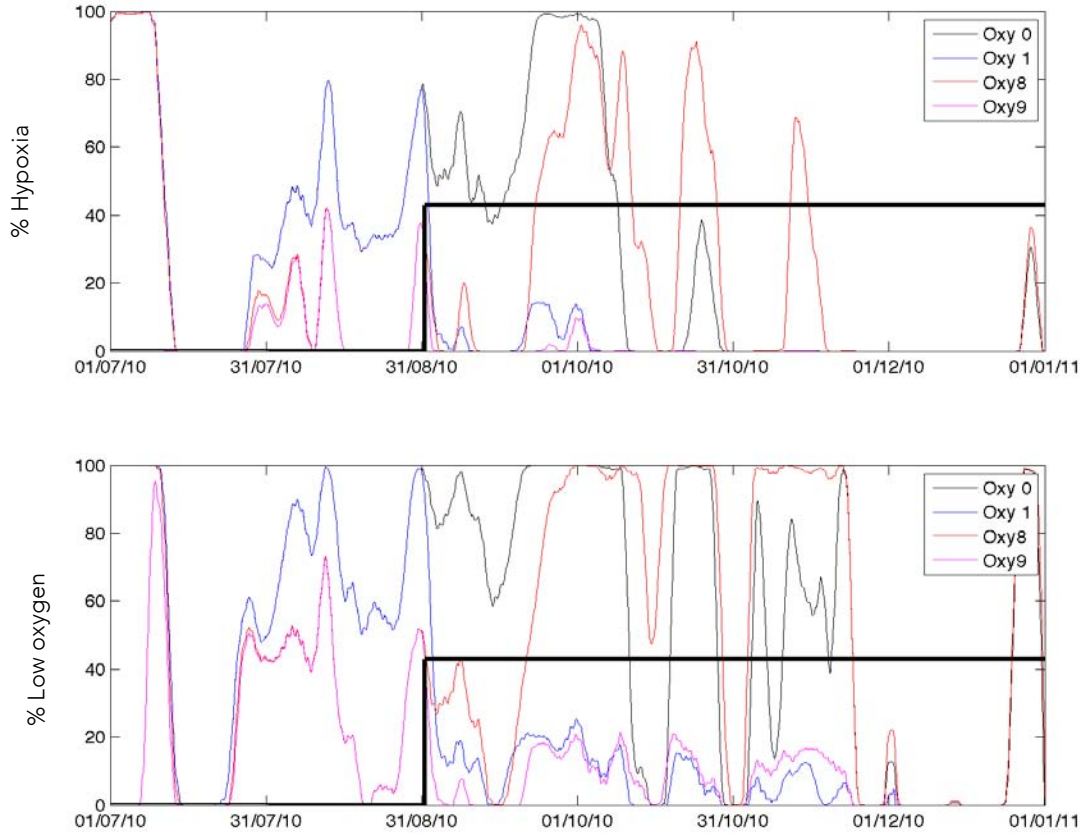

Figure 31: Percent (%) of bottom waters under hypoxia (< 2 g O_2 m^{-3}) and low oxygen (< 4 g O_2 m^{-3}) for the smaller oxygenation plant domain. Thick black line represents operation period of oxygenation plants. Note date range.

The high influence of river flow rates on the observed patterns of anoxia and hypoxia response would suggest that an oxygenation plant operating procedure that responds to river inflow magnitude would maximise efficiency and potentially reduce unnecessary costs. Further work is required however to link the benefit of oxygenation inputs (in terms of benthic area improved) under a range of different flow and estuary antecedent conditions. Note that currently the Upper Swan plants now link their operation with locally measured oxygen (termed "DO control"), which essentially aggregates flow and other factors. This approach requires further assessment within the modelling scenarios to ensure the system-wide oxygenation benefits are maintained – for example, disabling oxygen input when a local sensor exceeds a limit may not account for requirements further away from the sensor.

To quantify the improvement of the oxygenation plant inputs Figure 32 shows how the percentage of time that a certain area of benthos experiencing hypoxia or general low oxygen conditions is impacted by the operational regimes. For example, Figure 32a shows that sOxy6 has 30% of the domain under low oxygen for 50% of the time, whilst sOxy0 has will have 30% for closer to 70% of the time. Note these calculations are based on integration over the period from Jan – Jul, and Jul – Dec, reflecting the different hydrology over these periods.

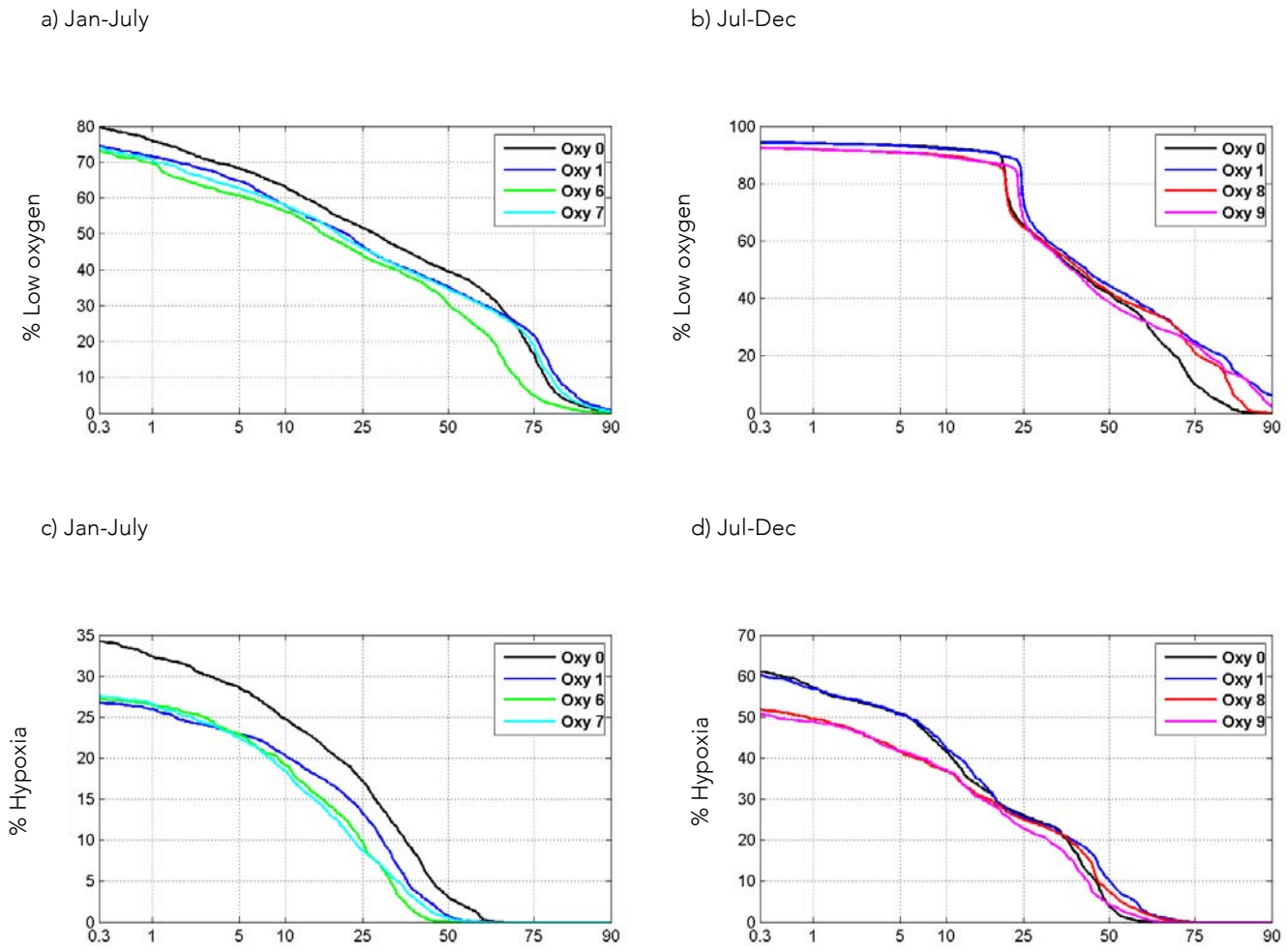

Figure 32: Exceedance probability curves indicating percentage of time (x-axis) that a designated % low oxygen (a,b) or % hypoxia (c,d) extent is equalled or exceeded. Note the y-axis scales vary between plots.

Given the large site-to-site and day-to-day variability, the effectiveness of the various scenarios is better illustrated through the spatially integrated total benthic area that has avoided hypoxia due to the presence of the oxygenation inputs – termed the "area of benthos saved" (Figure 33). To do this, each scenario is compared to the no-oxygenation scenario.

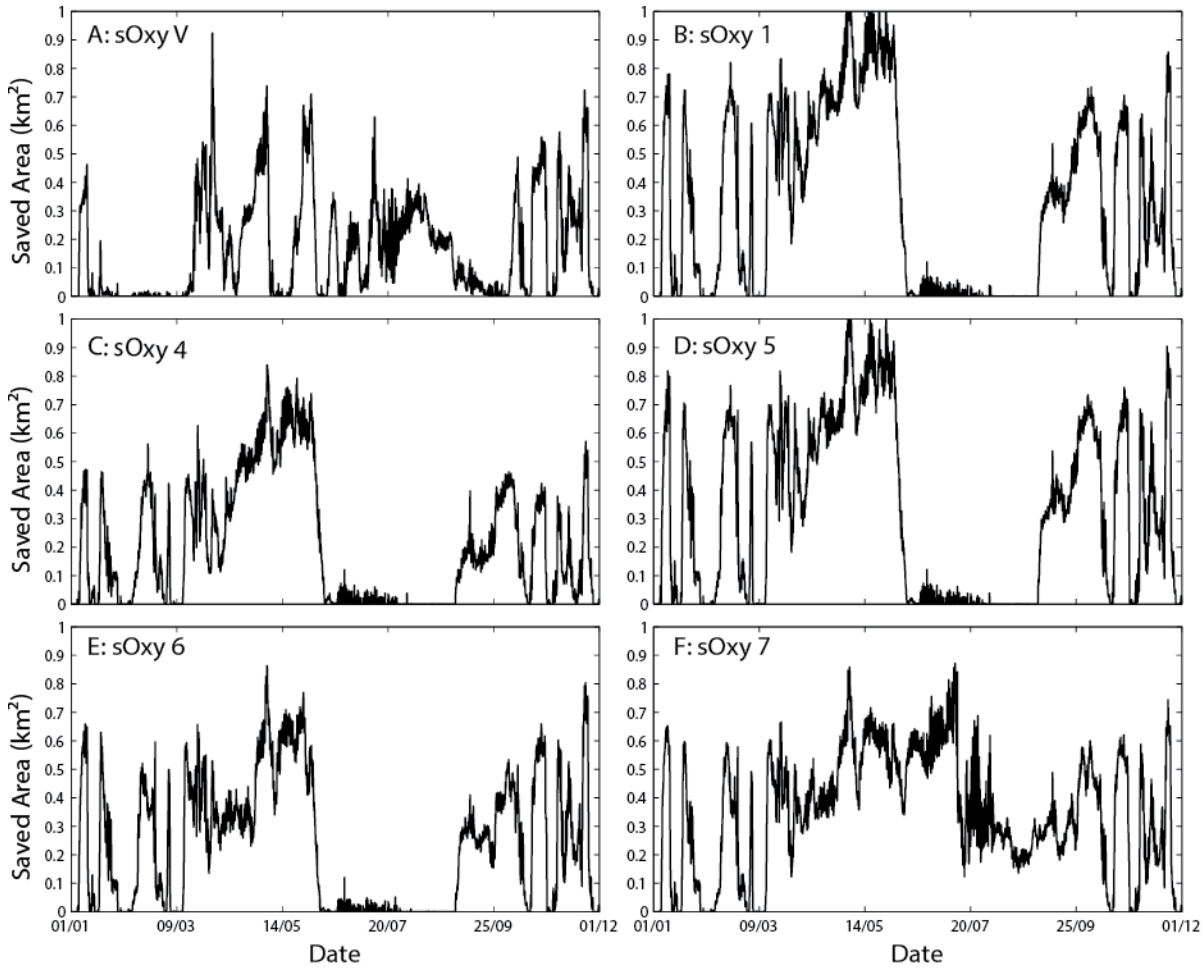

Figure 33: Time-series of total "benthic area saved from low oxygen" (km^2) by each scenario, calculated relative to sOXY0.

Across the different oxygenation scenarios, with both plants running, the area of benthos "saved" could range from 0.6 – 1.2 km^2 during peak of plant operations depending on the plant operation method. The effect is better summarised in Figure 34, which demonstrates the frequency (y-axis) along the length of the estuary (x-axis) of benthic area that has been saved by the oxygenation intervention. These graphs highlight the areas that receive the most benefit, compare the benefit of one versus two plants being operational, and illustrate how these benefits are affected by operational conditions.

These various scenarios are summarised in terms of their average areal benefit, in order to give a simple indication of the benefit of each to facilitate inter-comparison (Figure 35). This figure demonstrates the annual average benthic area saved relative to both oxygen input loading and expense to highlight scenario options that give the best environmental benefit for the least cost.

When the total area saved is compared to the total oxygen input amount, these scenarios summarise the non-linear relationship between input and response. In particular, sOxy7 appear to be the most optimum in terms of amount of area saved per unit input. When factoring in the cost of oxygen inputs, and electricity (including simplified on-peak, off-peak rules), the resultant graph illustrates the relative benefit per unit cost. sOxy7 again came out as being the most optimum, highlighting tidal phases as being an important determinant of the total benefit.

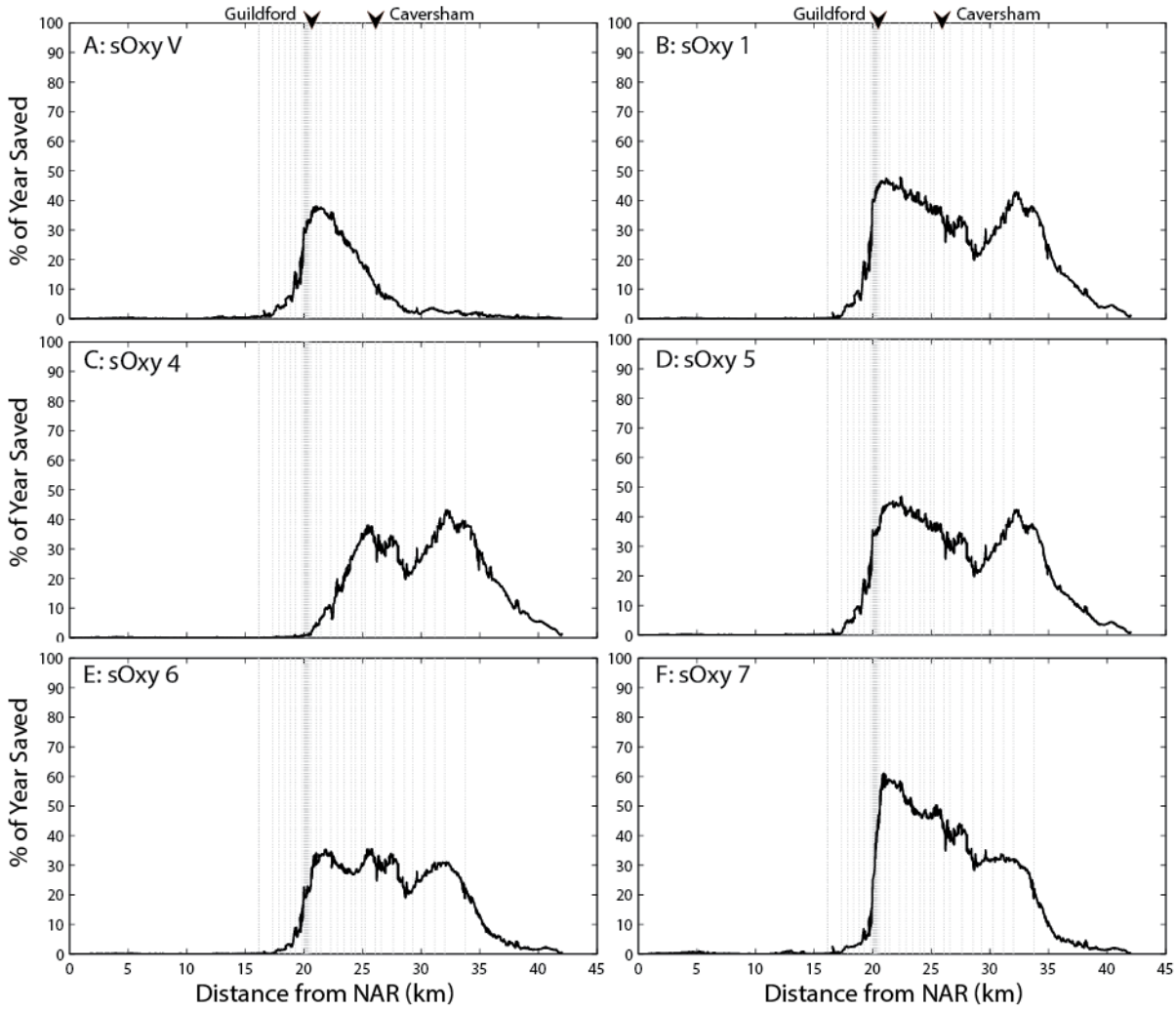

Figure 34: Percentage time during the simulation year that was saved from low oxygen conditions as a function of distance along the estuary. Results presented for each scenario are calculated relative to sOxy0. Grey lines indicate the monitoring sites in Figure 25.

a)

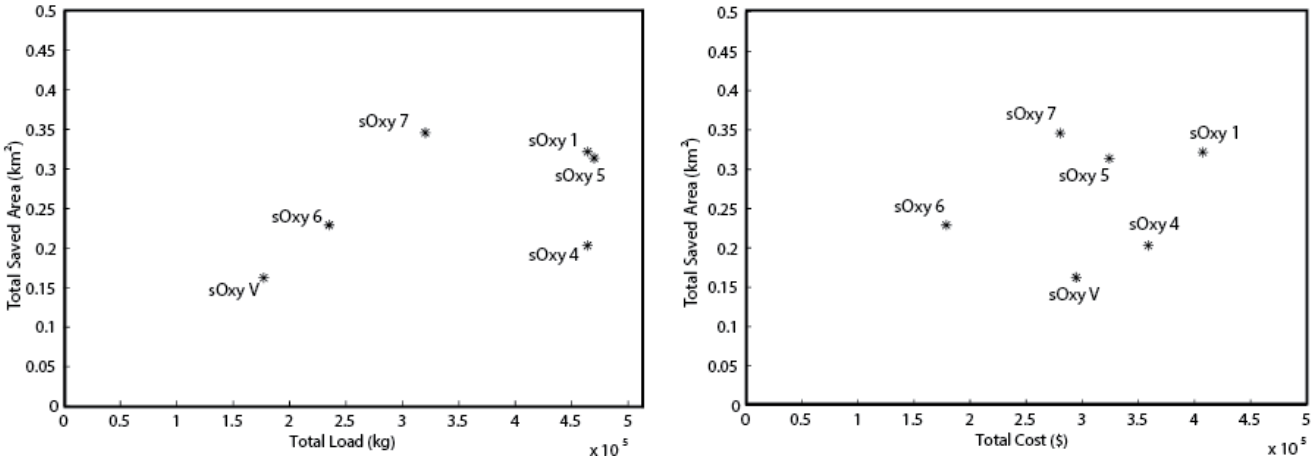

b)

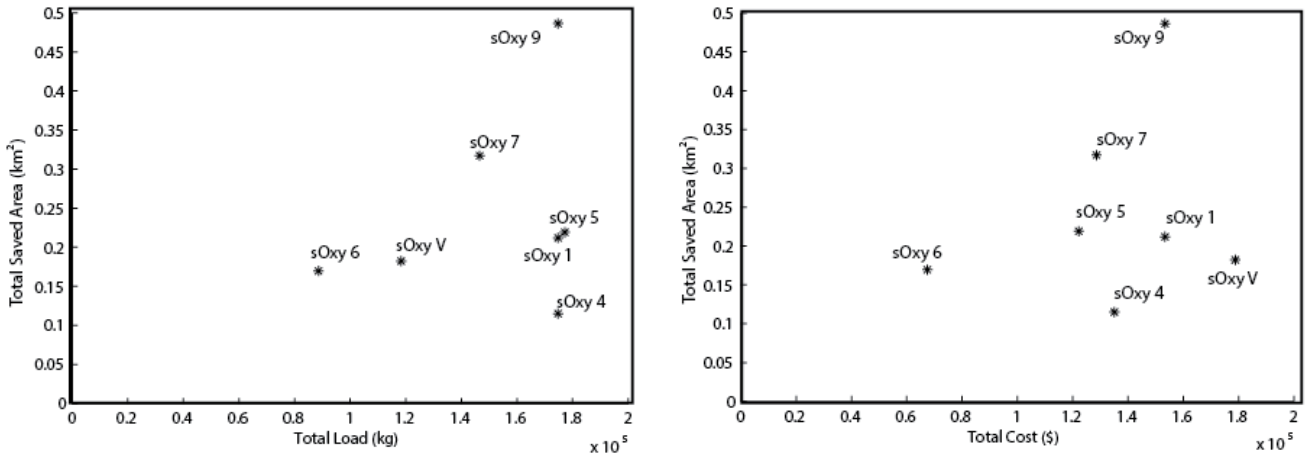

Figure 35: Average area of benthos (river bed) saved in the Upper Swan from hypoxia, as a function of oxygenation plant loading (left) and total cost (right): a) the top panels are simulations with 2010 flow regime and computed by averaging over the full year; and b) the bottom two panels are computed by averaging over the last 6 months (Jul – Dec) to demonstrate the relative significance of the "2011 winter flow" scenario (sOxy9) on the overall efficiency. The costs were calculated using Eq. 2-4, based on a price 0.278 $ kWh^{-1} for peak and 0.100 $ kWh^{-1} for off-peak, assuming a consumption of 44 kWh for Guildford and 65 kWh for Caversham.

5. Canning Weir Pool Model

Model application

The Canning Weir Pool domain spans from below the Kent St weir (near Castledare) to the Upper Canning gauging station. The mesh is loosely based on a curvilinear designed grid, but with custom elements around complex areas, including the around the Kent St weir structure itself. The channel has approximately 4 elements across the river near the weir pool, with only a single cell wide in the upstream reaches. The depths on the grid were interpolated from recently collected bathymetric data available from the Department of Transport (Figure 36). The vertical resolution of the model was set to be 0.2 m, with several variable thickness (sigma) layers for water levels above the weir crest.

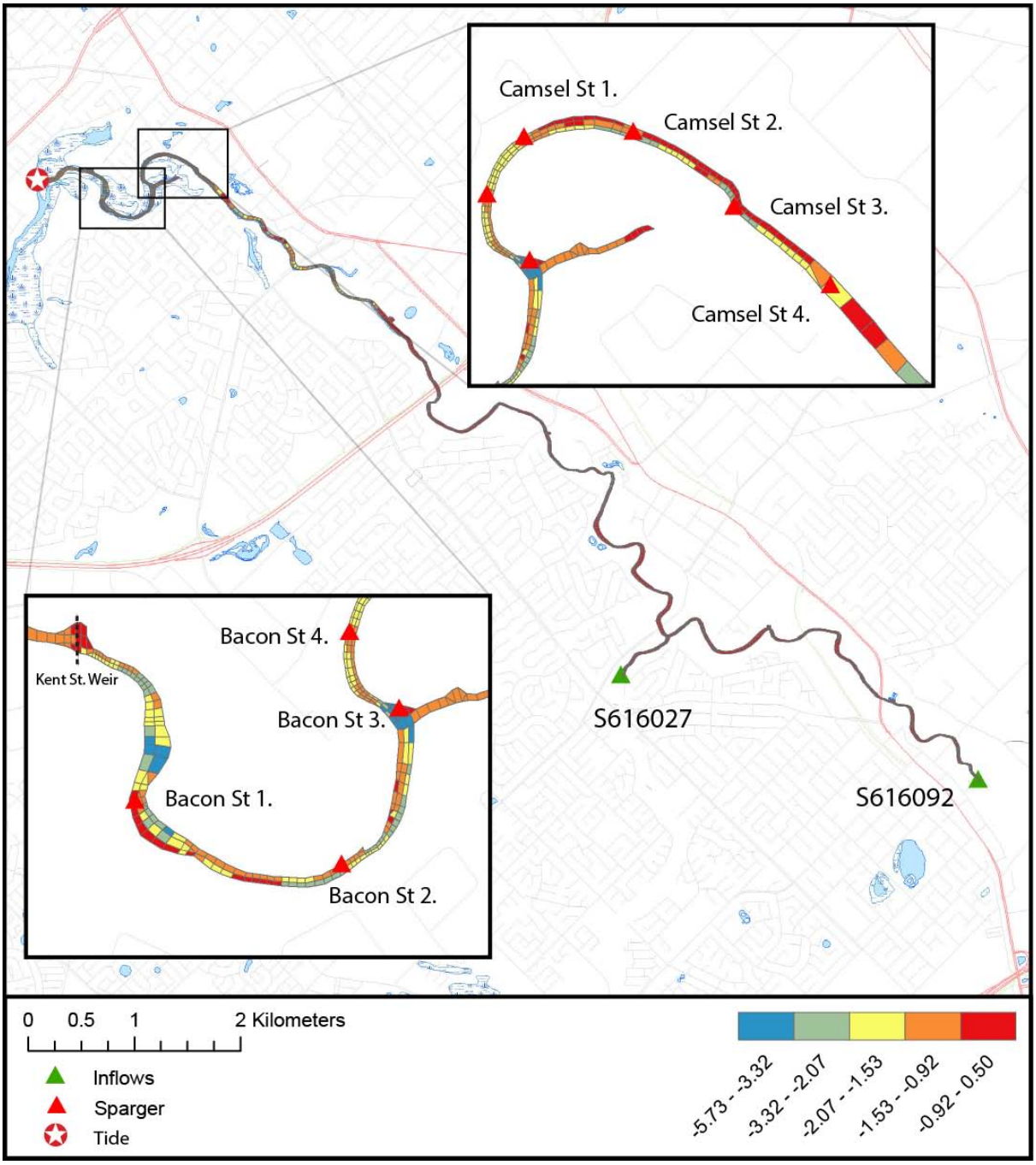

Figure 36: Canning Weir Pool computational mesh, with the colour scale indicating bathymetric depths, and locations of inflow points and Sparger input points for the Camsel and Bacon St plants indicated.

The domain is forced by inflows, meteorological and tidal information form various location:

- *Tidal data* – 15 minute water level data was input directly to the model downstream of the weir, and weekly water quality data interpolated to daily resolution:
  - Water level was from Kent St Downstream (Department of Water station 616094)
  - Water quality was from Casteldare (Department of Water station CAS)
- *Meteorological data* – As for the Upper Swan domain, South Perth meteorological station was used providing:
  - Solar radiation, wind, air temperature, humidity, rain, clouds
- *Inflow data* – daily gauging station data was used for flow (Figure 37) and salinity and weekly water quality data was interpolated to daily for the following stations:
  - Canning River (616092), Southern River (616027), Yule Brook (616042)

The model was run from Oct 1st 2008 – Jul 31st 2009. The simulation included the two oxygenation plants as inputs (Bacon and Camsel St plants, each with 4 spargers) as indicated in Figure 36 (see insets). Data for oxygenation plant input was estimated from data supplied form the Department for Water with an average plant input rate of 5 kg hr^{-1}.

Initial runs indicated we were unable to get the persistent cool water that observed at station NIC where there is a deep hole present, and we therefore added a small, cool groundwater influx (T = 18°C, flow = 0.0064 $m^3 s^{-1}$)

Model validation and assessment

Validation approach

The model was validated against all sites shown in Figure 38, with a summary of the model comparisons presented for the 8 sites indicated in (Table 11). Other assessments were conducted as for the Swan.

Table 11: Validation sites adopted in the Kent St Weir Pool domain, indicating the focus sites presented in the below validation time-series plots (denoted A-H). All 13 sites were used in curtain comparisons.

Station number	SiteID	Name	X	Y	Time series panel ID
1	CAS	Casteldare	397599	6456555	
2	KEN	Kent St Weir Pool	398104	6456676	
3	KENU300	300m upstream of Kent St Weir	398214	6456487	A
4	BACD500	500m downstream of Bacon St	398415	6456264	B
5	BACD300	300m downstream of Bacon St	398570	6456298	C
6	BAC	Bacon St	398652	6456567	D
7	BACU300	300m upstream of Bacon St	398621	6456804	E
8	PO2	Phoslock and Oxy Section Site 2	398993	6456763	
9	GRE	Greenfield St Footbridge	399251	6456530	F
10	MAS	Masons Landing	399698	6456184	
11	NIC	Nicholson Rd Bridge	400108	6455782	G
12	HES	Hester Park	400308	6455779	
13	ELL	Ellison Parade	401012	6455148	H

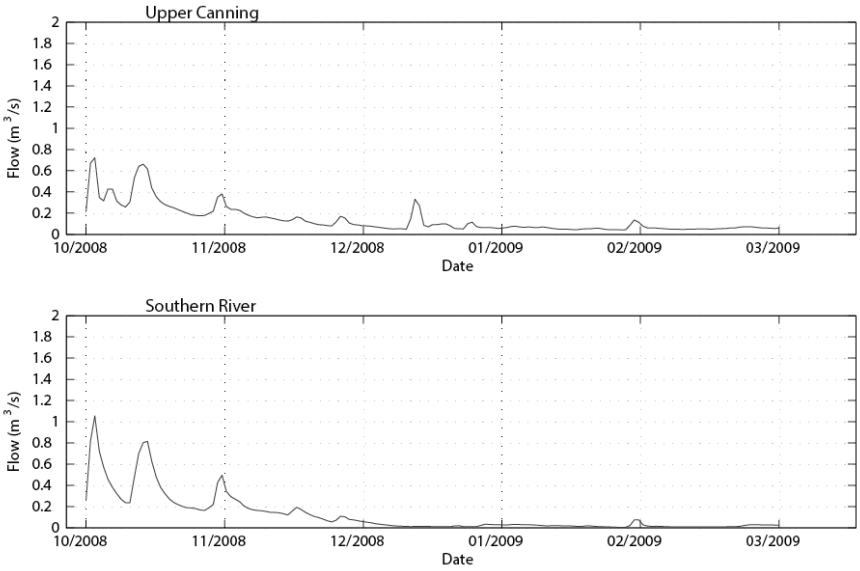

Figure 37: Inflows for Upper Canning (616092) and Southern River (616027) entering the Canning Weir Pool domain.

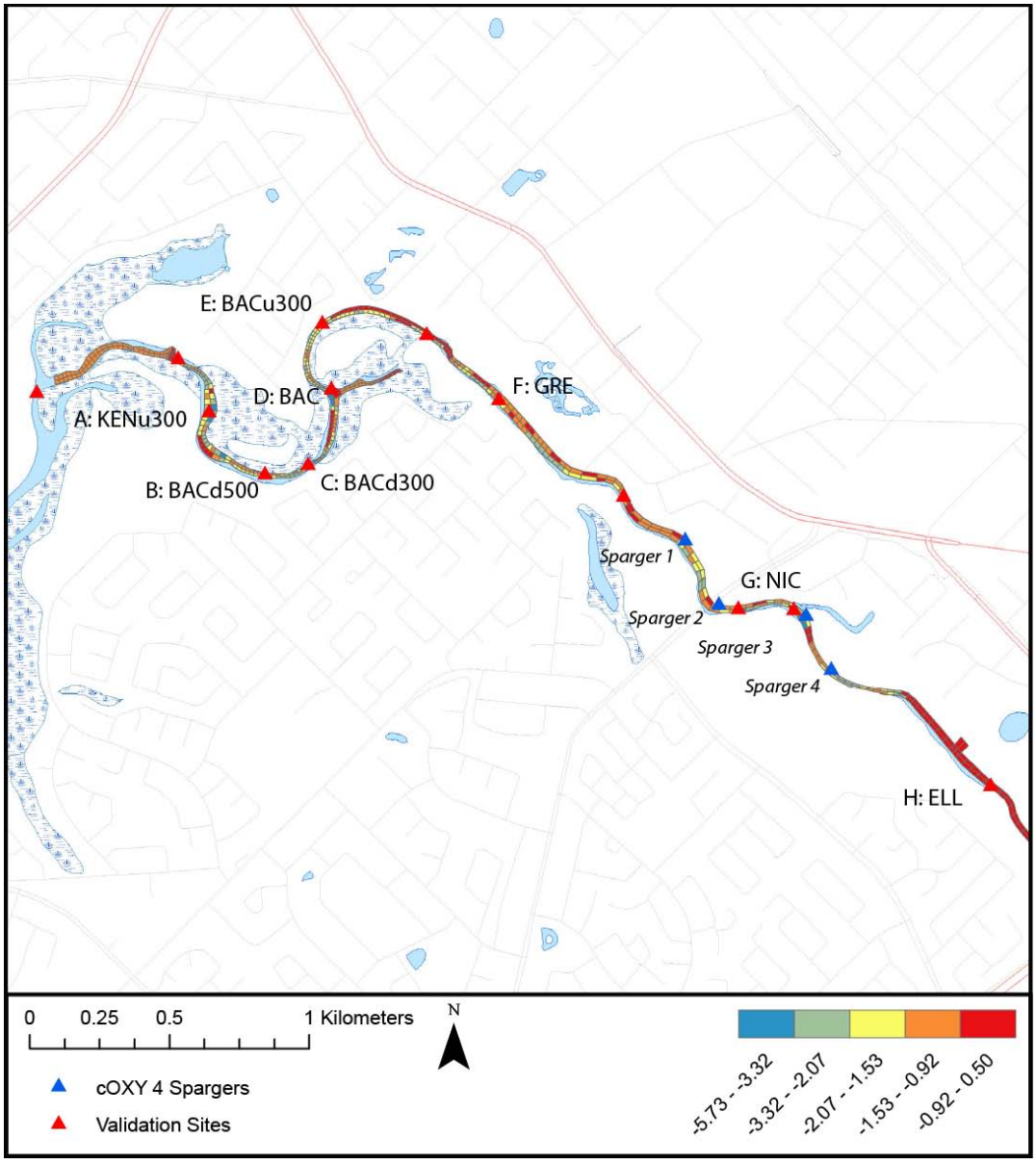

Figure 38: Canning Weir Pool computational mesh showing validation points.

Water level, salinity and temperature

The water level predictions in the Canning (Figure 39) are accurately captured with relatively minor peaks occurring following small flows after the boards were put in place.

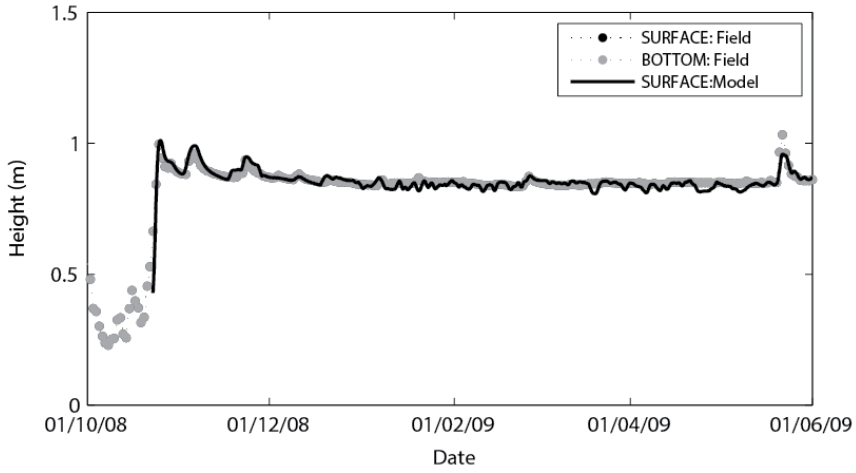

Figure 39: Canning Weir Pool surface height validation.
Data from Department of Water station: Kent St U/S (616093).

The salinity was captured well for the simulation period (Figure 40 – 41) with small inputs of salinity over the weir during high tides, and large inputs during May, where a significant overtopping event occurred bringing saline estuarine water into the weir pool. The model accurately captures this pulse and the lateral extent that this penetrates.

Unlike the Upper Swan simulation, temperature is the main driving force of vertical stratification for much of the simulation period (when the saline water pulse is absent). Substantial error was found in the original hydrodynamic simulations due to significant overheating of the domain when using the South Perth meteorological data. To improve the predictions, adjustments were made to the extinction coefficient, wind speed and solar radiation input. The best calibration occurred with solar radiation reduced to 70% of the value of the South Perth data, which was thought to reflect the potential significant effect of shading caused by riparian vegetation. The simulations with the reduced solar radiation (Figure 42) demonstrate good performance by the model in capturing the seasonal warming and cooling, with a notable over-prediction in January by ~1 – 2°C. In general the surface and bottom temperatures only varied by a small amount throughout the year (~1°C), but this was under-predicted by the model.

Two notably different areas were around KENU300 and NIC, where deep regions experienced a persistent cool bottom layer throughout the summer months. This was not originally captured in the model, but after consultation with Department of Water staff this was concluded to be seepage of groundwater into the domain. Adding a cool groundwater flow (as described above) meant that this trend was able to be captured with the model, though not perfectly at KENU300. Due to the importance of temperature in simulating oxygen solubility, improving the model simulation through collection of local meteorological data, and gaining a better understanding of groundwater inputs, would be beneficial.

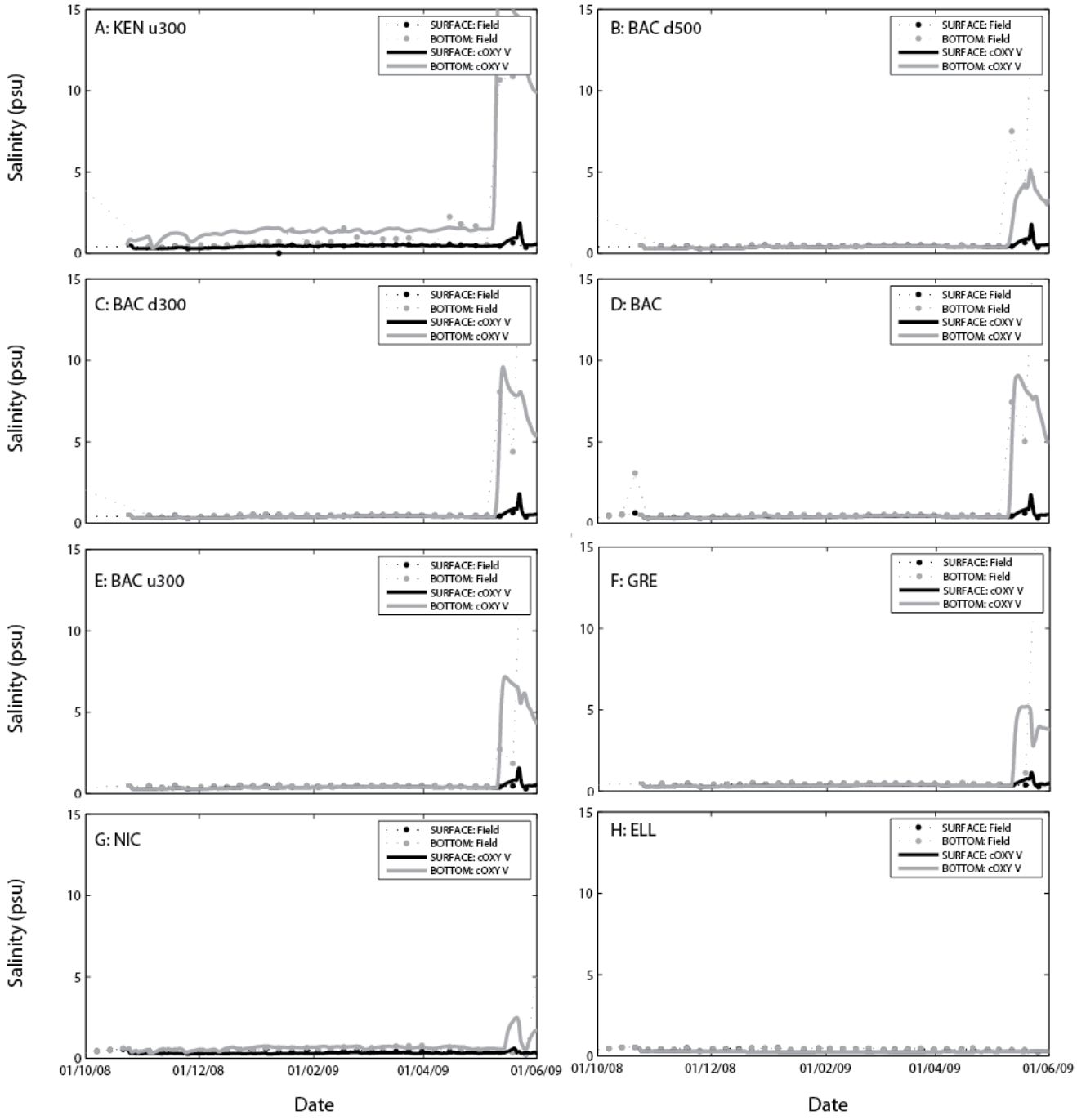

Figure 40: Canning Weir Pool simulated versus observed salinity (psu) predictions for Canning stations A-H.

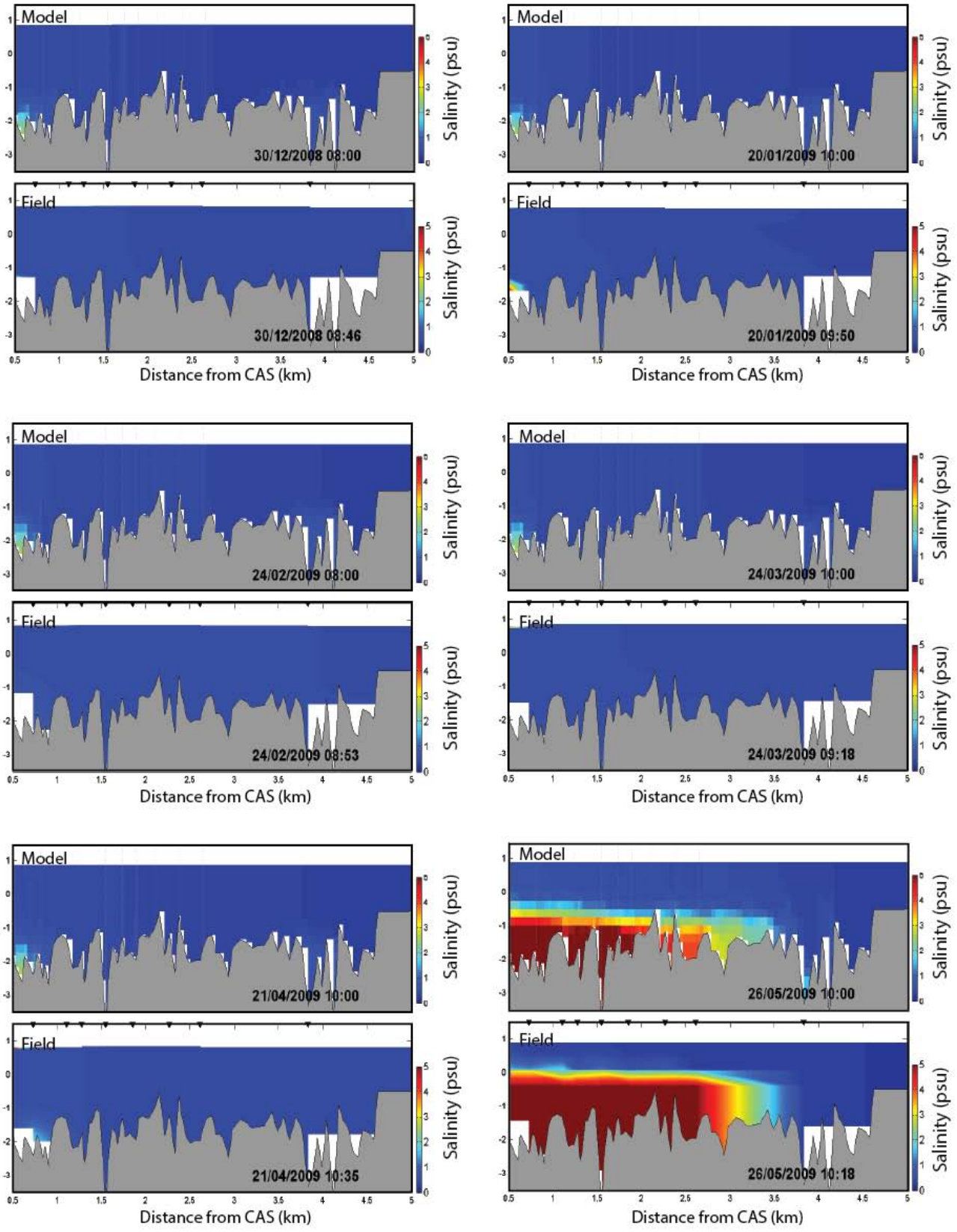

Figure 41: Cross-section ('curtain') plots showing depth variation (y-axis, m AHD) of salinity (psu) along the centre of the weir pool (x-axis, distance upstream from CAS in km). Plots are comparing modelled and observed salinity for several monthly snapshots. The field plots are based on a linear contouring around the 13 profile data points (Table 11), identified as triangles on the water surface (note some sites up or downstream of the plot axis are used in the interpolation). The Kent St Weir is situated at approximately x = 0.5 km.

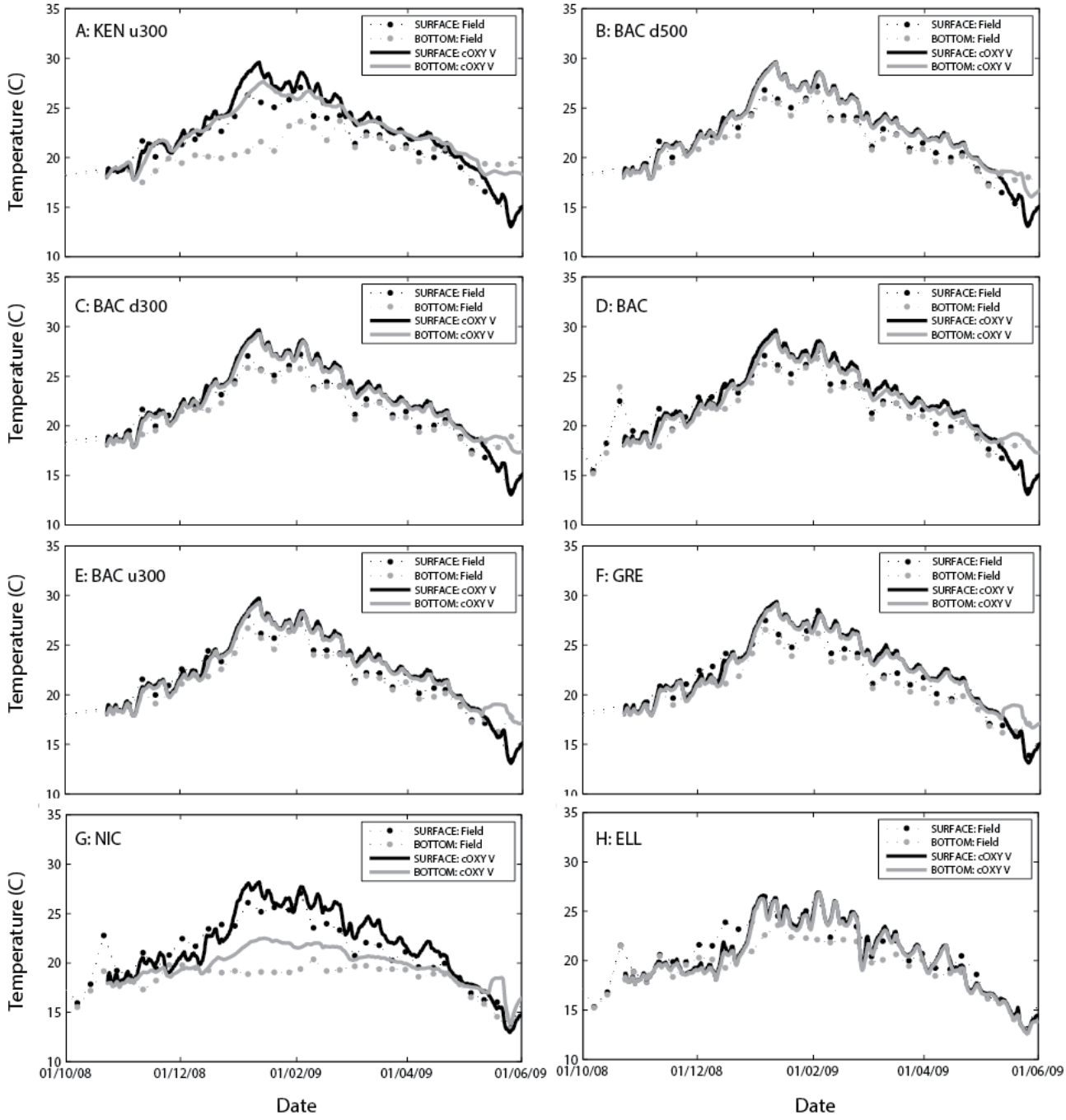

Figure 42: Canning Weir Pool simulated versus observed temperature (C) predictions for Canning stations A-H.

Dissolved Oxygen

The oxygen concentration predictions from the Canning simulation compared well with the field data (Figure 43), though not as closely as for the Upper Swan simulation. The region from KEN – BACU300 was simulated the best, most likely due to the dominance of the numerous (8) oxygenation plant inputs in this region dominating the observed concentration profiles. Within the region further upstream from GRE – ELL, the bottom oxygen concentrations were well simulated, but the surface oxygen concentrations were generally under-predicted by ~2 – 3 g O_2 m^{-3} at GRE and ELL. Based on our analysis, this is understood to be from insufficient temperature stratification in this region of the domain predicted by the model, or may also be contributed to by lack of algal production in the simulation as was discussed previously.

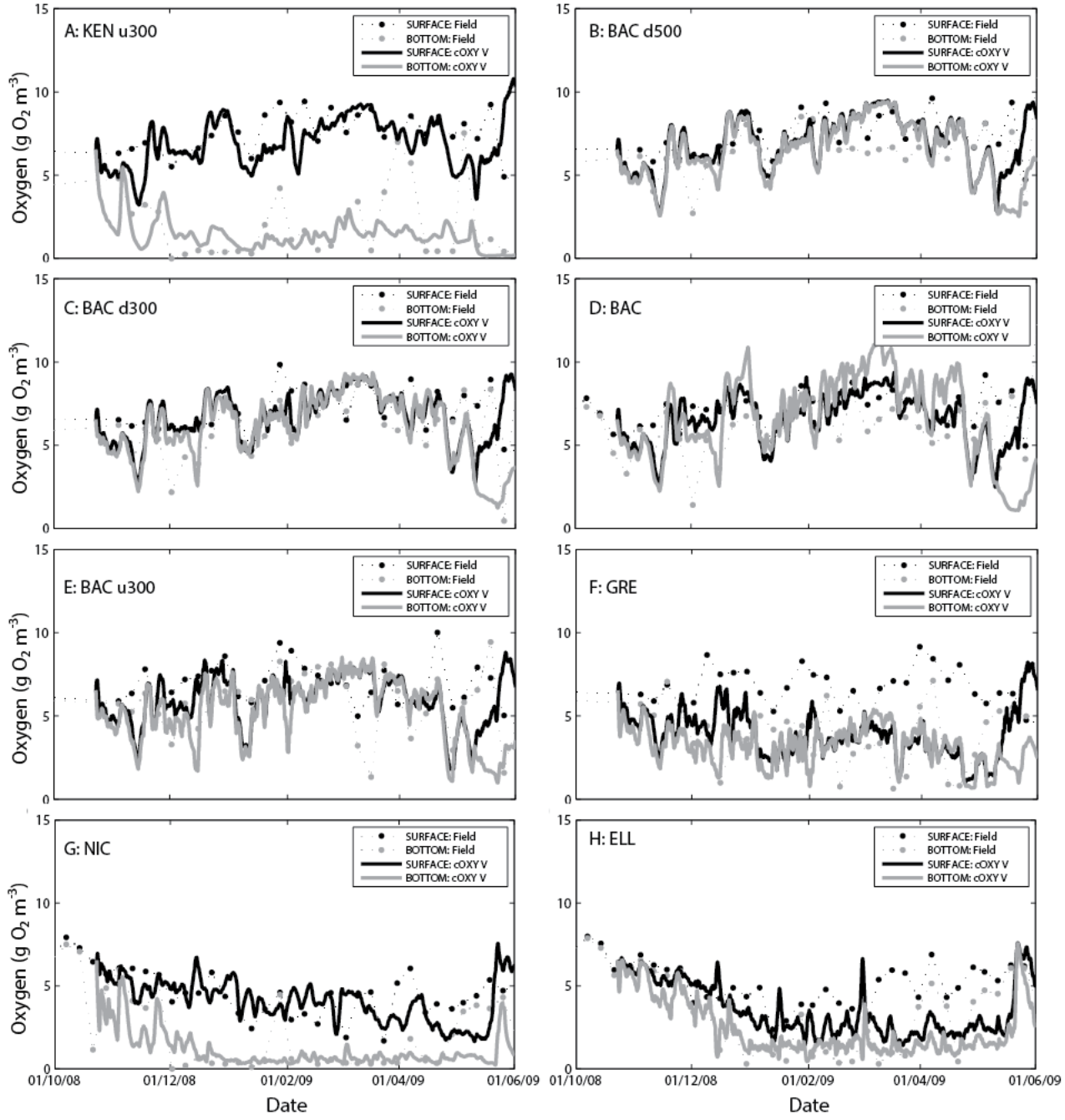

Figure 43: Canning Weir Pool simulated versus observed dissolved oxygen concentrations (g O_2 m^{-3}) predictions for Canning stations A-H.

These discrepancies are most notably seen in the cumulative frequency distribution plots (Figure 44), which highlight the under-prediction of the surface concentrations in the upstream stations. Nonetheless, the frequency of bottom water hypoxia (<2 g O_2 m^{-3}) is predicted well in all sites.

Monthly cross-section plots of oxygen concentrations (Figure 45) demonstrate that whilst the time-series comparison is not perfect, that the model is in fact capturing the vertical and horizontal variation in oxygen through the simulation period very well. Note that compared to the Upper Swan curtains, the profile locations in the Canning domain are further apart in the upstream section and therefore the observed data are not able to resolve the level of detail seen in the model curtain plots. The main difference in the field plots that is not seen in the model is the upstream diffusion of oxygen at the surface, however, part of this inland extension of the may in fact be overly exaggerated by the coarse interpolation between GRE – NIC.

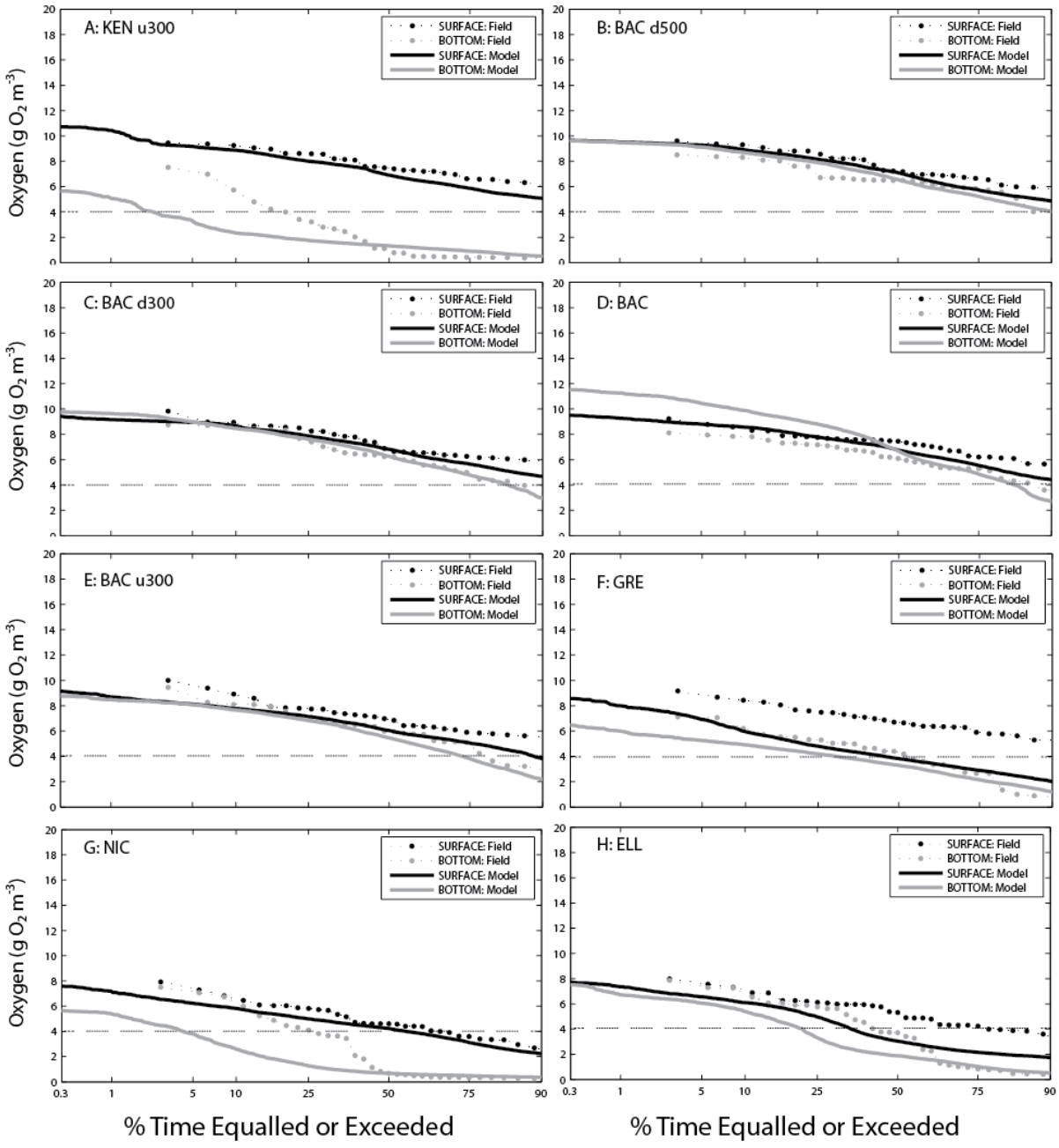

Figure 44: Cumulative frequency distribution (%) of simulated and observed dissolved oxygen (g O_2 m^{-3}) for several stations (A-H).

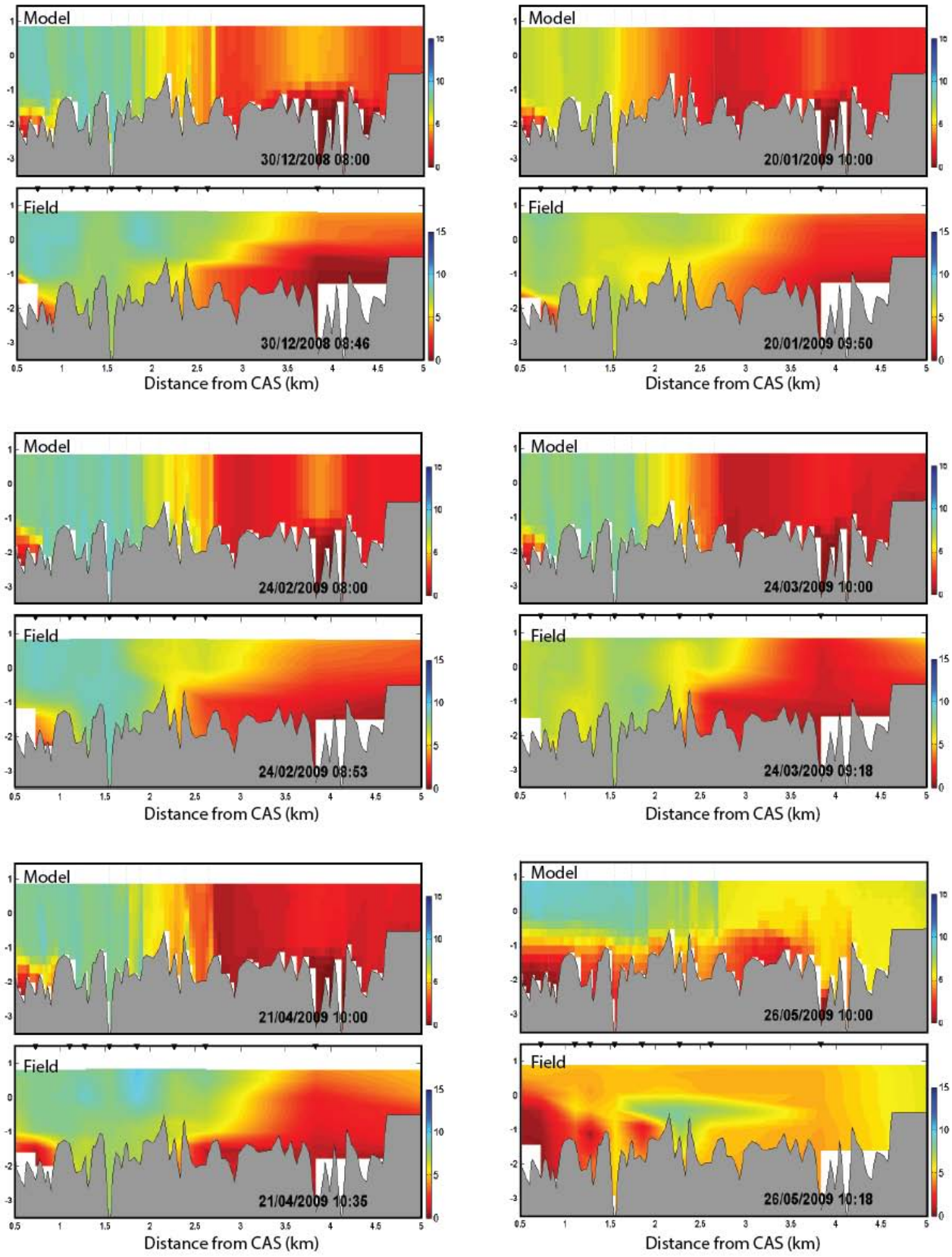

Figure 45: Cross-section ('curtain') plots showing depth variation (y-axis, m AHD) of dissolved oxygen (g O_2 m^{-3}) along the centre of the weir pool (x-axis, distance upstream from CAS in km). Plots are comparing modelled and observed oxygen for several monthly snapshots. The field plots are based on a linear contouring around the 13 profile data points (Table 11), identified as triangles on the water surface (note some sites up or downstream of the plot axis are used in the interpolation). The Kent St Weir is situated at approximately x = 0.5 km.

Oxygenation plant scenario assessment

A range of scenarios were explored to assess how sensitive the oxygen in the weir pool would be to alternate oxygenation operational scenarios. These were chosen in consultation with relevant stakeholders and are presented as an initial set of "what-if" scenarios to provide a broad indication of how the region responds to oxygenation. Unlike the Upper Swan, where various strategies are utilised in operating the plants, the Canning oxygenation plants consistently operate under "DO control" (whereby oxygenation input is triggered by an in situ sensor reading), and with a set oxygen delivery rate, wherever possible. Therefore the simplified scenarios applied here test aspects of the model capabilities and system responses, based on a single year of actual operation. In addition, a scenario has been included to model the effect of a new oxygenation plant on the Canning River. Please note, this was based on a preliminary design available at the time of modelling and is purely hypothetical. As with the Upper Swan, all scenarios had a relevant 'control scenario' where no artificial oxygenation took place.

Scenarios tested

The scenarios tested are listed in Table 12 and range from **cOxy0** – **cOxy5**, with the reference to the base simulation denoted as **cOxyV**. They explore the sensitivity to:

- Amount of oxygen input (33% and 67% of the validation simulation trialled)
- The number and operation of the spargers (2 versus 4 spargers tested, and bottom versus surface entry)
- The benefit of a third hypothetical plant in the upstream reaches with 4 spargers added.

Table 12: Summary of scenarios run to assess effectiveness of the oxygenation plants

Scenario Name	Flow condition	Bacon St plant operational regime	Camsel Wy plant operational regime	Hypothetical upstream plant regime
cOxy0 [A]	Dec 2008 – May 2009, low flow year	No oxygenation	No oxygenation	No oxygenation
cOxyV	Dec 2008 – May 2009, low flow year	Actual 2008/2009 input rates	Actual 2008/2009 input rates	No oxygenation
cOxy1	Dec 2008 – May 2009, low flow year	33% of cOxyV	33% of cOxyV	No oxygenation
cOxy2	Dec 2008 – May 2009, low flow year	67% of cOxyV	67% of cOxyV	No oxygenation
cOxy3	Dec 2008 – May 2009, low flow year	As cOxyV, but reduced to 2 spargers instead of 4	As cOxyV, but reduced to 2 spargers instead of 4	No oxygenation
cOxy4	Dec 2008 – May 2009, low flow year	As cOxyV	As cOxyV	Set to flow rate of Camsel Way, with 4 spargers
cOxy5	Dec 2008 – May 2009, low flow year	Oxygen diffusers adjusted to prevent rapid rising of the oxygen plume.	Oxygen diffusers adjusted to prevent rapid rising of the oxygen plume.	No oxygenation

[A] Control scenario which cOxyV – cOxy5 are compared to.

Bottom water oxygen comparison

The model results indicating the different bottom water oxygen predictions are shown in Figure 46 – 50 for the 8 sites across the river. These highlight the extent of the improvement the plants have in the region KEN to GRE. Substantial increases of the order of several times greater than cOxy0 (do nothing) were predicted for the cOxyV (base case). The relative impact of the 33%, 67% and 100% (cOxyV) scenarios demonstrates an expected degree of change in bottom oxygen concentration (Figure 46), though not a directly proportional response is observed (see analysis below).

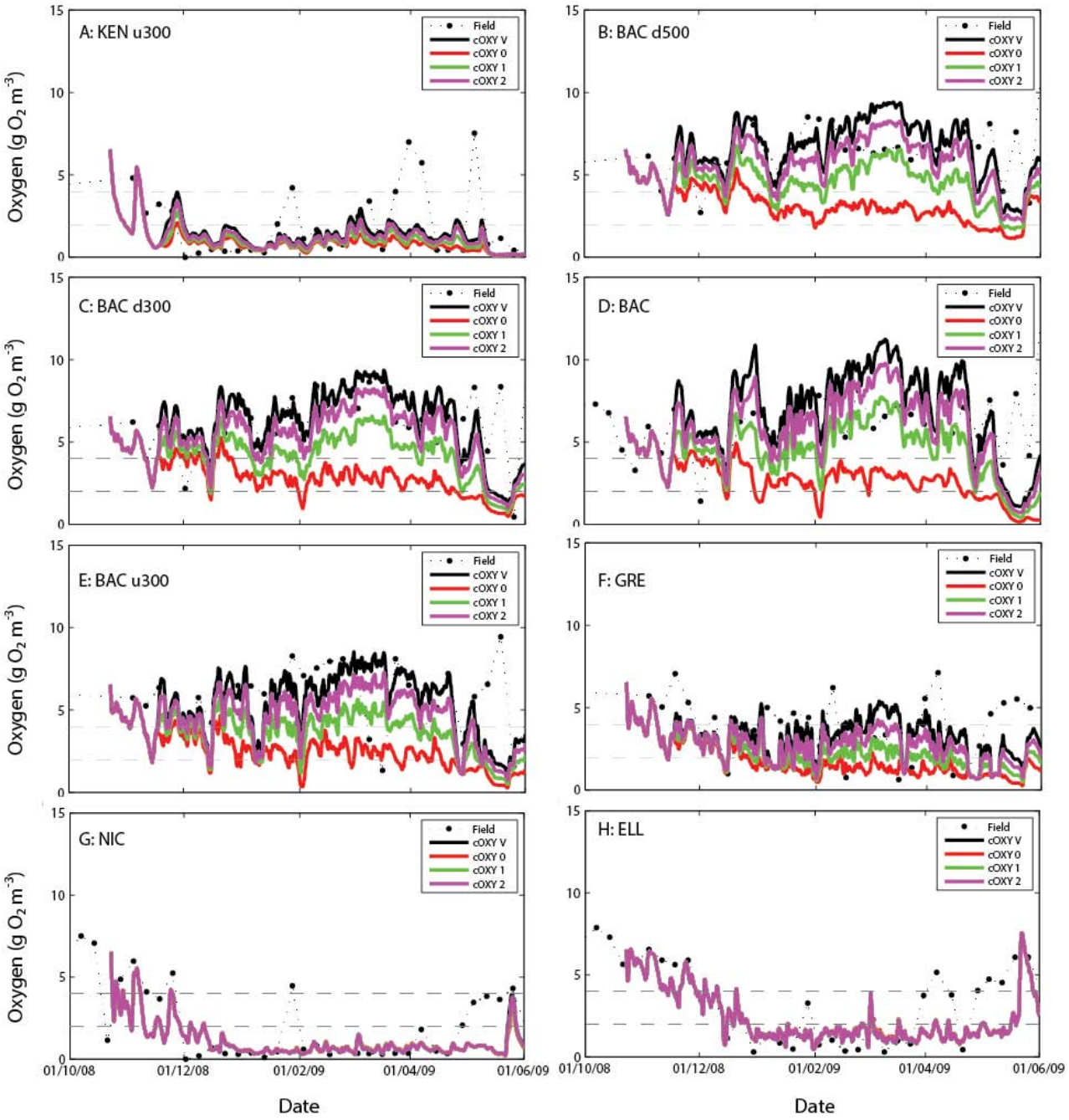

Figure 46: Bottom water dissolved oxygen concentrations for the 8 sites (A-H) in the Canning Weir Pool for the oxygenation scenarios assessing sensitivity to the input flow from the oxygenation plant (refer to Table 12 for scenario detail).

The scenarios comparing sensitivity to input configuration are shown in Figure 47. These show a high sensitivity to the vertical input point of the oxygen (cOxy5 versus cOxyV), and relative insensitivity to the number of spargers (cOxy3 versus cOxyV). For cOxy5, the input of oxygen is assumed to not rise rapidly, as opposed to the buoyant rise of the plume as happens in cOxyV, and leads to very large increases in bottom water concentrations, sometimes twice as high as that currently seen, for the same amount of input oxygen. Figure 48 demonstrates the advantages of this approach.

The final scenario tested was to assess if a third oxygenation plant situated in the upstream reaches near the NIC station would improve water quality in this region (Figure 49, note the different stations used on this plot). The time-series does not clearly show the potential benefit of the hypothetical plant, however the benefit is seen in the curtain plots (Figure 50). Based on the configuration adopted in these simulations, the additional inputs mainly benefit the surface layer by increasing surface concentrations, and do not combat the low concentrations in the deep holes around this region. This could potentially be mitigated through careful design of the spargers to minimise plume buoyancy.

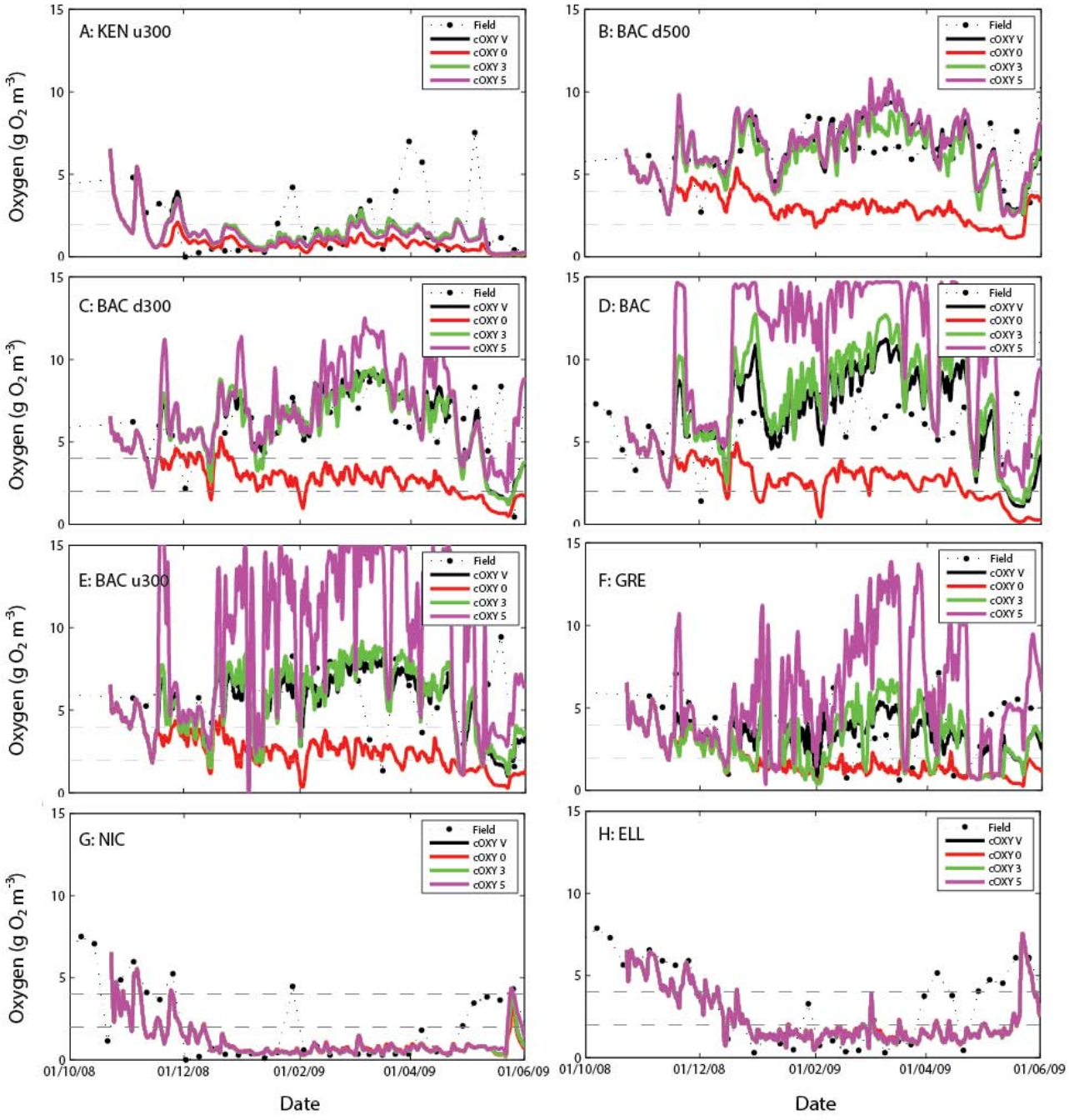

Figure 47: Bottom water dissolved oxygen concentrations for the 8 sites (A-H) in the Canning Weir Pool for the oxygenation scenarios assessing sensitivity to the input configuration (refer to Table 12 for scenario detail).

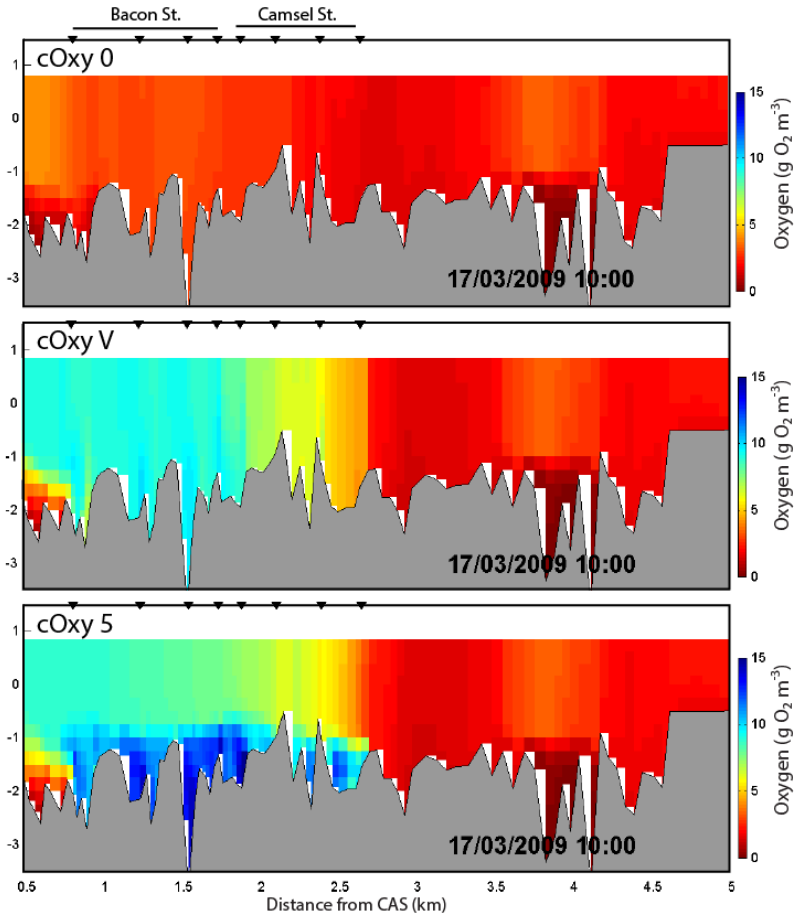

Figure 48: Dissolved oxygenation concentrations for cOxy0, cOxyV and cOxy5, demonstrating the benefit from having the oxygenation plume inserting and persisting at the bottom without rising.

Given the large site-to-site and day-to-day variability, the effectiveness of the various scenarios is better illustrated through the spatially integrated total benthic area that has been prevented from going into hypoxia due to the presence of the oxygenation inputs (Figure 51). Given the scenarios have not tested altered input temporal regimes, they tend to follow the same pattern with higher or lower peaks depending on the total amount of oxygen input. The spatial pattern is seen clearly in Figure 52, which demonstrates the remediation effect created for each scenario as a percentage of the simulation period, and position upstream of the weir.

These various scenarios are summarised below in order to give a simple indication of the benefit or otherwise of each (Figure 53). When the relative efficiency is compared to the relative input amount, these scenarios summarise the non-linear relationship between input and response. In particular, the curve shows that the beneficial response for unit of input decreases with increasing input and approaches a point where increases lead to minor improvement for amounts above the cOxyV amount. Also notable is that whilst the altered input configuration scenarios made substantial impacts at some locations (Figure 48), the overall effect on the system-scale total area of remediated benthic area was minimal; in general terms the response of the weir pool to oxygenation was larger related to the amount of input rather than the physical method of how it is introduced. This reflects the relatively small and disconnected nature of this system compared to the Upper Swan case.

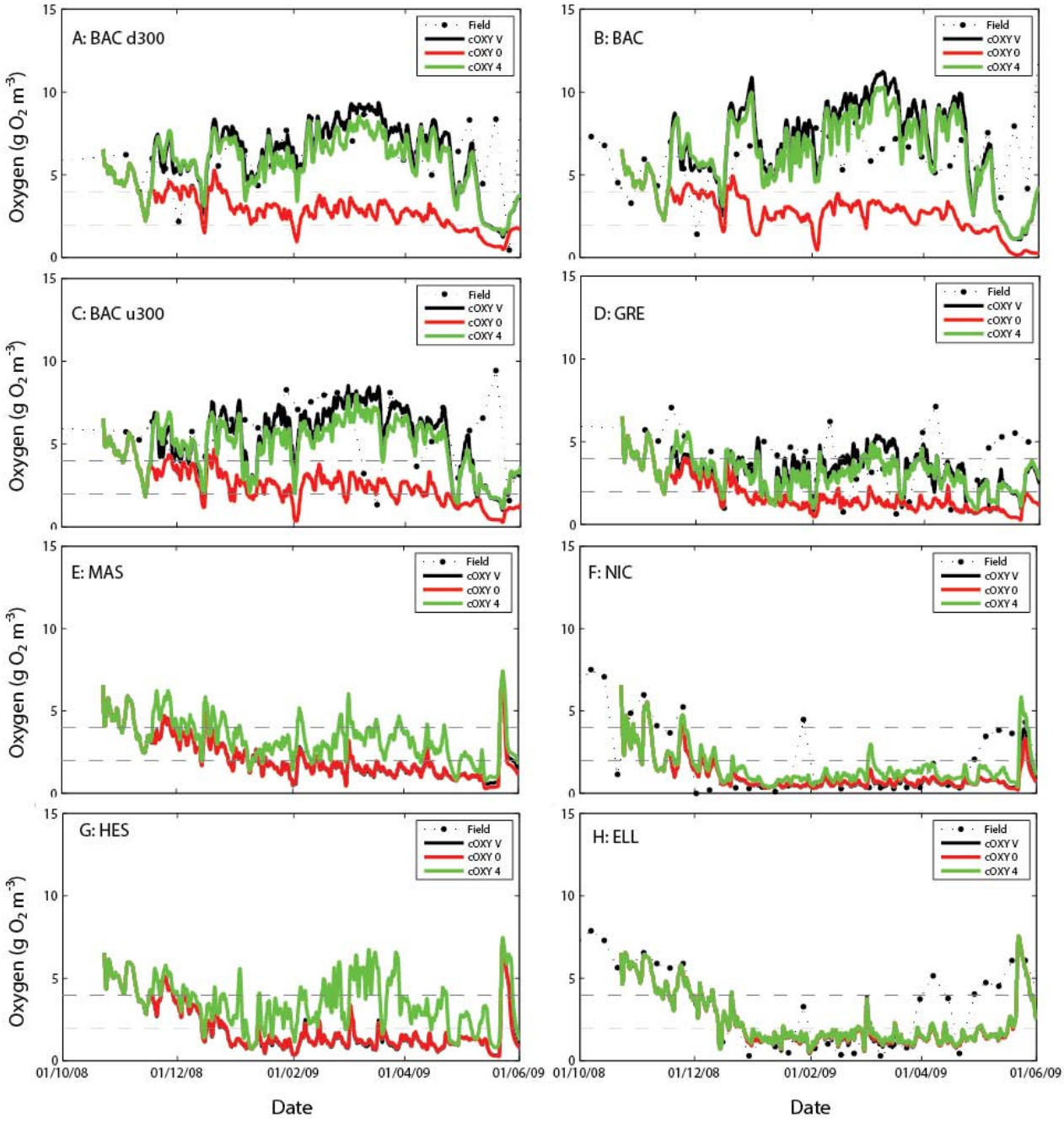

Figure 49: Bottom water dissolved oxygen concentrations for the 8 sites (A-H) in the Canning Weir Pool for the oxygenation scenarios assessing sensitivity to number of oxygenation plant inputs (refer to Table 12 for scenario detail).

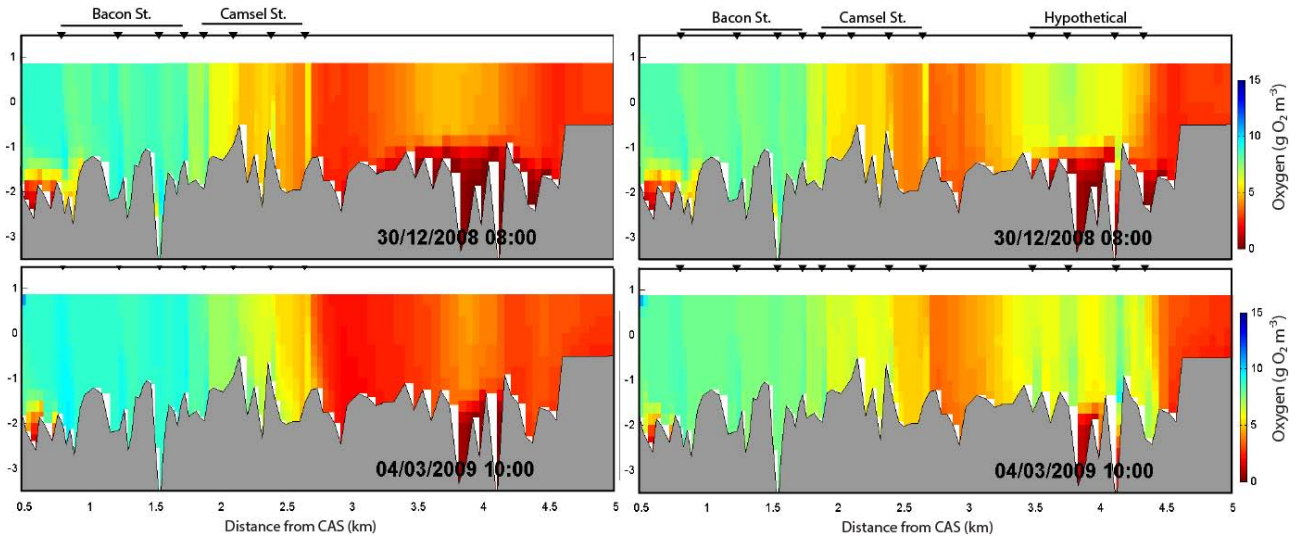

Figure 50: Dissolved oxygenation concentrations for cOxyV (left) and cOxy4 (right), for two snap shots, demonstrating the potential benefit of the hypothetical spargers placed around the NIC site.

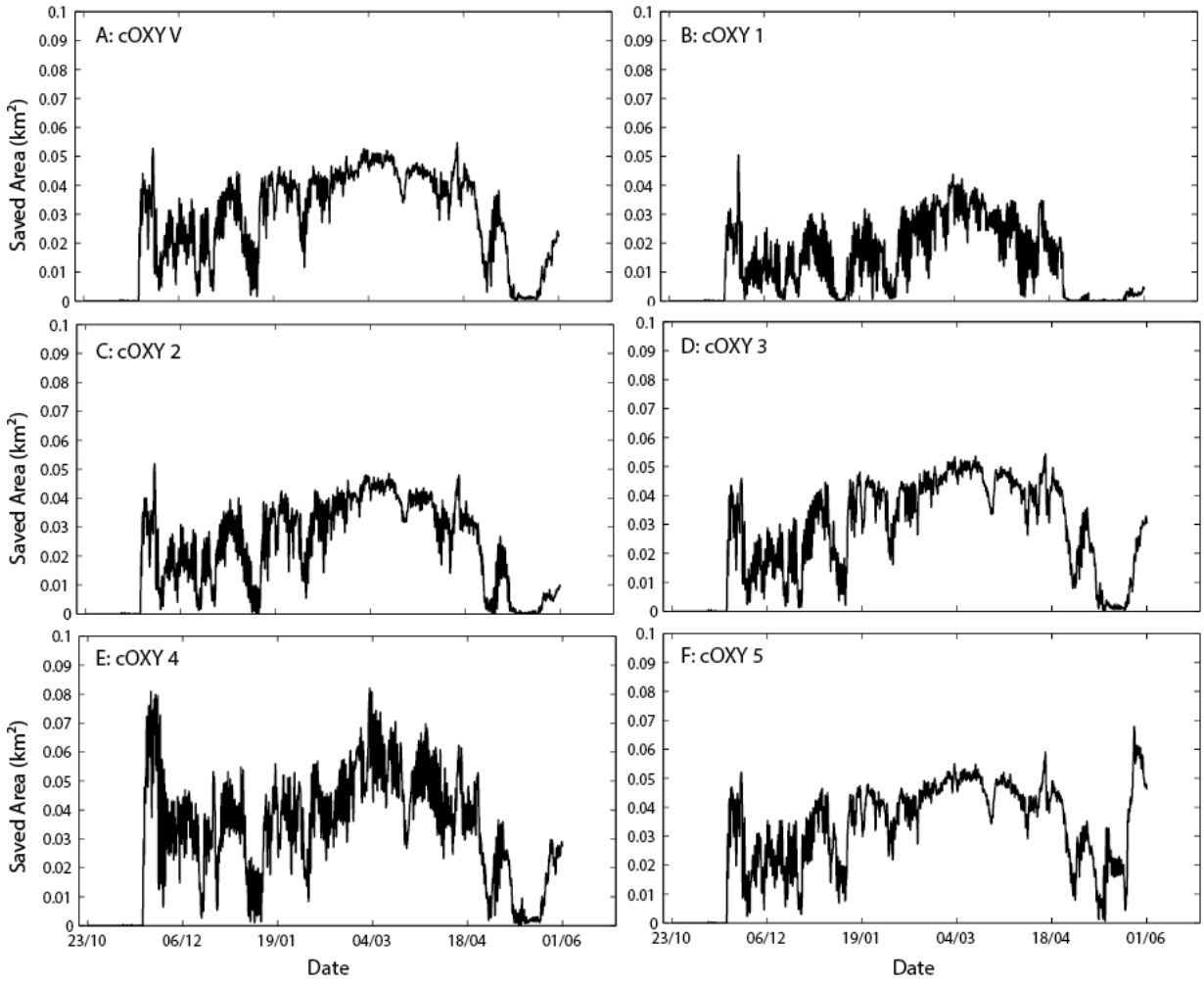

Figure 51: Time-series of total "benthic area saved from low oxygen" (km^2) calculated for each scenario relative to cOxy0 (do nothing).

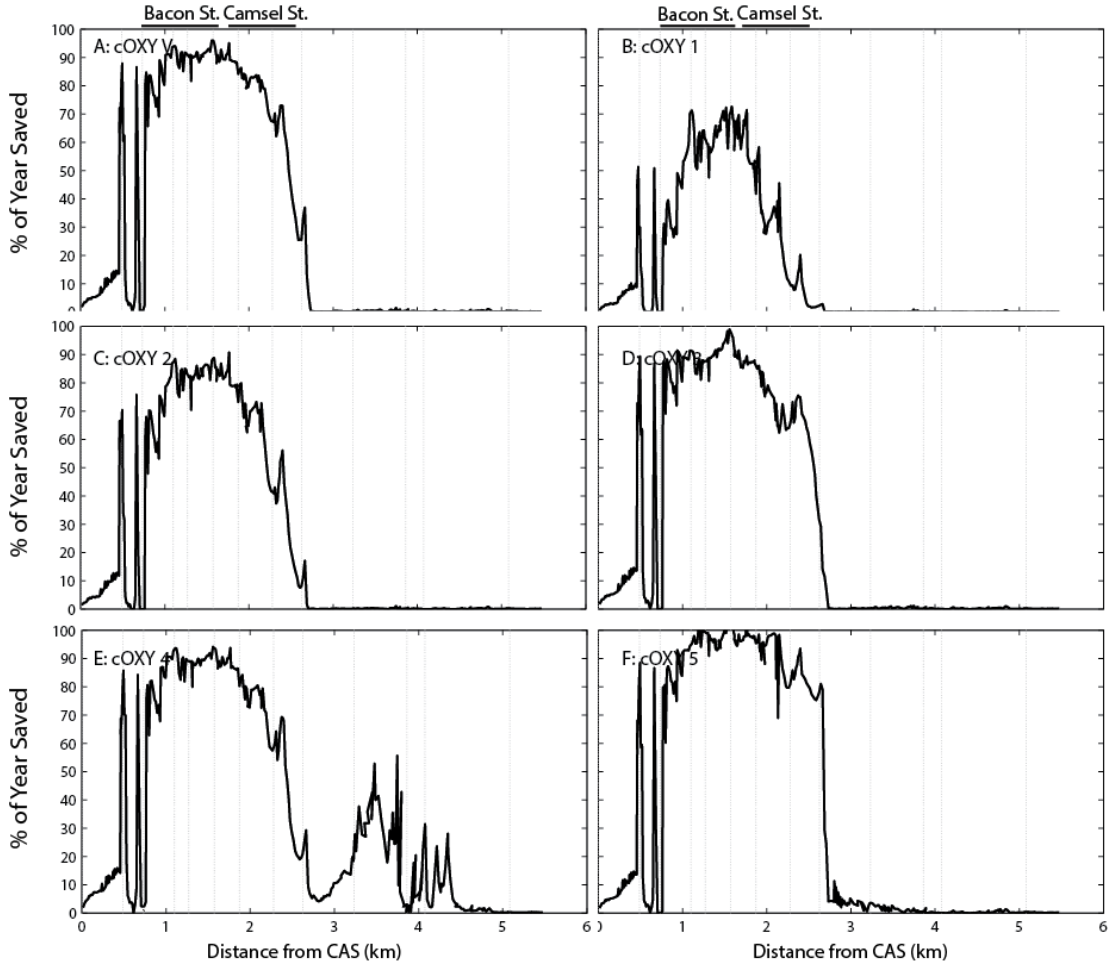

Figure 52: Along-stream transect of "benthic area saved from low oxygen" (relative units) for each scenario, summed over the length of the simulation, calculated relative to cOXY0.

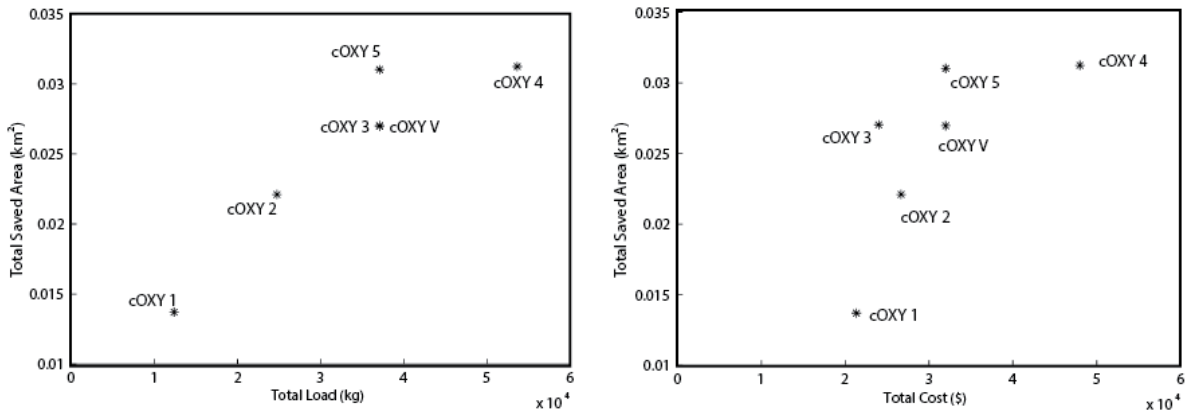

Figure 53: Daily average area of benthos (river bed) saved in the Kent St Weir Pool from low oxygen (< 4 g O_2 m^{-3}) concentrations as a function of oxygenation plant input (left) and total cost (right). Several scenarios are shown comparing oxygen input regime and amount (refer to Table 12 for details). The cost was calculated using Eq. 2-4, based on a price 0.278 \$ kWh^{-1} for peak and 0.100 \$ kWh^{-1} for off-peak, assuming a consumption of 44 kWh for both plants.

6. Conclusions & Recommendations

Through development and validation of an estuary response model, the project has collated a wide variety of data and historical information in order to better understand the effectiveness and dynamics of the oxygenation plants managed by the Western Australia State Government. Specifically, the model has been used to assess the hydrodynamics and biogeochemistry of the Upper Swan estuary and Canning Weir Pool in relation to various oxygenation scenarios.

Overall, the model has been configured according to the project aims, and has been proven to be fit-for-purpose for assessing:

- the benefit of oxygenation plants on the Upper Swan estuary and the Canning Weir Pool;
- different oxygenation plant operational scenarios under different hydrological conditions;
- the area of benthic habitat improved by oxygenation;
- the effect of oxygenation changes on sediment biogeochemical processes; and
- cost-benefit analyses of different management decisions.

To date there has been no proven examples of models used to simulate the dynamics of estuary artificial oxygenation, particularly in estuarine rivers with high curvature and complex morphometries, and therefore this work has invested a significant amount of effort into testing different model setups and parameterisation, and assessing model performance (validation). In particular, a substantial amount of data from all available monitoring stations (20 long-term plus 38 ad hoc sites for the upper Swan River and 13 sites for the Canning) has been processed for the purposes of testing the model against these dynamics. Overall, the model performed very well in capturing the spatio-temporal variability in estuarine temperature, salinity and oxygen concentrations. Whilst the model was configured to simulate nutrients, turbidity and chlorophyll-a, it was run using default parameters and not the focus of this present report. However, it has been implemented as a first step towards allowing the development of a full-featured biogeochemical model that can be further developed in future studies.

One of the key drivers for estuarine deoxygenation is the sediment oxygen demand. Therefore a parallel sediment biogeochemical model was constructed, validated and used to simulate the high-resolution vertical dynamics of surficial sediment under various conditions, including the highly dynamic conditions as created by the diel changes in redox conditions created by periodic oxygenation. This analysis at the small-scale was able to unravel the potential complex effects oxygenation could have on sediment chemistry and the associated changes in nutrient and oxygen fluxes. The results from this complex and high-resolution sediment model were used to justify the development of simpler sediment flux relationships that were incorporated into the 3D hydrodynamic-biogeochemical model. This approach ensures that we have confidence that the large-scale model was capturing the essential sediment biogeochemical dynamics relevant to the dynamically changing environmental conditions experienced by the sediment.

An overview of the key outcomes for the two simulated domains is provided below, outlining the current limitations of the model and recommendations for further work.

Upper Swan estuary

Model validation and suitability

Validation was conducted for the 2008 and 2010 calendar years, with specific focus on the salinity, temperature and oxygen patterns. This included in particular the salt wedge propagation and the extent of low oxygen conditions (<4 g O_2 m^{-3}), including hypoxia (<2 g O_2 m^{-3}).

- *Model performance: hydrodynamics*
    - After several iterations of model mesh refinement, the model demonstrated it was able to confidently predict the salt-wedge dynamics (R^2 >0.9 at most sites; relative error ~5-10%), both at the estuary scale, and at the focus area surrounding Guildford and Caversham.
    - The river has a high degree of curvature here that hydrodynamic models typically find challenging to resolve the sharp pycnocline in this environment, so the accurate hydrodynamic simulations presented

here, both during normal flow conditions (2008) and very low flow conditions (2010), gives us confidence the model is suitable for this environment and fit-for-purpose.

- *Model performance: water quality*
    - The oxygen dynamics were also thoroughly assessed across the estuary for both flow years. The relative error estimates for oxygen were higher (~20%) than for salinity, which was considered given the relatively large degree of variability within the data. The broad scale seasonal trends and both the surface and bottom oxygen concentration predictions were very well reproduced for a domain of this complexity, and the timing and extent of low oxygen and hypoxia was comparable to that observed in the monitoring data.
    - A detailed comparison of the model results with data collected in 2010 from around the Guildford oxygenation plant was able to demonstrate the model was able to effectively simulate the rise and dispersion of the oxygenation plume, though poor resolution of the forcing meteorological data in this region and lack of local algal bloom predictions in the model, meant that some discrepancies emerged in the model results during some of the comparisons with the high-resolution profile data.
    - Overall, the model was deemed to have accurately captured the underlying hydrodynamic and biogeochemical processes that drive the dynamics of oxygen in the estuary near the oxygenation plants for the purposes of assessing operational and flow scenarios.
    - Nutrient predictions using the default model process and parameter values showed reasonable predictions with variability due to inflow nutrient pulses captured, however, further work is required to further validate the nutrient cycling in the model before it can be used to assess the oxygenation affect on the overall nutrient loss rates.

Outcomes from the oxygenation scenario simulations

The model was used to explore the effectiveness of several oxygenation operational scenarios. We assessed the oxygenation plant performance using several metrics, including along-stream distance of influence, the degree of reoxygenation of the bottom of the water column, and the percentage of benthic area experiencing low oxygen or hypoxic conditions. The scenario assessment concluded:

- Under 2010 low flow conditions, artificial oxygenation significantly improved oxygen conditions over a wide range. This was assessed by using a tracer injection, which showed that the along-stream distance of influence influenced by the addition of oxygen at Guildford and Caversham could exceed 30 km, depending on the magnitude of the river flow.

- Our assessment of the "saved benthic area" was conducted to assess benthic oxygen improvements relative to a reference "no oxygenation" (do nothing) simulation. Across the different oxygenation scenarios, with both plants running, the area of benthos saved could reach between 0.6 – 1.2 km^2 during the peak of plant operation. On an annual time-scale average values of ~0.3 km2 could be achived, which covers most of the 0.38 km^2 Swan River Trust oxygenation target zone. The results depend on the plant operation method (e.g., night operation, all day operation or tidally-optimised operation), with an estimated operating cost ranging from $200,000-400,000 per annum.

- There is a non-linear relationship between increasing oxygen supply and increased benefit, with the scenarios highlighting that adding more oxygen would improve the oxygen conditions to a greater extent up to a limit (i.e., the law of diminishing returns). This relationship emerges because higher input rates also enhance the area of the water column that is over-saturated and thereby potentially decrease its cost-effectiveness as a result of increasing atmospheric losses. From a cost-benefit point of view, there is an optimum amount that is able to see the benthic area experiencing low oxygen to increase just above 4 g O_2 m^{-3}. Once this level of improvement has been reached then increased inputs are less effective and do not necessarily penetrate further upstream or downstream.

- The spatial analysis conducted highlighted the benefit of having two plants adding oxygen compared to one plant inputting oxygenation at twice the rate.
- Simulations showed that timing of oxygen input (e.g. night time versus aligned with tidal cycles) could potentially lead to some modest differences in plant effectiveness, though cost savings associated with running during off-peak times highlights this as an effective approach.
- The relative efficiency was compared under two flow conditions and showed that the total area benefiting from oxygenation was highly sensitive to the prevailing flow regime; the area of benthos saved was approximately twice has high when comparing the 2011 winter-spring flows (high flow rate) compared with the 2010 flow regime (low flow rate).
- Scenario outputs were also presented in probabilistic terms in order to help guide decision-making in terms of setting management targets related to low oxygen conditions, such the expected frequency/likelihood of low oxygen conditions being experienced.

Canning Weir Pool

Model validation and suitability

The Canning River validation was conducted from the period the boards went up at the end of 2008 until the end of June 2009.

- *Model performance: hydrodynamics*
    - The model captured the salinity regime during this period including the salt water input events.
    - Accurately simulating temperature was more problematic and modifications to the available South Perth meteorological data were required to get an accurate prediction. In particular, it was necessary to reduce solar radiation to 70% of the observed value to prevent overheating, and this was justified given the likely effect that tree shading of the riparian areas has on the river heat budget.
- *Model performance: water quality*
    - Overall the extent of bottom water hypoxia and seasonal changes were considered to be well captured.
    - The oxygen predictions were most accurate in the downstream end of the weir pool (where the model was forced with known artificial oxygen inputs), with some under-prediction of the surface oxygen noticed in the upstream end where oxygen concentrations in the model were less well constrained.
    - The model validation was best when the majority of the oxygenation plume was configured to enter the middle to upper layers of the water column, suggesting the buoyancy of the plume is significant and the full reoxygenation of the deeper waters is not occurring.
    - With modifications outlined above the model well captured the seasonal and spatial trends that exist in the domain and the model was deemed to be suitable for the purposes of the oxygenation scenario assessments.

Outcomes from the oxygenation scenario simulations

Several scenarios were simulated to test the relative effectiveness of the oxygenations plant inputs:

- In general, the two plants are estimated to have saved up to 0.05 km^2 of benthic habitat during the simulation period (which has a total area of 1.3 km^2 from Kent St weir to Roe Hwy), with annual average values of ~0.03 km^2.

- The range of scenarios tested show a clear non-linear relationship to the amount of money spent on oxygen and electricity and the environmental benefit.

- The data and simulations suggest that the oxygenated input water rapidly rises near the diffusers. A further scenario was run to test the benefit of maintaining the injected oxygen lower in the water column during injection. This demonstrated a potential benefit in the local area, however at the large-scale there was an improvement of approximately 15%.

- The model can be used to shape the design of the third oxygenation plant on the Canning River; in one scenario a hypothetical third oxygenation plant was placed in the upstream section. The results demonstrated an improvement as expected, however the total benefit to the river system in terms of total area of benthos saved did not increase in proportion to the extra cost spent on operating it.

Current limitations to use of the model

- The oxygenation dynamics in the model are largely driven by organic matter loading and sediment oxygen demand. The role of algal production in creating high surface concentrations of oxygen has not been validated and is under-predicting photosynthetic contribution.

- The oxygen surface exchange algorithm in the model uses a standard gas transfer velocity formulation developed for larger open estuaries, and the effect of having reduced fetch in the case of a narrow and sheltered river may mean the rate of oxygen exchange at the atmosphere is over predicted in the upper reaches of the domain.

- Whilst the simulations were configured to include the nutrient cycles and chlorophyll-a, further work is needed to predict the details of the nutrient cycles and algal bloom dynamics in more detail. Nonetheless, despite this reservation, the sediment biogeochemical model was validated in some detail and predictions of the effect of variable oxygen concentrations on sediment oxygen and nutrient fluxes are reliable. Further work to more fully validate the seasonal and spatial variability in nutrient and algal dynamics will allow therefore allow us to fully resolve the estuary nutrient budget.

- Scenarios to test the benefit of "DO control" (whereby oxygenation plant operation is linked to near real-time in situ oxygen concentrations) have not been conducted but is an area worth investigating further. This requires the model to dynamically adapt the rate of oxygenation input in response to internal predictions of the model. Further development of the AED oxygen module is required to enable an adaptive rate of oxygenation input that is able to vary in response to internal state of oxygen within the model.

- The model parameterization of inputs from the oxygenation plant simplifies the dynamics of the oxygenation plume, and doesn't consider detailed resolution of the bubble plume dynamics. Therefore the model is less well-suited to fine-scale studies of near-field oxygen plume dynamics and diffuser design simulations.

- The role of groundwater inputs into the domain have not been considered in the upper Swan domain, however this was crudely approximated for the Canning Weir Pool simulations. The role of groundwater in shaping estuarine water quality is largely unknown and could be contributing to organic matter and nutrient loading.

General recommendations and further work

Based on the work conducted, several recommendations are provided relating to the operation of the oxygenation plants.

- Implementation of practices to encourage less rapid rising of the oxygenation bubble plume. Exploring these options has been beyond the scope of this study but would allow management options to prevent degassing to be explored. These could include modification to the diffusers or installation of baffles to encourage horizontal dispersion and reduce the rise of the plume.

- Whilst not explicitly assessed in these scenarios, the use of "DO control" as defined above and which is currently being conducted by plant operators, is potentially not the most optimum scenario for improving water column oxygen. Further work is recommended to identify how DO control operational rules lead to the benefit at the larger system scale (e.g. in terms of area of benthos saved), and how this compares with other alternatives.

- Investment in the collection of local weather station data, including net-radiation fluxes. This should be within the upper riverine reaches of the two domains to better capture the local conditions near the oxygenation plants.

The model application and validation effort reported here has been conducted in order to establish a base model platform, with several oxygenation scenarios assessed. Ongoing model development, improvement and further validation will continue to improve the predictive ability of the model for tackling questions relevant to management. Some priority areas for further research effort include:

- Sediment flux studies, including sediment oxygen penetration assessments, are recommended to better describe how nutrient release responds to dynamic benthic oxygen conditions.

- Using the model to run whole operational year scenarios for all years that plants have been in operation to determine 'benthic area saved' versus actual expenditure (i.e., to quantify how the management intervention and associated costs have improved the estuarine environment. Extending this study to a range of flow and operational conditions will allow us to be more confident and accurate in estimation of the plant benefits and gain insights into how different flow conditions influence the degree of success of oxygenation.

- Collection of improved data on the organic matter loading in the major and minor tributaries of the Upper Swan, considering both coarse and fine particulate material, and dissolved organic matter.

- Improved spatial mapping of sediment condition to allow specification of localized sediment flux rates within the model.

- Using the model presented here, it is also possible to develop an "optimal" operational regime based on knowledge of hydrological, biogeochemical and operational conditions in the days/weeks immediately prior. In this way effective forecasts could be introduced in order to gain the maximum plant operational savings.

For wider use of the model for assessing estuary response, the following further recommendations are made:

- Nutrient cycling in the Swan Canning estuary is complex as has been reported in numerous previous studies. Further skill in modelling nutrient cycles, including the organic matter and inorganic nutrients is possible with further work required to customize the model validation beyond the initial effort reported here. Improved model validation of the nutrient and carbon pools will allow the preparation of more detailed nutrient budgets of the estuary to better inform decision making.

- Improved phytoplankton model setup and validation. Given the likely role of blooms in controlling surface oxygen concentrations, this will also lead to improved accuracy in the oxygenation plant related model scenarios. Modelling the bulk community dynamics and different functional groups is possible by building on past modelling studies and integrating with recent cell count and cytometric data that has been collected.

- The simulation of benthic oxygen condition provides improved opportunities to simulate benthic infauna habitat and community structure. This has been reported in previous studies to be significantly affected by persistent low oxygen conditions.

References

Adiyanti, S., Eyre, B.D., Maher, D.T., Santos, I., Golsby-Smith, L., Hipsey, M.R., 2014. A carbon isotope-enabled model for quantifying carbon flux pathways in a salt-wedge estuary, Manuscript submitted to *Environmental Modelling and Software*, available on request.

Arhonditsis, G., Adams-Vanharn, B., Nielsen, L., Stow, C. and Reckhow, K.H., 2006. Evaluation of the current state of mechanistic aquatic biogeochemical modeling: citation analysis and future perspectives. *Environmental Science and Technology*, 40: 6547–54.

Arhonditsis, G. and Brett, M., 2004. Evaluation of the current state of mechanistic aquatic biogeochemical modeling. *Marine Ecology Progress Series*, 271: 13–26.

BMTWBM, 2013a. TUFLOW FV Science Manual. Available from: http://www.tuflow.com/Download/TUFLOW_FV/Manual/FV_Science_Manual_2013.pdf

BMTWBM, 2013b. Three dimensional receiving water quality modelling of the Maroochy River: Calibration report. Prepared for SEQ Healthy Waterways Partnership. 142pp.

Bruce, L.C., Cook, P.L.M. and Hipsey, M.R., 2011. Using a 3D hydrodynamic-biogeochemical model to compare estuarine nitrogen assimilation efficiency under anoxic and oxic conditions. *19th International Congress on Modelling and Simulation*. p3691–3697.

Bruce, L.C., Cook, P.L.M., Teakle, I. and Hipsey, M.R., 2014. Hydrodynamic controls on oxygen dynamics in a riverine salt-wedge estuary, the Yarra River estuary, Australia. *Hydrology and Earth System Sciences*, 18: 1397 - 1411

Bruggeman, J. and Bolding, K., 2014. A general framework for aquatic biogeochemical models. *Environmental Modelling and Software*, DOI: 10.1016/j.envsoft.2014.04.002.

Chan, T., Hamilton, D.P. Robson, B.J., Hodges, B.R. and Dallimore, C., 2002. Impacts of hydrological changes on phytoplankton succession in the Swan River, Western Australia. *Estuaries and Coasts*, 25: 1406–1415

Chao, X., Jia, Y., Shields, F.D., Wang, S.S.Y. and Cooper, C.M., 2010. Three-dimensional numerical simulation of water quality and sediment-associated processes with application to a Mississippi Delta lake. *Journal of Environmental Management*, 91: 1456 – 1466.

Cottingham, A., Hesp, S.A., Hall, N.G., Hipsey, M.R. and Potter, I.C., 2014. Changes in condition, growth and maturation of Acanthopagrus butcheri (Sparidae) in an estuary reflect the deleterious effects of environmental degradation. *Estuarine, Coastal and Shelf Science*, in press.

Crowe, S. A., Canfield, D. E., Mucci, A., Sundby, B. and Maranger, R., 2012. Anammox, denitrification and fixed-nitrogen removal in sediments from the Lower St. Lawrence Estuary. *Biogeosciences*, 9: 4309-4321.

Department of Water 2010 & 2011. Quarterly Swan Canning estuarine data reports.

Fellman, J.B., Petrone, K.C. and Grierson, P.F., 2011. Source, biogeochemical cycling, and fluorescence characteristics of dissolved organic matter in an agro-urban estuary. *Limnology and Oceanography*, 56: 243-256.

Fofonoff, N. and Millard, R., 1983. Algorithms for computation of fundamental properties of seawater. UNESCO technical papers in marine science, 44: 1–53.

Gal, G., Hipsey, M.R., Paparov, A., Makler, V. and Zohary, T., 2009. Implementation of ecological modeling as an effective management and investigation tool: Lake Kinneret as a case study. *Ecological Modelling*, 220: 1697-1718

Gedaria, A.I., and Paparini, A. and Hipsey, M.R., 2013. Integration of cytometric, bio-molecular and nutrient data to explore microbial dynamics in the Swan River Estuary. University of Western Australia Technical Report prepared for the Swan River Trust, Perth, Australia. 94pp.

Gillibrand, P.A., Andrewartha, J.R., Herzfeld, M., 2012. Numerical hydrodynamic modelling of the Leschenault Estuary. CSIRO Technical Report, Hobart, Australia. 79pp.

Hamilton, D.P., Douglas, G.B., Adeney, J.A. and Radke, L.C., 2006. Seasonal changes in major ions, nutrients and chlorophyll a at two sites in the Swan River estuary, Western Australia. *Marine and Freshwater Research*, 57: 803-815.

Herzfeld, M., Hamilton, D.P. and Douglas, G.B., 2001. Comparison of a mechanistic sediment model and a water column model for hindcasting oxygen decay in benthic chambers. *Ecological Modelling*, 136: 255-267.

Herzfeld, M., Jones, E., Margvelashvili, N., Mongin, M., Skerratt, J., Andrewartha, J., Rizwi, F., McAlister, T., Holmes, R., Barry, M., Weber, T., Teakle, I. and Baird, M. 2014. SEQ RWQM V3 Phase II Final Report. Prepared for the SEQ Healthy Waterways Partnership. 170pp.

Hipsey, M.R., Bruce, L.C. and Hamilton, D.P., 2014. AED – Aquatic Ecodynamics Modelling Library: Model overview and user information. The University of Western Australia, Perth, Australia. 50pp. ISBN: 978-1-74052-303-5

Hipsey, M.R., Salmon, S.U., Aldrige, K.T. and Brookes, J.D., 2010. Impact of hydro-climatological change and flow regulation on physical and biogeochemical dynamics of the Lower River Murray, Australia. *8th International Symposium on Ecohydraulics* (ISE2010), September, 2010, Korea.

Hipsey, M.R. and Busch, B.D., 2012. Lower Lakes water quality recovery dynamics. University of Western Australia Technical Report prepared for South Australian Department of Environment and Natural Resources, Adelaide, Australia. 81pp.

Howarth, R., Chan, F,. Conley, D.J., Garnier, J., Doney, S.C., Marino, R., Billen, G. 2011. Coupled biogeochemical cycles: eutrophication and hypoxia in temperate estuaries and coastal marine ecosystems. *Frontiers in Ecology and the Environment*, 9: 18–26.

Kemp, W.M., Testa, J.M., Conley, D.J., Gilbert, D. and Hagy, J.D., 2009. Temporal responses of coastal hypoxia to nutrient loading and physical controls. *Biogeosciences*, 6: 2985-3008.

Kangas, M.I, Chandrapavan, A., Hetzel, Y.L. and Sporer, E.C., 2012. Minimising gear conflict and resource sharing issues in the Shark Bay trawl fisheries and promotion of scallop recruitment. *Fisheries Research Report No. 229*. Department of Fisheries, Western Australia. 136pp.

Kilminster, K., Goss, Z., Evans, S., Evans, G., Robb, M.S., Bryant, L.D., Mcginnis, D.F. and Damgaard, L., 2011. Artificial oxygenation of the Swan River: assessing sediment condition. *AMSA conference*, Fremantle, Western Australia.

Kurup, R.G., Hamilton, D.P. and Patterson, J.C., 1998. Modelling the effect of seasonal flow variations on the position of salt wedge in a microtidal estuary. *Estuarine Coastal and Shelf Science*, 47: 191-208.

Kurup, R.G. and Hamilton, D.P., 2002. Flushing of dense, hypoxic water from a cavity of the Swan River estuary, Western Australia. *Estuaries*, 25: 908-915.

Lavery, P.S., Oldham, C.E. and Ghisalberti, M., 2001. The use of Fick's First Law for predicting porewater nutrient fluxes under diffusive conditions. *Hydrological Processes*, 15: 2435-2451.

Middelburg, J.J. and Levin, L.A., 2009. Coastal hypoxia and sediment biogeochemistry. *Biogeosciences*, 6: 1273-1293.

Norlem, M., Paraska, D. and Hipsey, M.R., 2013. Sediment-water oxygen and nutrient fluxes in a hypoxic estuary. In: Piantadosi, J., Anderssen, R.S. and Boland J. (eds) *MODSIM2013, 20th International Congress on Modelling and Simulation*. Modelling and Simulation Society of Australia and New Zealand, December 2013, pp. 1777-1783. ISBN: 978-0-9872143-3-1. http://www.mssanz.org.au/modsim2013/H7/norlem.pdf

Paerl, H., Pinckney, J. and Peierls, B., 1998. Ecosystem responses to internal and watershed organic matter loading: consequences for hypoxia in the eutrophying Neuse River Estuary, North Carolina, USA. *Marine Ecology Progress Series*, 166: 17–25.

Peña, M. A., Katsev, S., Oguz, T. and Gilbert, D., 2010. Modeling dissolved oxygen dynamics and hypoxia. *Biogeosciences*, 7: 933-957.

Petrone, K., Richards, J. and Grierson, P., 2009. Bioavailability and composition of dissolved organic carbon and nitrogen in a near coastal catchment of south-western Australia. *Biogeochemistry*, 92: 27-40.

Petrone, K.C., Hughes, J.D., Van Niel, T.G. and Silberstein, R.P., 2010. Streamflow decline in southwestern Australia, 1950-2008, *Geophysical Research Letters*, 37: 11401-11407.

Petrone, K.C. 2010. Catchment export of carbon, nitrogen, and phosphorus across an agro-urban land use gradient, Swan-Canning River system, southwestern Australia. *Journal of Geophysical Research (Biogeosciences)*, 115.

Roberts, K. L., V. M. Eate, B. D. Eyre, D. P. Holland, and P. L. M. Cook. 2012. Hypoxic events stimulate nitrogen recycling in a shallow salt-wedge estuary: The Yarra River Estuary, Australia. *Limnology and Oceanography*, 57: 1427–1442.

Robson, B.J., and Hamilton, D.P., 2004. Three-dimensional modelling of a *Microcystis* bloom event in the Swan River estuary, Western Australia. *Ecological Modelling*, 174: 203–222.

Robson, B.J., Hamilton, D.P., Webster, I.T., Chan, T., 2008. Ten steps applied to development and evaluation of process-based biogeochemical models of estuaries. *Environmental Modelling and Software*, 23: 369–384.

Robson, B., Webster, I., Rosebrock, U., 2006. Biogeochemical modelling and nitrogen budgets for the Fitzroy Estuary and Keppel Bay. Cooperative Research Centre for Coastal Zone, Estuary & Waterway Management Technical Report 40 CRC for Coastal Zone, Estuary & Waterway Management.

Romero, J.R., Antenucci, J.P. and Imberger, J., 2004. One- and three-dimensional biogeochemical simulations of two differing reservoirs, *Ecological Modelling*, 174: 143-160.

Salmon, S.U., Hipsey, M.R., Wake, G., Ivey, G., Oldham, C.E., 2014. Testing internal vs. external controls on lake water quality: Coupling geochemistry, hydrodynamics, and aquatic ecology, and application to an acidic pit lake. Manuscript submitted to *Water Resources Research*, available on request.

Hamilton, D.P. and Schladow, S.G., 1997. Water quality in lakes and reservoirs. Part I Model description. *Ecological Modelling*, 96: 91–110.

Silberstein, R.P., Aryal S.K., Durrant, J., Pearcey, M., Braccia, M., Charles, S.P., Boniecka, L., Hodgson, G.A., Bari, M.A., Viney, N.R., McFarlane., D.J., 2012. Climate change and runoff in south-western Australia. *Journal of Hydrology*, 475: 441-455.

Smith, C.S., Haese, R.R. and Evans, S. 2010. Oxygen demand and nutrient release from sediments in the upper Swan River estuary. Geoscience Australia Record, 2010/28. Commonwealth Government, Canberra.

Smith, C.S., Murray, E.J., Hepplewhite, C. and Haese, R.R. 2007. Sediment water interactions in the Swan River estuary: Findings and management implications from benthic nutrient flux surveys, 2000-2006. Geoscience Australia Record 2007/13. Commonwealth Government, Canberra.

Storer, T, Robb, M, Norton, S, Kilminster, K. and Nice, H., 2013. Ecosystem health in the Canning River, focusing on the influence of the Kent Street Weir, *Water Science Technical Series, report no. 50*, Department of Water, Western Australia.

Trolle, D., Hamilton, D.P., Hipsey, M.R., Bolding, K., Bruggeman, J., Mooij, W. M., Janse, J. H., Nielsen, A., Jeppesen, E., Elliott, J. E., Makler-Pick, V., Petzoldt, T., Rinke, K., Flindt, M. R., Arhonditsis, G.B., Gal, G., Bjerring, R., Tominaga, K., Hoen, J., Downing, A. S., Marques, D. M., Fragoso Jr, C. R., Søndergaard, M. and Hanson, P.C., 2012. A community-based framework for aquatic ecosystem models. Hydrobiologia, 683: 25-34.

Tweedley, J.R., Hallett, C.S. and Hoeksema, S.D., 2011. The effects of artificial oxygenation on the benthic macroinvertebrate fauna of the Swan-Canning Estuary. Presentation to the *Swan River Trust Forum*, 2 November 2011, Perth, Western Australia.

Umlauf, L. and Burchard, H., 2003. A generic length-scale equation for geophysical turbulence models. *Journal of Marine Research*, 61: 235–265.

Vaquer-Sunyer, R. and Duarte, C.M., 2008. Thresholds of hypoxia for marine biodiversity. *Proceedings of the National Academy of Sciences*, 105: 15452-15457.

Vaquer-Sunyer, R. and Duarte, C.M., 2011. Temperature effects on oxygen thresholds for hypoxia in marine benthic organisms. *Global Change Biology*, 17: 1788-1797.

Vilhena, L.C., 2013. Physical-biological coupling in aquatic ecosystems: the role of hydrodynamics in structuring phytoplankton communities. PhD Thesis, Centre for Water Research, The University of Western Australia, Perth, Australia. 146pp.

Wanninkhof, R., 1992. Relationship between windspeed and gas exchange over the ocean. *Journal of Geophysical Research (Oceans),* 97(C5): 7373–7382.

Wildsmith, M.D., Rose, T.H., Potter, I.C., Warwick, R.M. and Clarke, K.R., 2011. Benthic macroinvertebrates as indicators of environmental deterioration in a large microtidal estuary. *Marine Pollution Bulletin*, 62: 525-538.

Wild-Allen, K., Skerratt, J., Whitehead, J., Rizwi, F. and Parslow, J., 2013. Mechanisms driving estuarine water quality: A 3D biogeochemical model for informed management. *Estuarine, Coastal and Shelf Science*.

Yeates, P.S., Okely, P., Dallimore, C.J., Antenucci, J.P, Imberger, J., and Hipsey, M.R., 2007. Three dimensional modelling of a seawater desalination plant discharge into Cockburn Sound, Western Australia. In: Qihau, Z., Xiping, D., Jiufeng, G. (eds), Proceedings of the *4th International Conference on Asian and Pacific Coasts* (APAC 2007), Nanjing, China, pp: 811-816. ISBN: 978-7-5027-6883-6.

Zhang, J., Gilbert, D., Gooday, A. J., Levin, L., Naqvi, S. W. A., Middelburg, J. J., Scranton, M., Ekau, W., Peña, A., Dewitte, B., Oguz, T., Monteiro, P. M. S., Urban, E., Rabalais, N. N., Ittekkot, V., Kemp, W. M., Ulloa, O., Elmgren, R., Escobar-Briones, E., and Van der Plas, A. K., 2012. Natural and human-induced hypoxia and consequences for coastal areas: synthesis and future development. *Biogeosciences*, 7: 1443-1467.

Zhu, Y., Cook, P.L.M. and Hipsey, M.R., 2013. Hydrodynamic modeling of the Gippsland Lakes. Proceedings of the *35th International Association for Hydraulic Research World Congress* (IAHR2013), September 2013, Chengdu, China.

Appendix A: Upper Swan Nutrients

Nutrient validation is shown for NH_4, NO_3 and PO_4 for each of the validation years 2008 and 2010 in the below 6 figure sets. Generally the level of predictions is not as good as for salinity and oxygen, however, the mean concentrations and much of the observed variability is captured reasonably. Since the focus of the study was oxygen dynamics, parameters associated with nutrient modules were not adjusted to improve the predictions and further improvements for these variables are left to a further study.

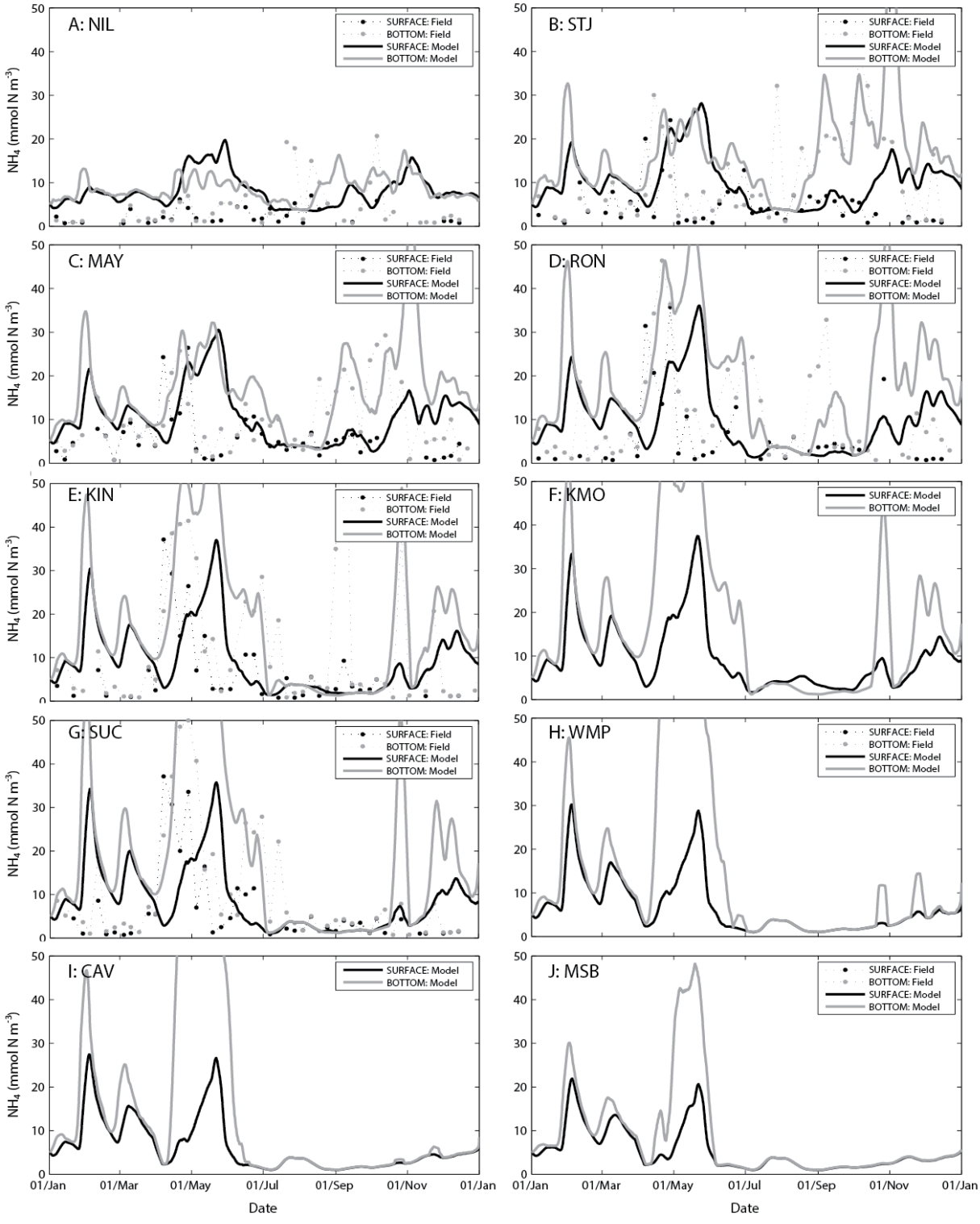

Figure A1: Upper Swan estuary NH_4 concentration (mmol N m^{-3}) for the year 2008 comparing simulated and observed values at 10 sites, labelled A-J.

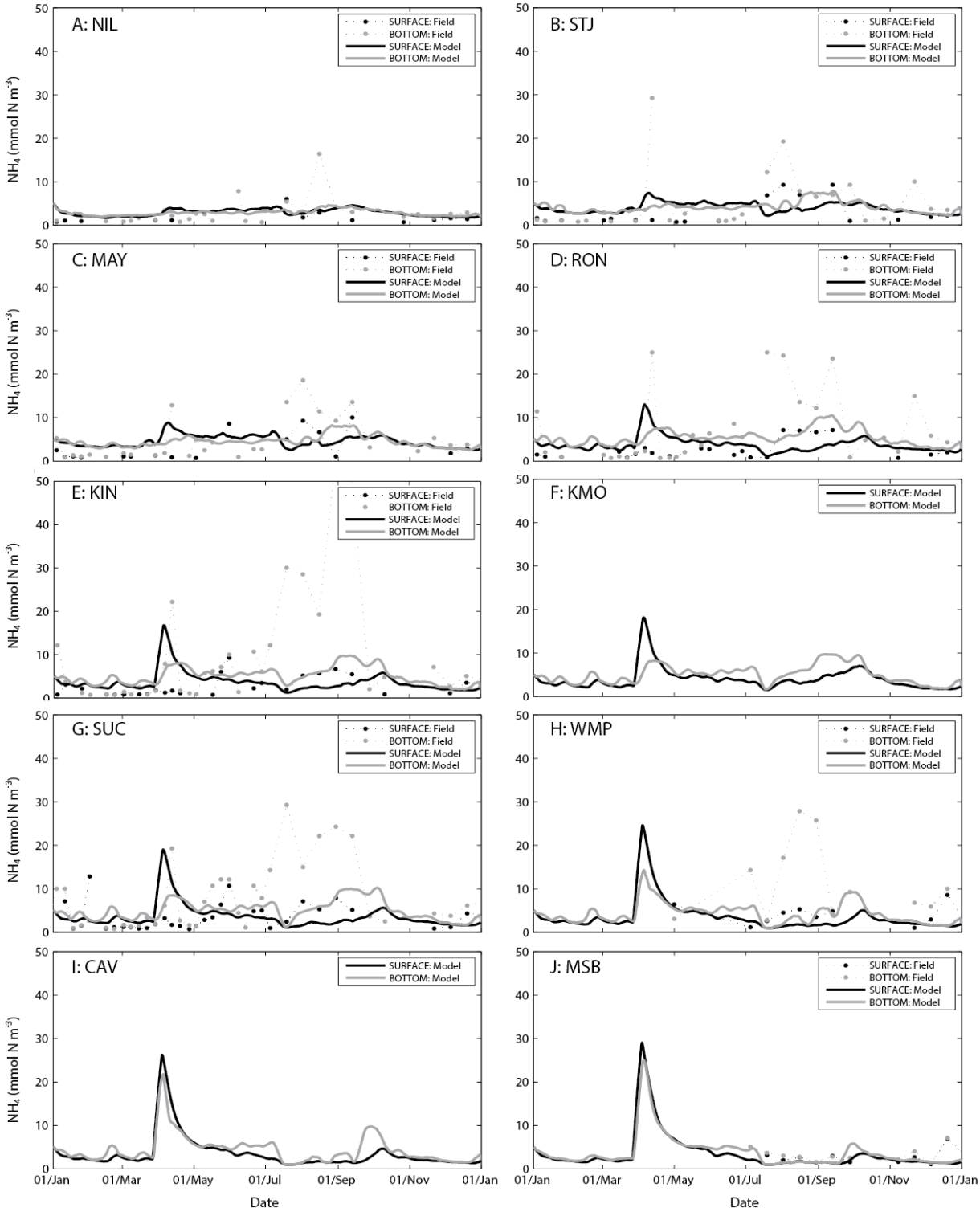

Figure A2: Upper Swan estuary NH_4 concentration (mmol N m^{-3}) for the year 2010 comparing simulated and observed values at 10 sites, labelled A-J.

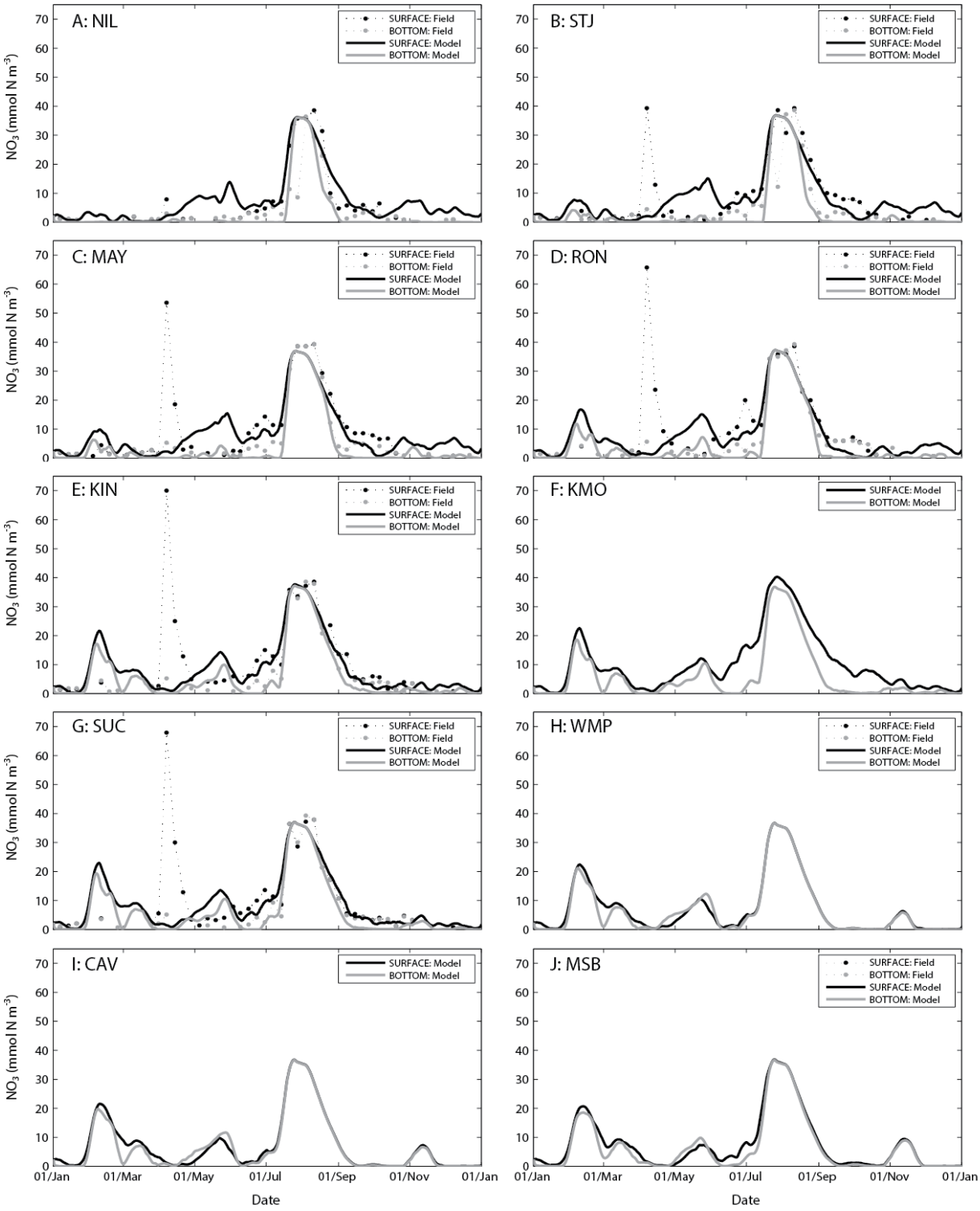

Figure A3: Upper Swan estuary NO_3 concentration (mmol N m^{-3}) for the year 2008 comparing simulated and observed values at 10 sites, labelled A-J.

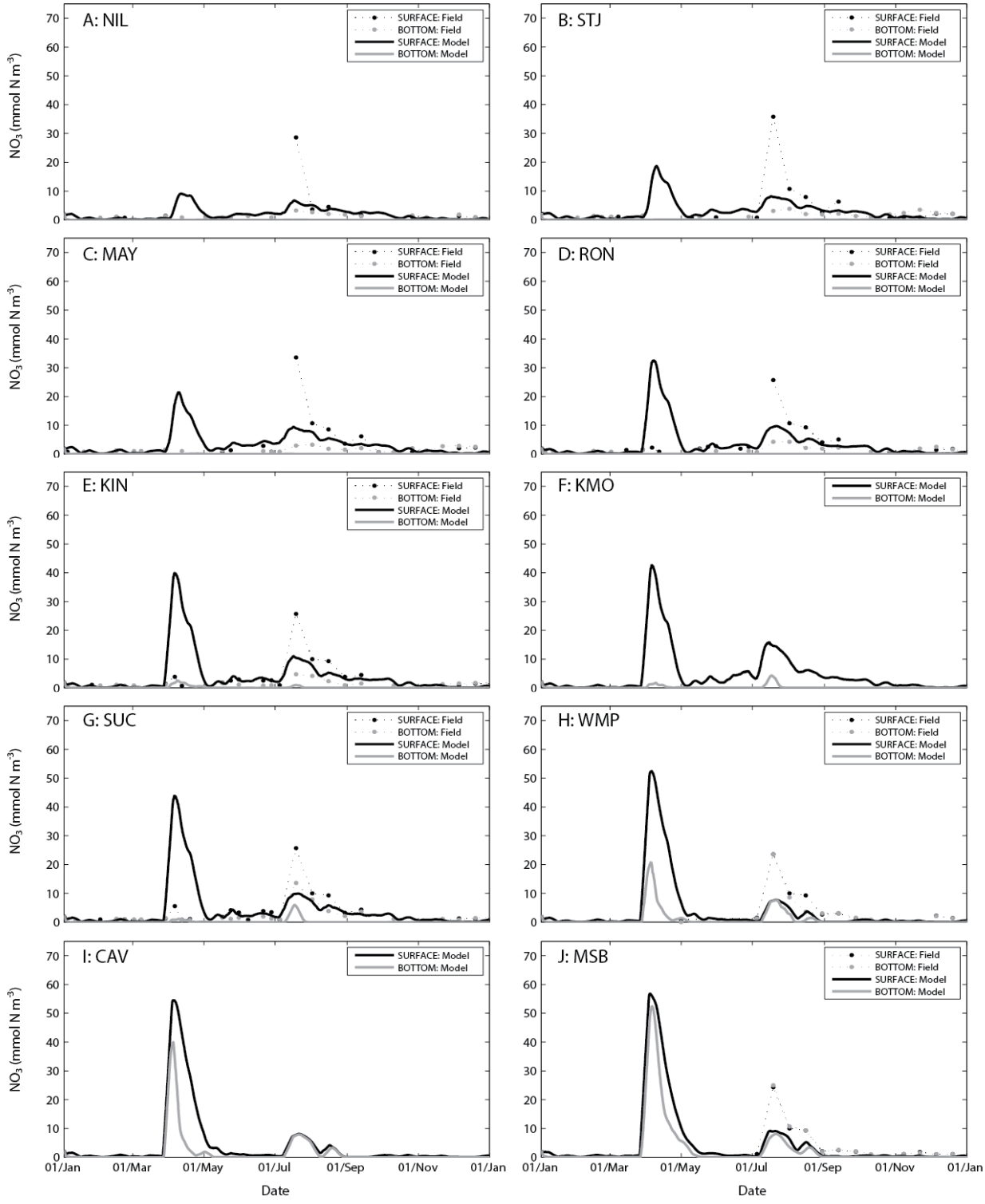

Figure A4: Upper Swan estuary NO_3 concentration (mmol N m^{-3}) for the year 2010 comparing simulated and observed values at 10 sites, labelled A-J.

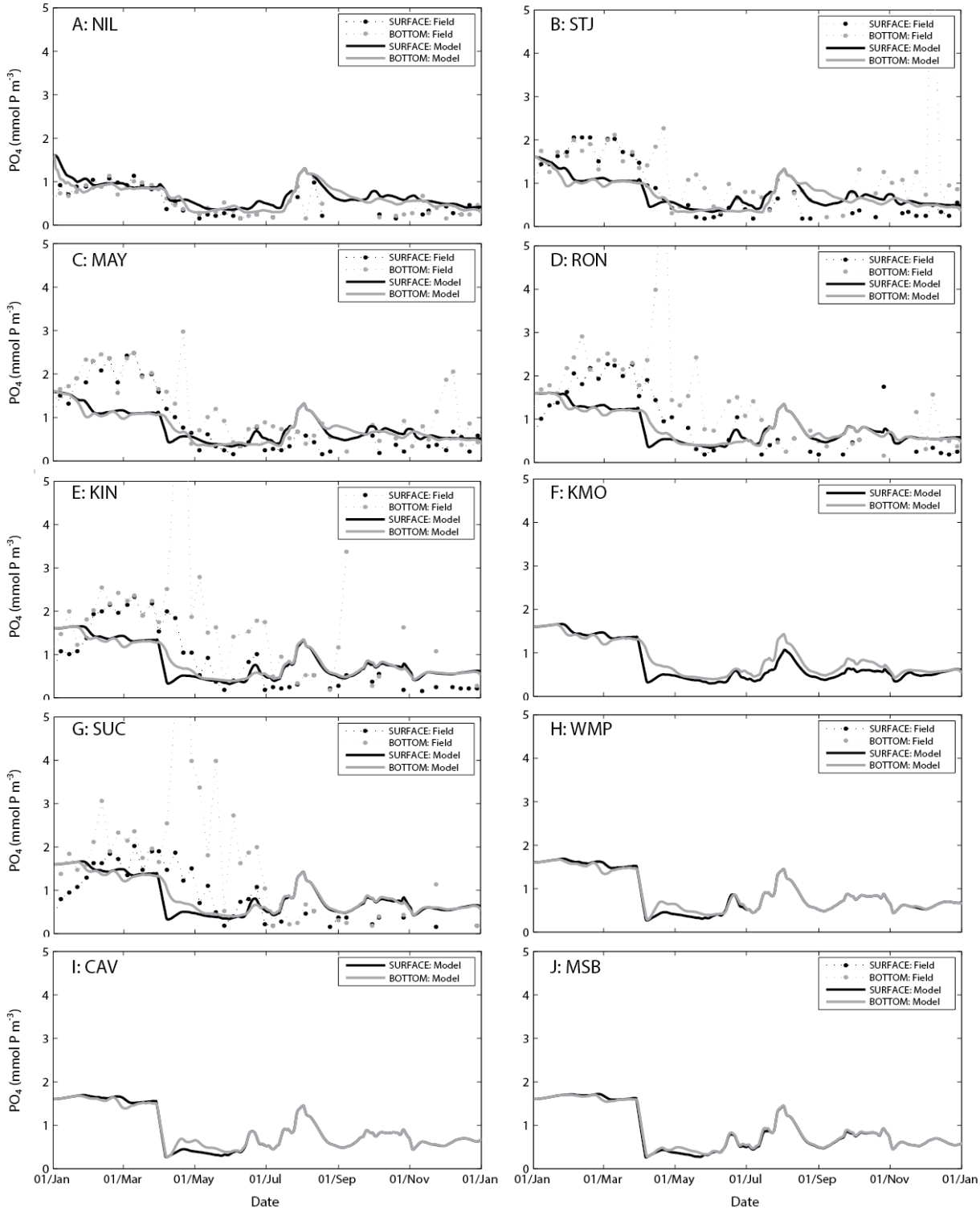

Figure A5: Upper Swan estuary PO_4 concentration (mmol P m^{-3}) for the year 2008 comparing simulated and observed values at 10 sites, labelled A-J.

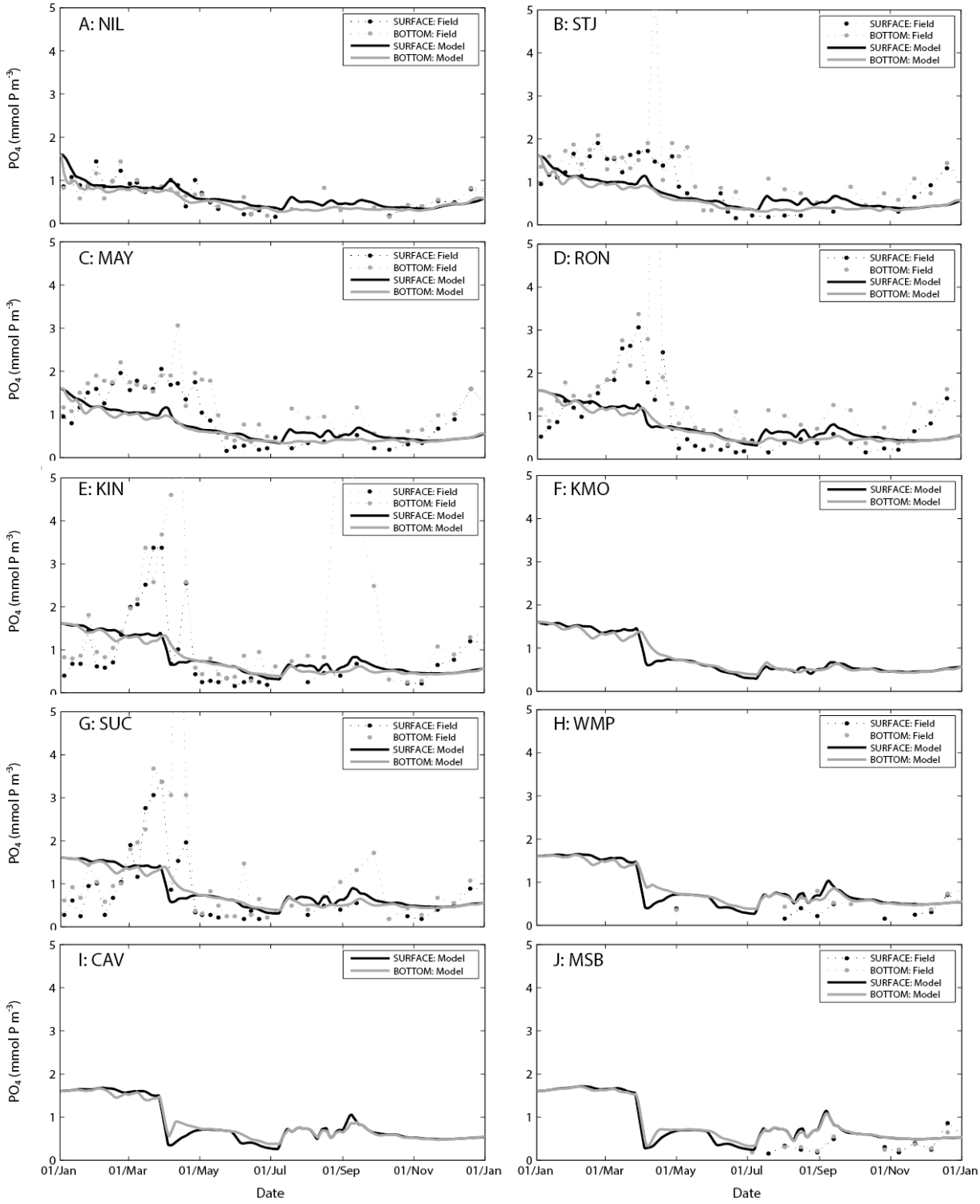

Figure A6: Upper Swan estuary PO_4 concentration (mmol P m^{-3}) for the year 2010 comparing simulated and observed values at 10 sites, labelled A-J.

Appendix B: Canning Weir Pool Nutrients

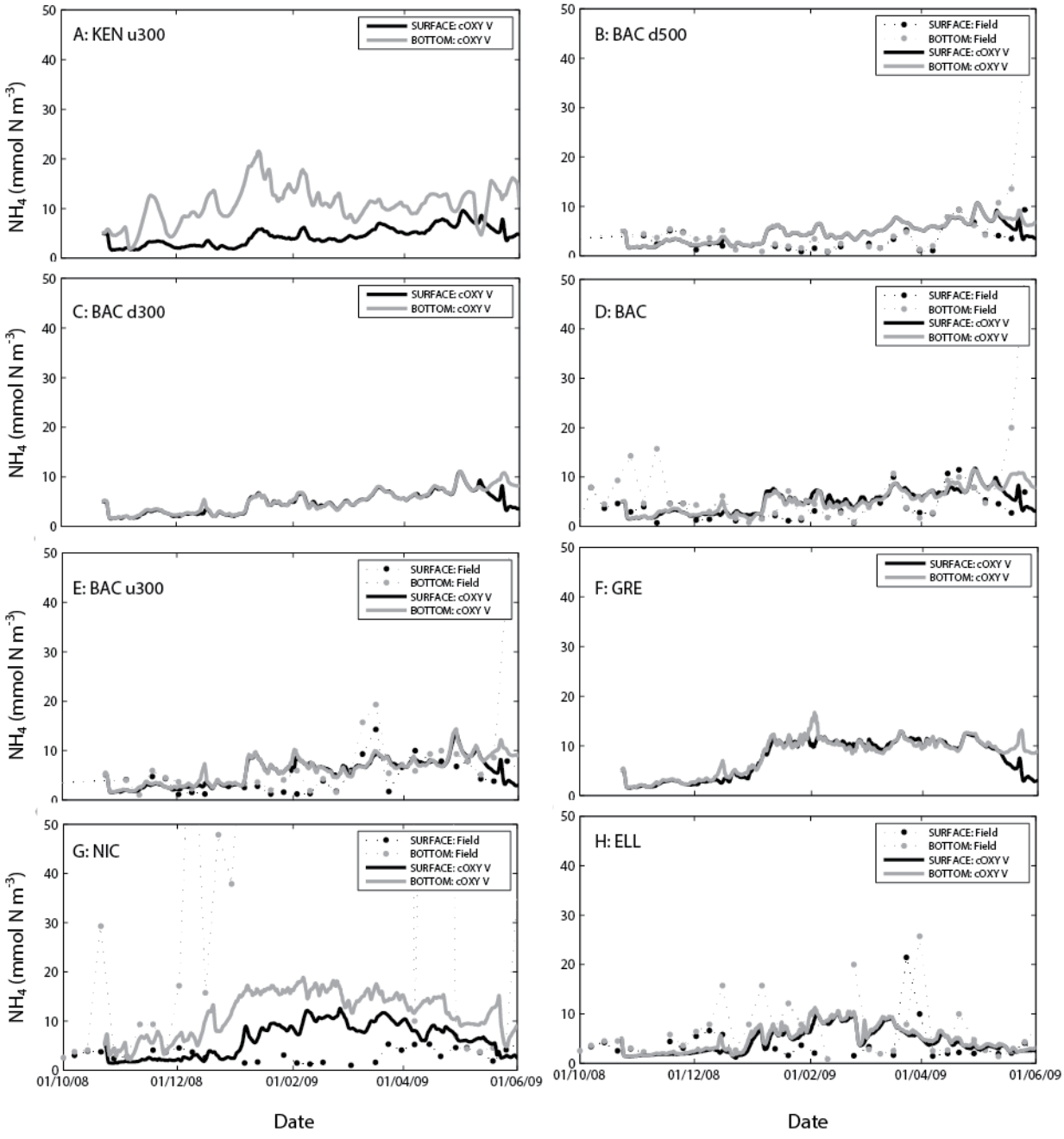

Figure B1: Canning Weir Pool simulated versus observed NH_4 concentrations (mmol N m^{-3}) predictions for Canning stations A-H.

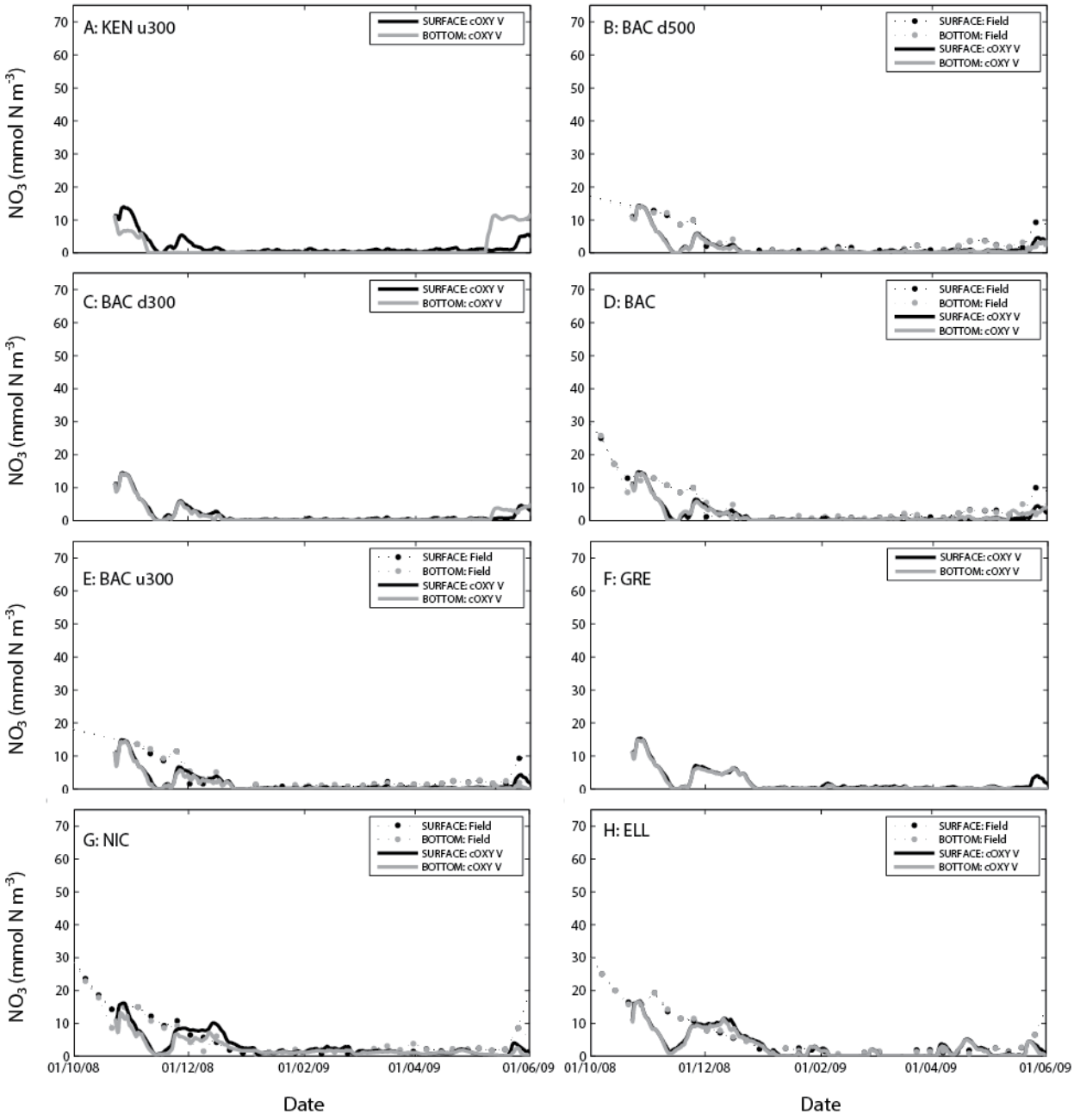

Figure B2: Canning Weir Pool simulated versus observed NO_3 concentrations (mmol N m^{-3}) predictions for Canning stations A-H.

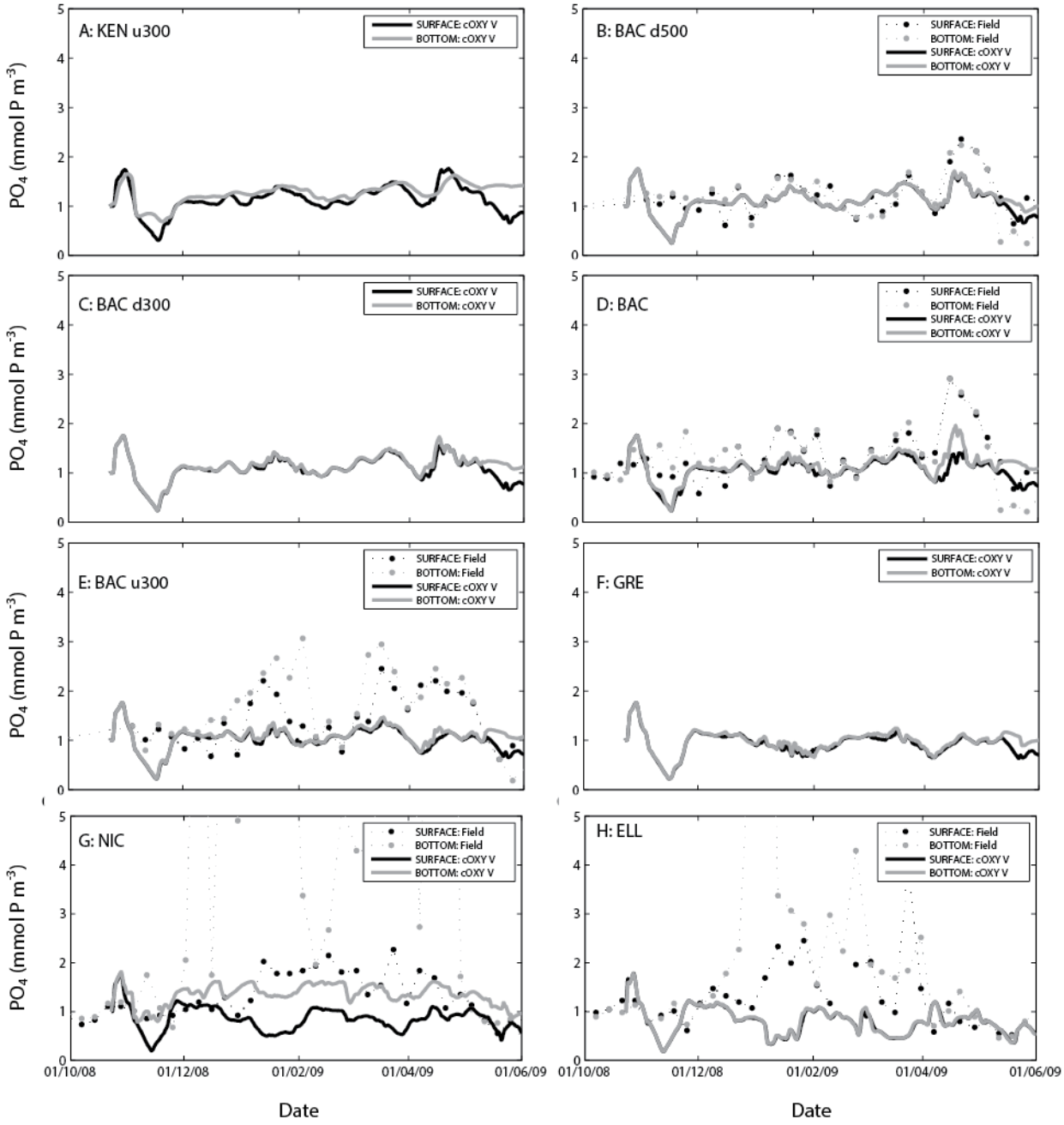

Figure B3: Canning Weir Pool simulated versus observed PO_4 concentrations (mmol P m^{-3}) predictions for Canning stations A-H.